16th ETH-Conference on Combustion Generated Nanoparticles
June 24th – 27th 2012

Summary

Name of Author: Simon Payne[1,2]
Co-Authors: Nick Collings[1]
Affiliation: [1] University of Cambridge, UK
[2] Cambustion, Cambridge, UK
Mailing address: Hopkinson Laboratory, Department of Engineering, University of Cambridge, Trumpington Street, CB2 1PZ. UK
E-mail: spayne@physics.org

Title: Study of Diesel Particulate Bridging Behaviour with SEM

Abstract:

The rapid initial increase in exhaust back pressure as a clean Diesel Particulate Filter (DPF) is loaded is caused by filling of the filter pores. It is of significant advantage to engine operation to minimise deposition of particles within the walls prior to cake formation in order to mitigate the pressure drop penalty. Understanding of the pore bridging process is immensely aided by visualisation with scanning electron microscopy (SEM), which offers sufficiently high resolution to capture images of particulate deposit microstructure. The development of a monitoring technique and a study of filtration in cordierite and silicon carbide (SiC) pores were reported at last year's conference [1].

The nature of pore bridging is best characterised by a locally defined interception parameter, R, which is the ratio of particle to pore size. Particle size is interpreted as the electrical mobility diameter up to 1 μm; the physical diameter estimated using the SEM images more appropriate for the super-micron agglomerates. Images of SiC and cordierite pores with diameters less than 10 μm showed that they were all bridged at a PM mass load between 0.025 and 0.05 g/l in a seemingly abrupt manner facilitated by deposition of aggregates from right side of the accumulation mode (not the larger agglomerates), for which R would approach 0.1. In contrast, the bridging of pores with diameters in the range 30-50 μm was a gradual process achieved between 0.2 and 0.4 g/l that approximated shrinking pore behaviour; in these cases, $R < 0.02$.

Successive stages of SiC wall loading with diesel particles of two different size distributions were subsequently compared. The first aerosol was sampled from the exhaust of the Cambustion Diesel Particulate Generator (DPG) and the second from an Iveco medium-duty diesel (MDD) engine via a catalytic stripper; the modal electrical mobility diameters were 120 nm and 60 nm respectively.

While initial filtration efficiency in the SiC wall was higher with the smaller engine aerosol, the transition from deep-bed to cake filtration occurred at a higher pressure drop and SEM images show a greater amount of particulate matter from the smaller aerosol was deposited deep within the walls (see Figure 1). Smaller particles appear to deposit uniformly along the necks of pores giving the appearance of gradually shrinking pores. It was found that particles of several hundred nm contribute to the growth of dendrites that extend over pores up to 20 μm in diameter, which is particularly evident with the DPG aerosol. If particles several microns in size are present, these can cause sudden plugging of smaller pores which substantially reduces the pre-cake pressure drop penalty. A threshold value of $R = 0.05$ was estimated for the transition between shrinking pore behaviour and the dominant action of dendrites.

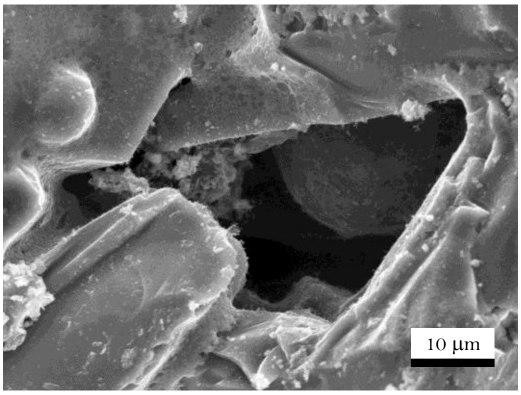

▲ Engine exhaust PM load = **0.05** g/l

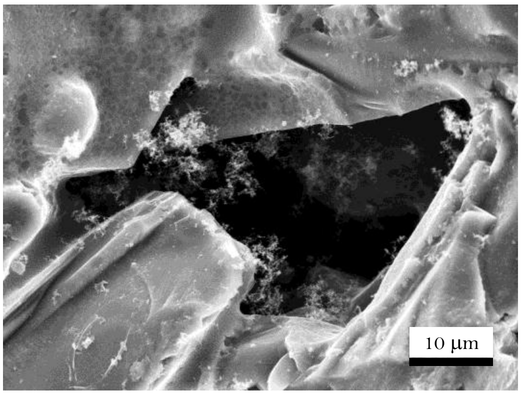

▲ DPG exhaust PM load = **0.05** g/l

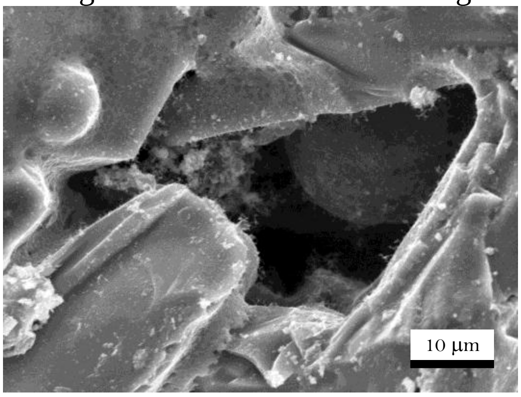

▲ Engine exhaust PM load = **0.1** g/l

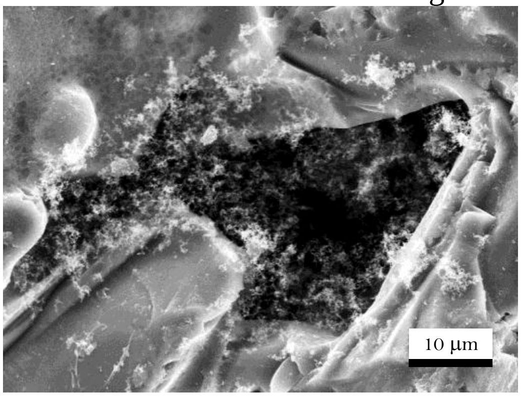

▲ DPG exhaust PM load = **0.1** g/l

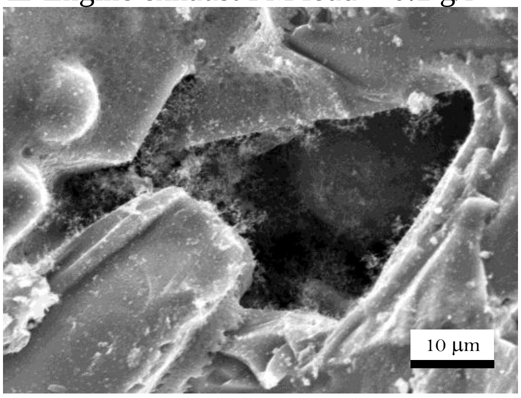

▲ Engine exhaust PM load = **0.2** g/l

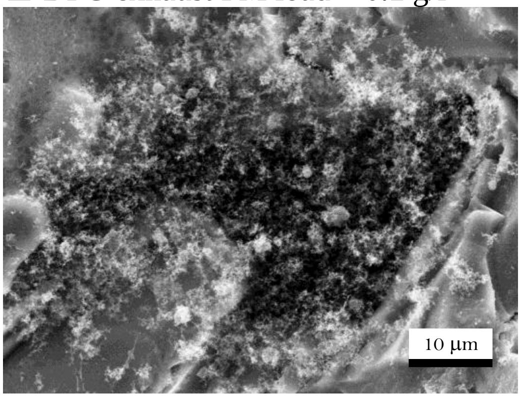

▲ DPG exhaust PM load = **0.2** g/l

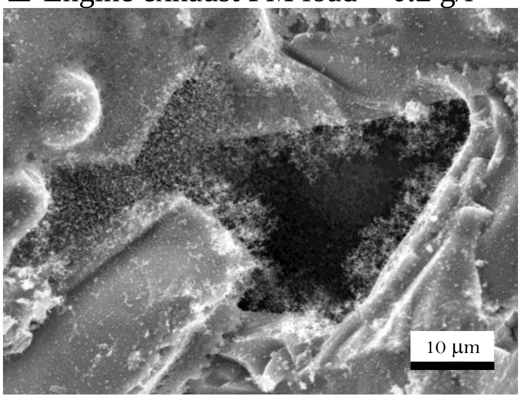

▲ Engine exhaust PM load = **0.4** g/l

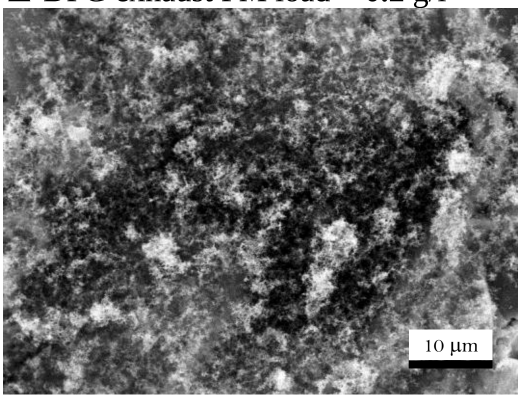

▲ DPG exhaust PM load = **0.4** g/l

Figure 1: Successive SEM images of the same SiC pore loaded at a clean pore velocity of 5 cm/s compared side-by-side at the same full-scale DPF mass loading with PM sampled from a medium-duty diesel engine exhaust and from a Cambustion DPG.

In a subsequent study a custom filter wall was fabricated that consisted of nearly uniform circular micro-channels laser-drilled in tungsten – loading of this with the Iveco MDD engine aerosol provided the basis to develop a pressure drop model for pore bridging. These experiments confirmed that for R < 0.02 (a condition satisfied throughout, since the concentration of particles with mobility diameters larger than 300 nm was vanishingly small) confirmed that the 20 µm diameter channels are filled in a radial manner. There is little deposition beyond the entrance prior to bridging; particulate deposits at the rim of each channel grow as dendrites to lengths of several microns and then merge with neighbouring dendrites, leading to a nearly circular open flow area that contracts almost uniformly as loading continues. Viewed at a 45° angle to the plane of the disc, the complete particulate cake, once established, is torus-shaped and begins to grow out of the channel as a dome (see Figure 2).

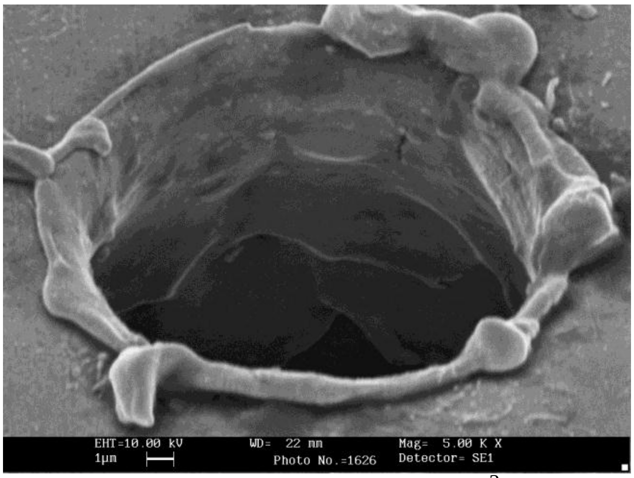

▲ Engine exhaust PM load = **0** mg/m^2

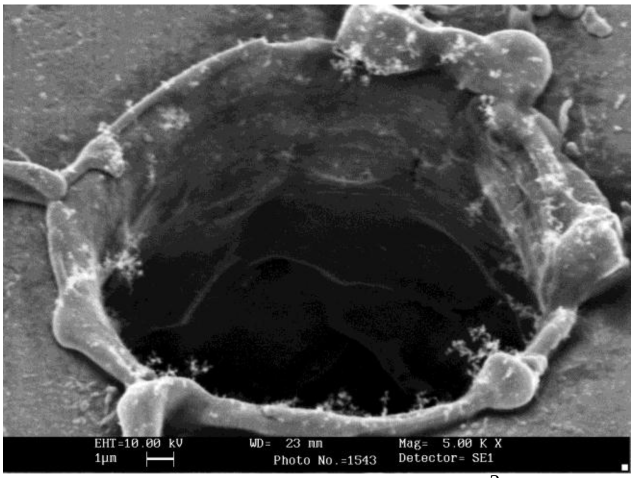

▲ Engine exhaust PM load = **8** mg/m^2

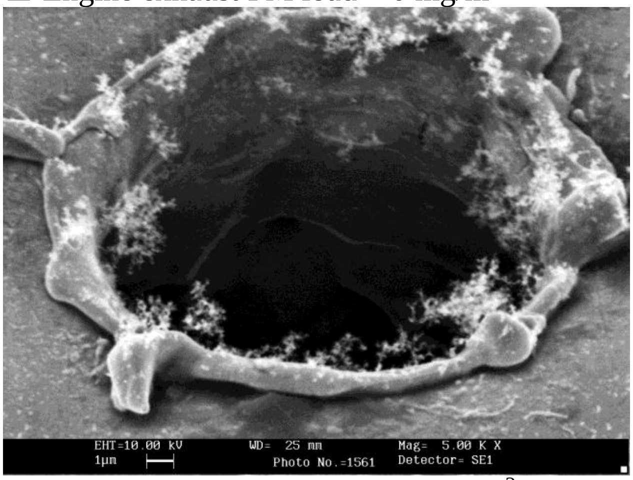

▲ Engine exhaust PM load = **16** mg/m^2

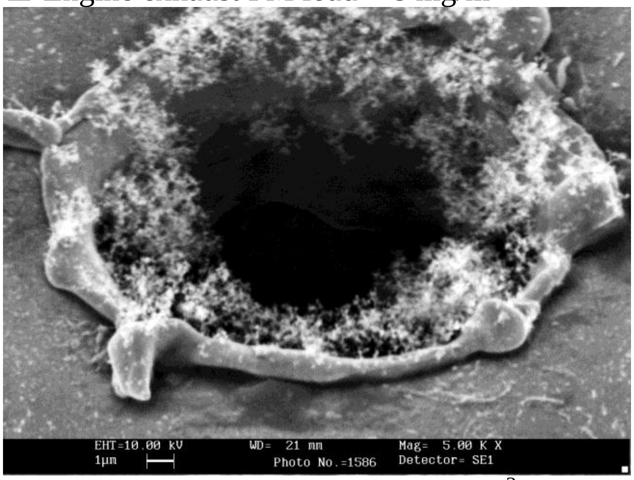

▲ Engine exhaust PM load = **32** mg/m^2

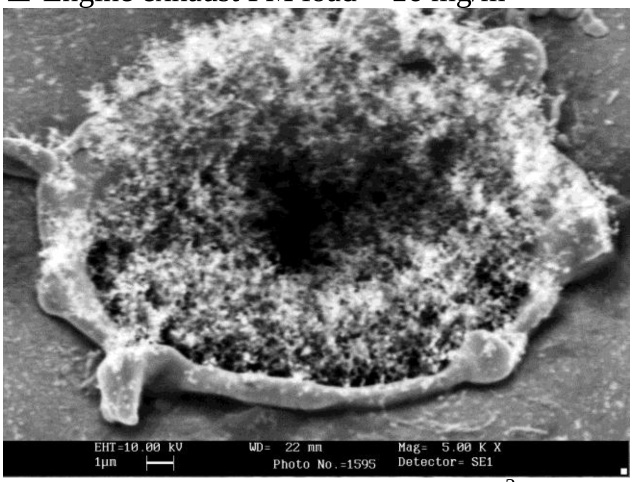

▲ Engine exhaust PM load = **64** mg/m^2

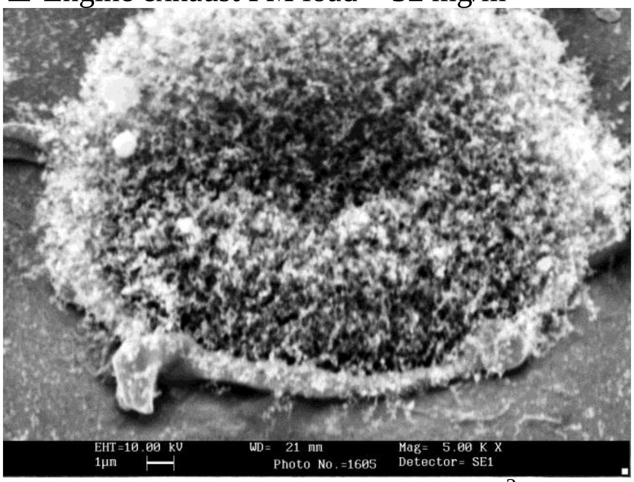

▲ Engine exhaust PM load = **96** mg/m^2

Figure 2: SEM images of the same micro-channel (20 µm entry diameter) for successive stages of PM loading of a laser-drilled tungsten disc at a flow velocity of 10 cm/s at the clean channel entrance.

Partitioning of the flow between the rim deposits and central open area was estimated at successive stages of loading using a simple model based on a parallel electric circuit analogy. This led to a description of the evolving pressure drop across the channel. The dimensions of the particulate cake at successive stages were measured using the SEM images and a fit of the model to the experimental data yielded values for the permeability of the particulate deposits. The provisional values obtained indicate that the permeability decreases from 3×10^{-13} m^2 to 8×10^{-14} m^2 as the particulate layer closes up; a possible cause of this reduction is deposition of incident particles deep within the cake as well as on its surface.

Reference:

[1] Payne, S., and Collings, N., "Visualisation and Monitoring of Diesel Particulate Filtration": Poster presented at the 15th ETH-Conference on Combustion-Generated Nanoparticles, Zürich 2011

Study of Diesel Particulate Bridging Behaviour with SEM

Simon Payne and Nick Collings
University of Cambridge

16th ETH Conference on Combustion Generated Nanoparticles
Zürich, 24-27 June 2012

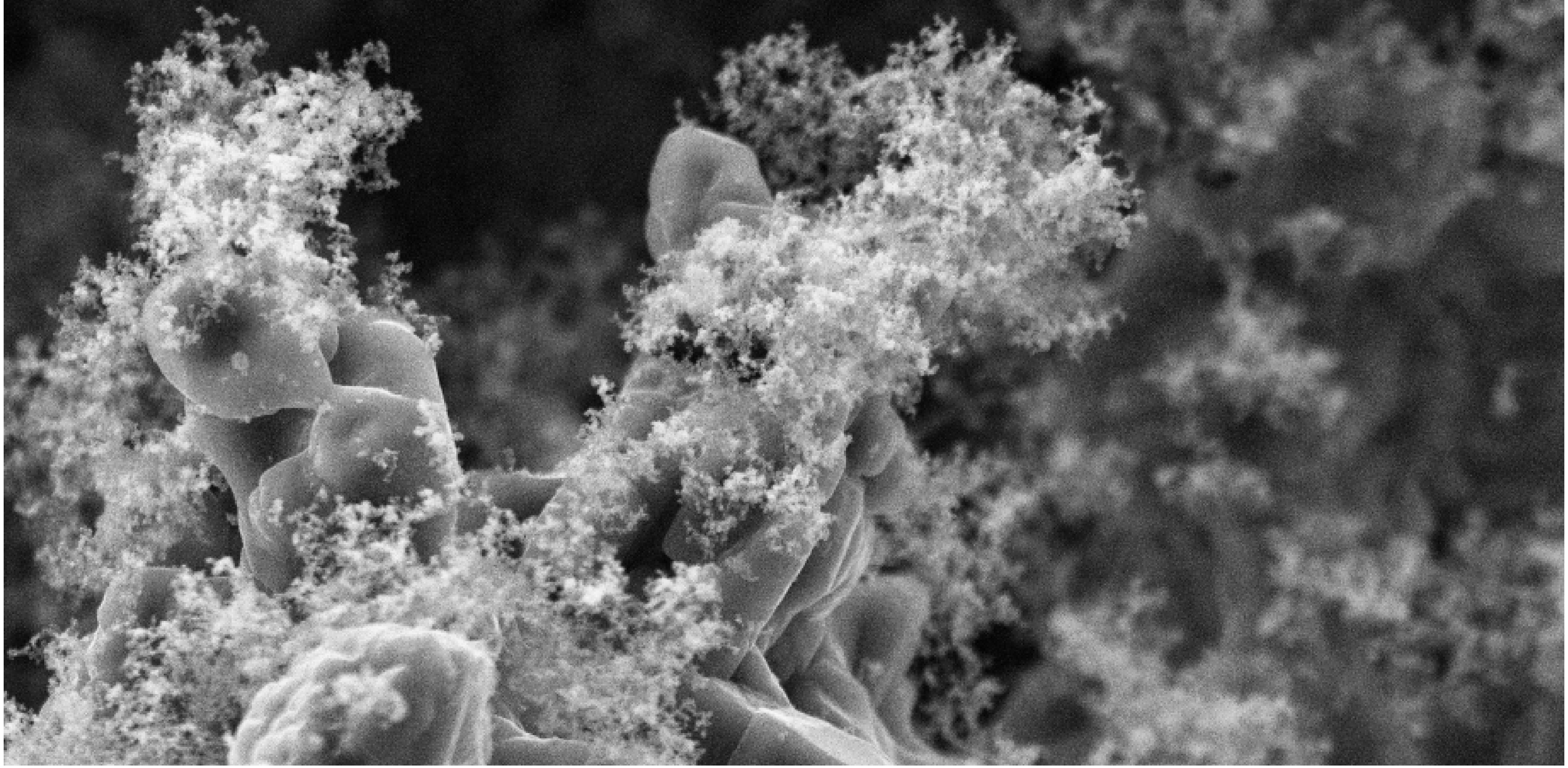

Outline

- Development of visualisation and monitoring technique
  - Mapping of pores with SEM
  - Characterisation of nature of pore bridging with interception parameter
- Monitoring of filtration of diesel exhaust particulate matter (PM) from two different size distributions in the same SiC filter pores
- Monitoring of deposition of diesel exhaust PM in circular micro-channels laser-drilled in tungsten
  - Development of pressure drop model for particulate bridging

Diesel Particle Filter (DPF): wall-flow honeycomb design

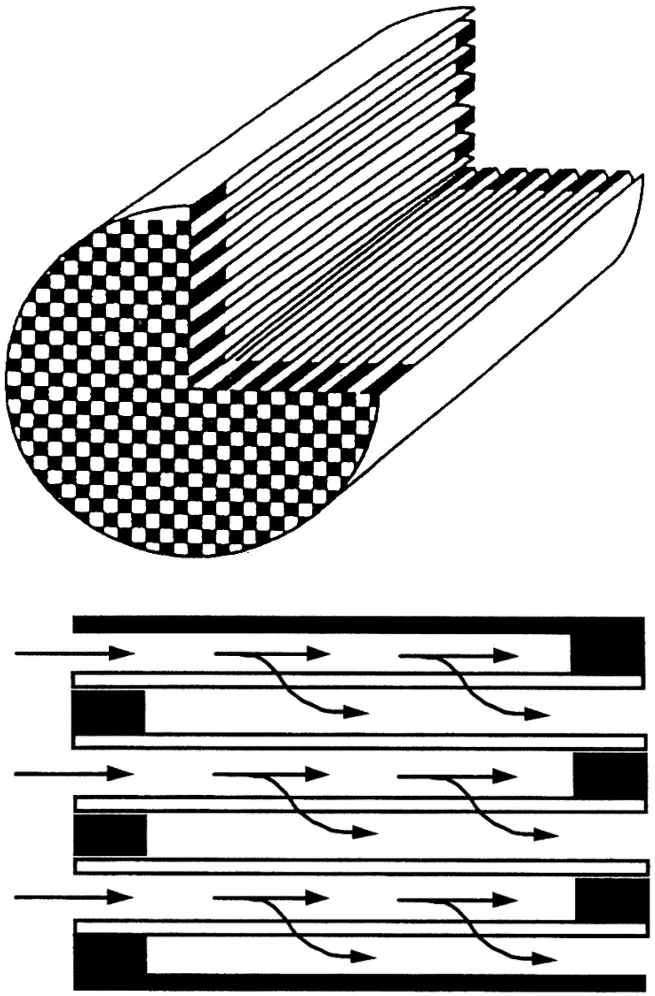

Murati et al. *"Catalytic Air Pollution Control"* 2002

◄ Isometric projection with cut-away section showing alternately plugged channels; bottom left: axial cross-section showing aerosol flowlines

▼ SEM image of sliced radial cross-section of loaded SiC DPF (JM Autocatalyst Technology Centre)

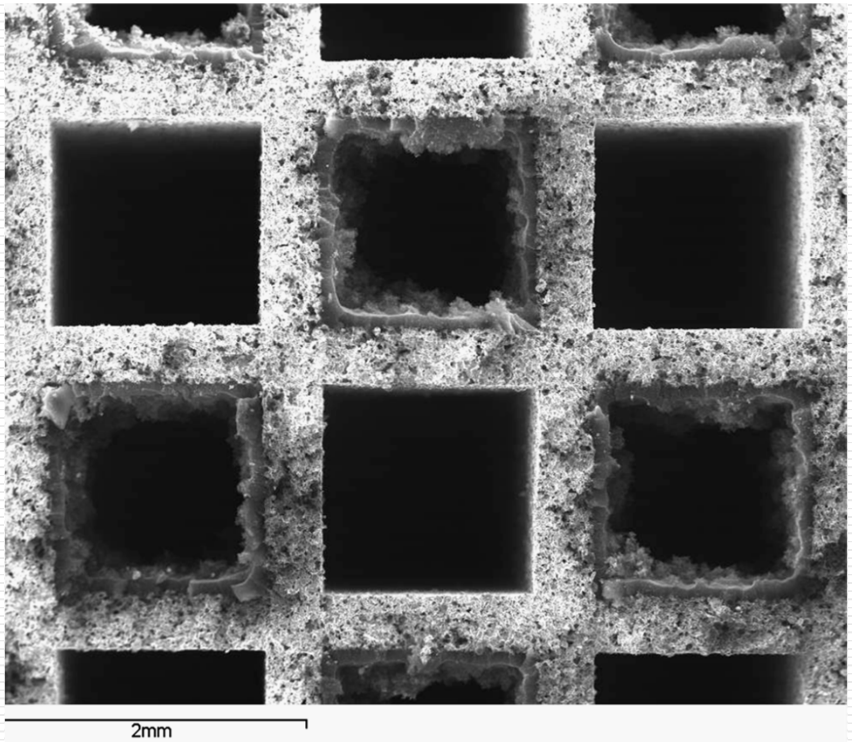

Visualisation of pore-filling process with SEM

- SEM provides sufficiently high resolution to capture images of individual aggregates and particulate deposit microstructure

- ΔP and filtration efficiency monitored during particulate loading of wall samples under ambient conditions with cessation of loading at regular intervals for visualisation (Leica Stereoscan 440)

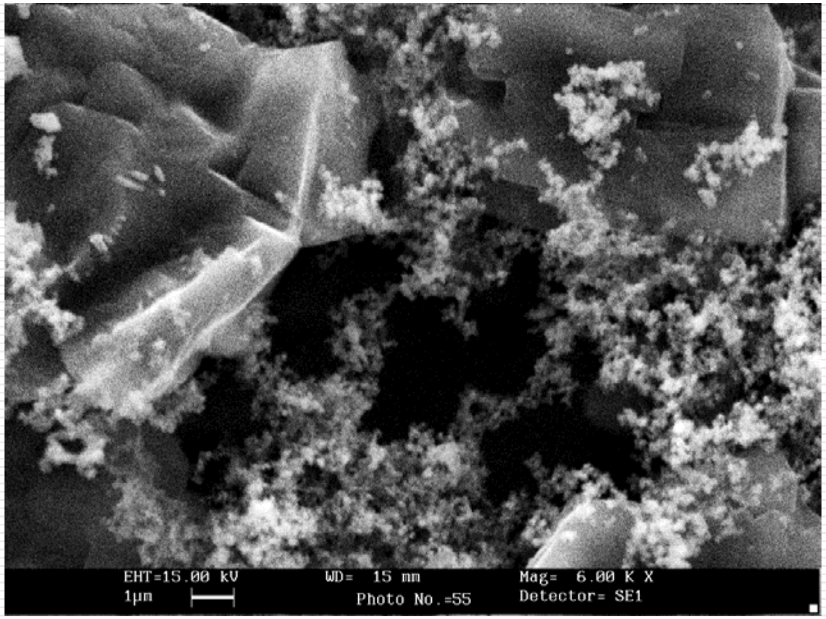

◄ Evidence of chains of deposits extending across pores motivates study of particulate bridging dynamics

DPF wall parameters: recap of ETHZ 2011 poster*

	Material	Wall thickness (µm)	Porosity (%)	Mean pore diameter (µm)
Porous wall A	Cordierite	305	48	12
Porous wall B	Silicon carbide	305	42	14

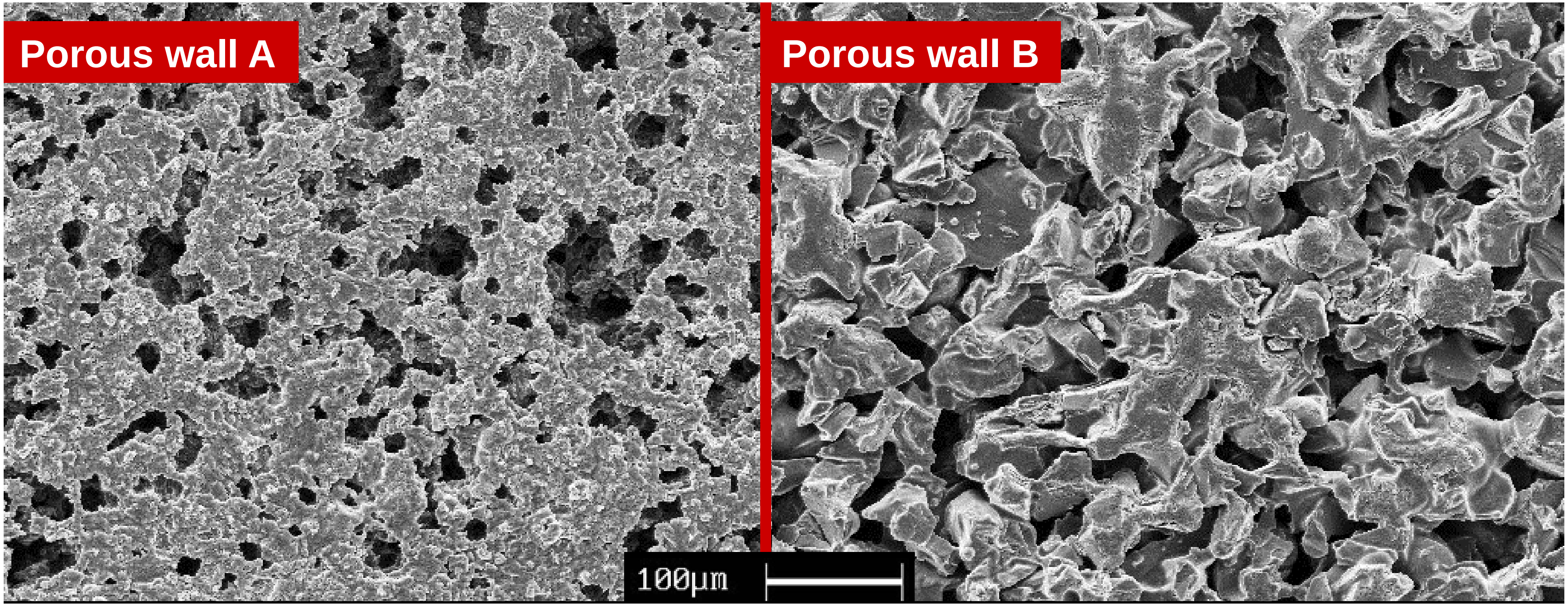

8 pores selected for loading analysis by SEM:

Pore diameter (µm)	<10	10-20	20-30	>30
No. of pores	2	3	2	1

** Payne, S., and Collings, N., "Visualisation and Monitoring of Diesel Particle Filtration": 15th ETH-Conference on Combustion-Generated Nanoparticles, Zürich 2011*

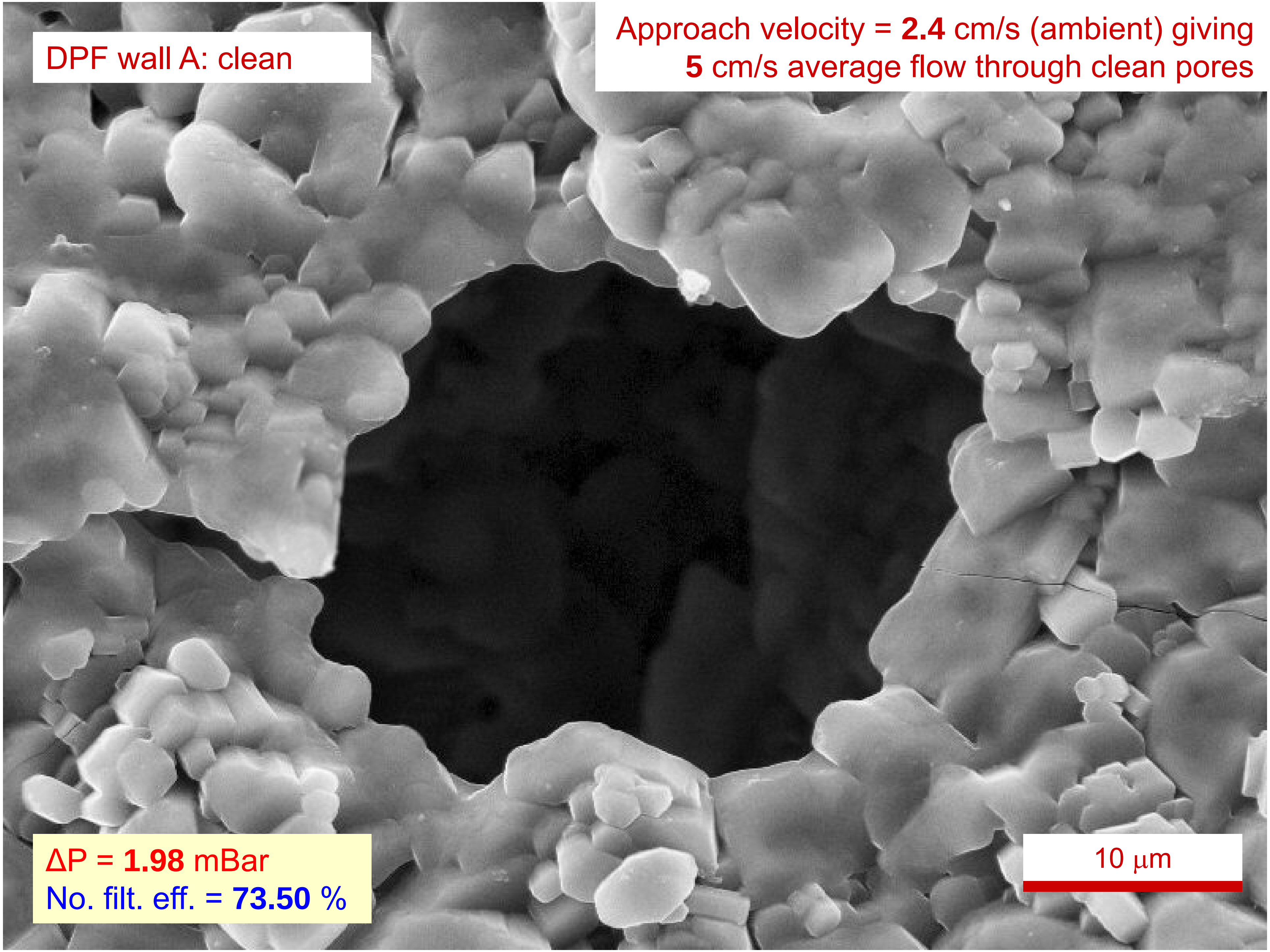
DPF wall A: clean
Approach velocity = **2.4** cm/s (ambient) giving
5 cm/s average flow through clean pores
ΔP = **1.98** mBar
No. filt. eff. = **73.50** %
10 µm

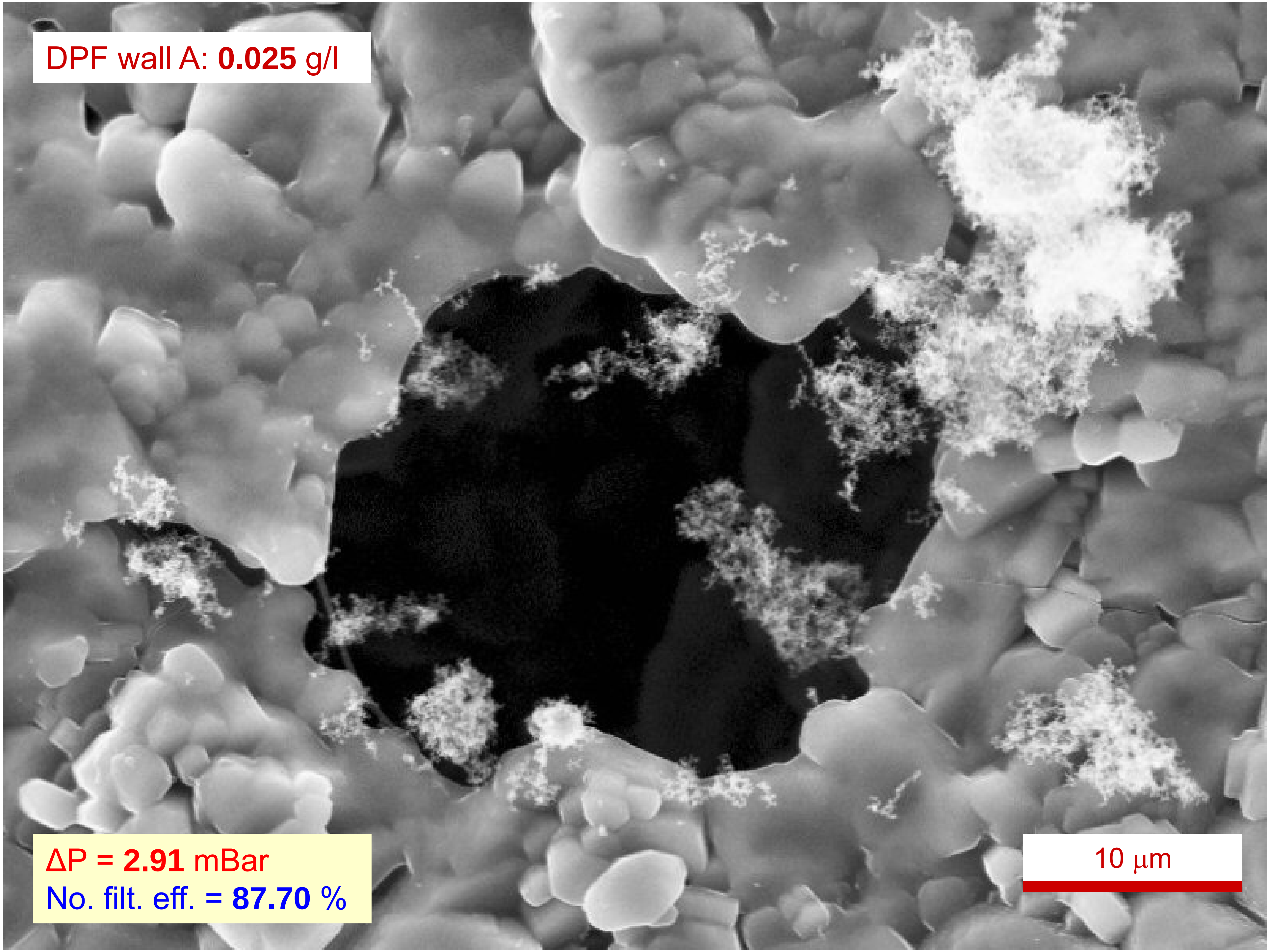
DPF wall A: 0.025 g/l
ΔP = 2.91 mBar
No. filt. eff. = 87.70 %
10 μm

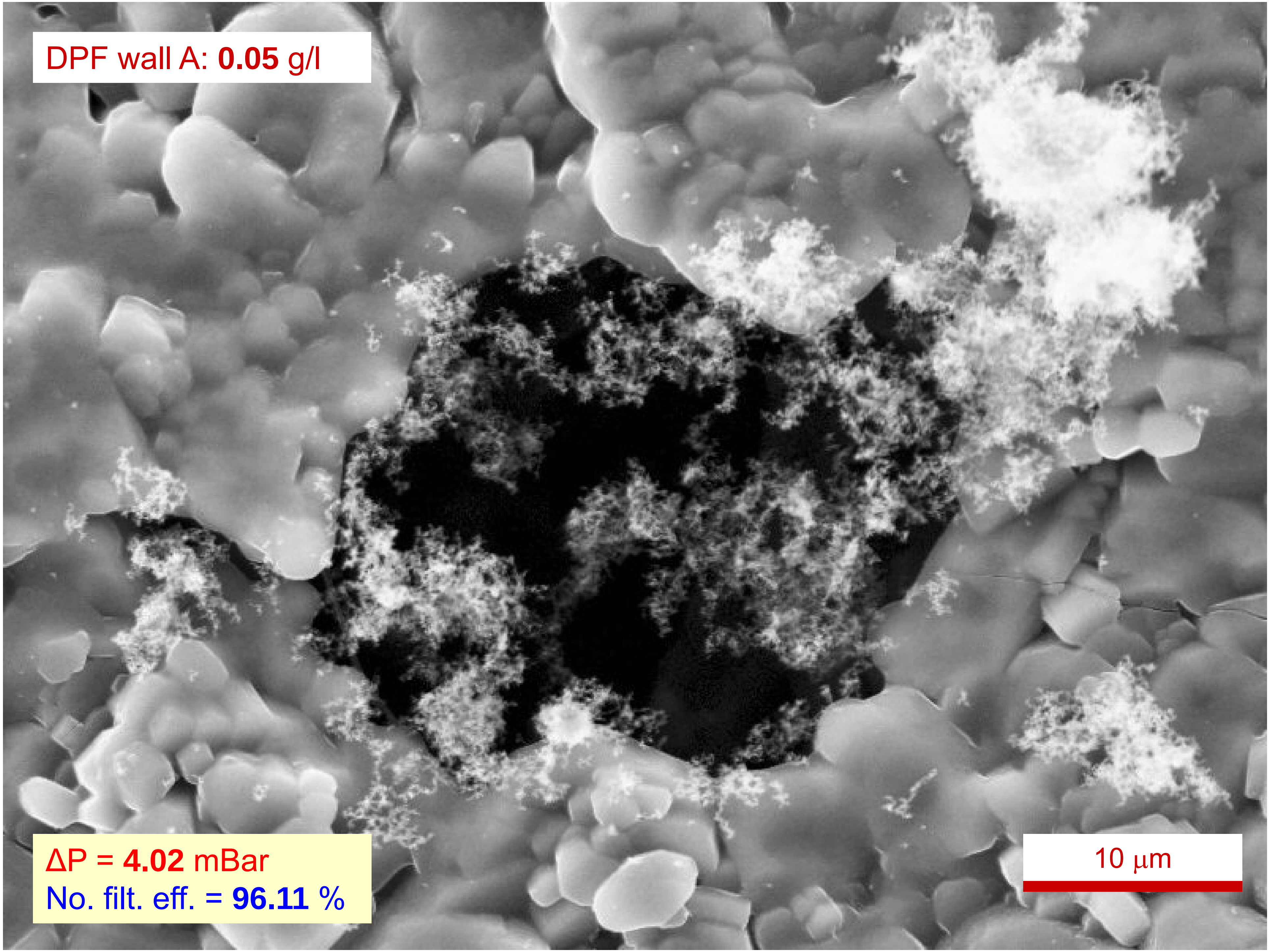
DPF wall A: **0.05** g/l
ΔP = **4.02** mBar
No. filt. eff. = **96.11** %
10 μm

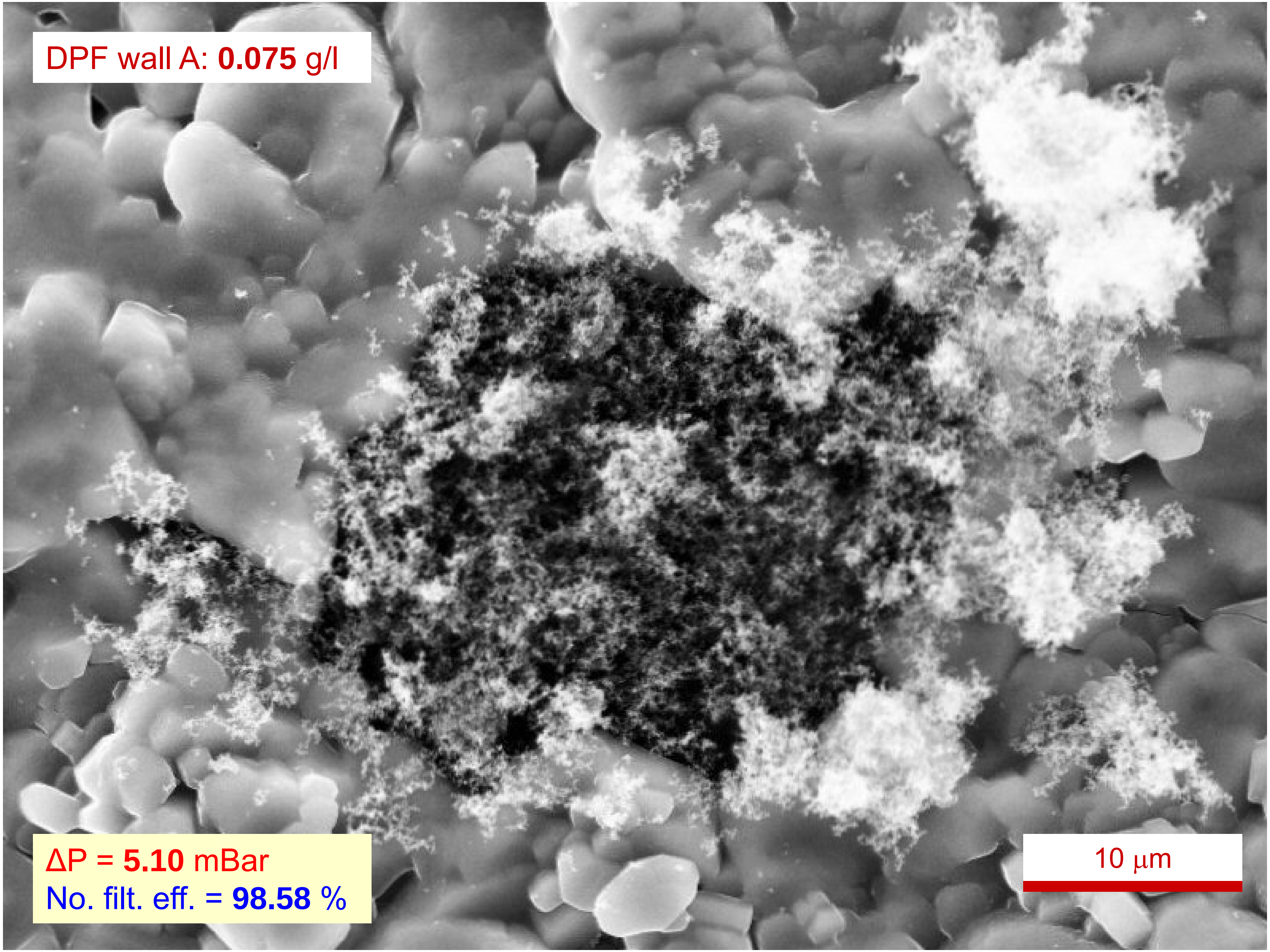
DPF wall A: **0.075** g/l
ΔP = **5.10** mBar
No. filt. eff. = **98.58** %
10 μm

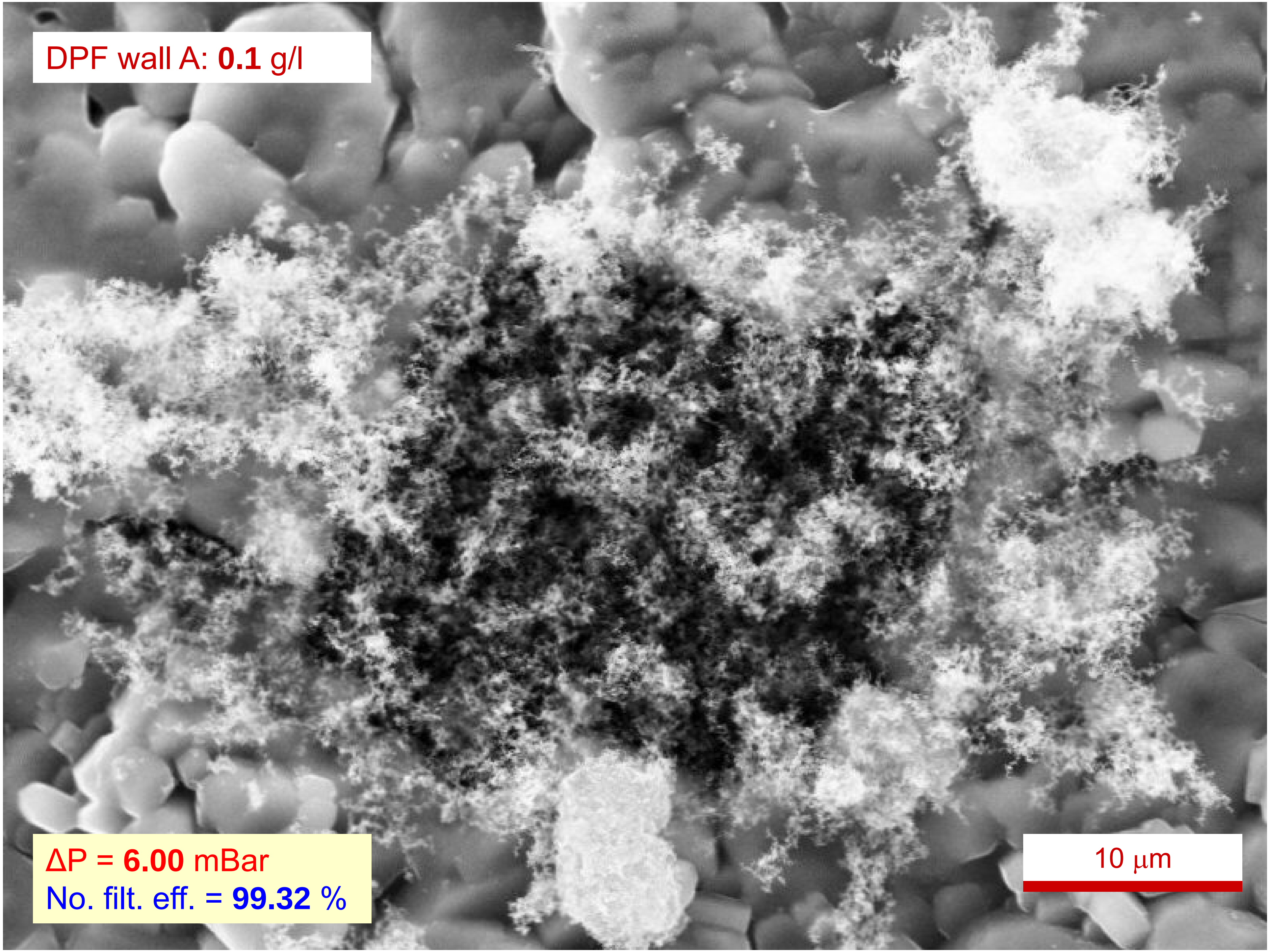
DPF wall A: **0.1** g/l
ΔP = **6.00** mBar
No. filt. eff. = **99.32** %
10 μm

Interception parameter, *R* (ratio of particle to pore size)

- Images of SiC and cordierite pores with diameters less than 10 μm showed that they were all bridged at a PM mass load between 0.025 and 0.05 g/l in a seemingly abrupt manner facilitated by deposition of aggregates from the right side of the accumulation mode (not the larger agglomerates), for which ***R* ~ 0.1**

- In contrast, the bridging of pores with diameters in the range 30-50 μm was a gradual process achieved between 0.2 and 0.4 g/l that approximated shrinking pore behaviour; in these cases, ***R* < 0.02**

- Threshold value of *R* exists between these two values:
  Shrinking pore behaviour ↔ Rapid bridging with dendrites

- More detailed observations possible by comparing filtration in same pores with two different particle size distributions

Cambustion Diesel Particulate Generator (DPG)

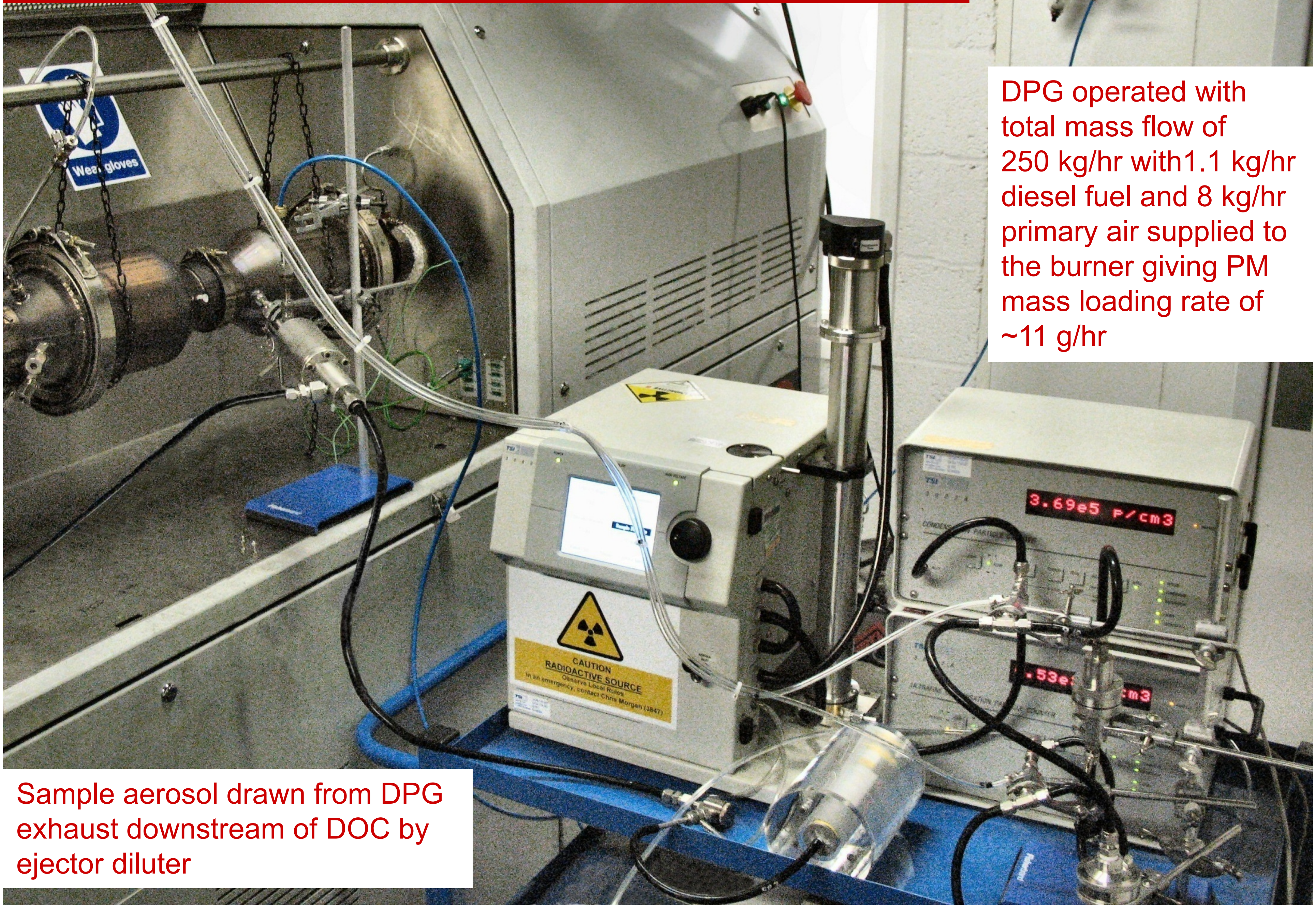

DPG operated with total mass flow of 250 kg/hr with1.1 kg/hr diesel fuel and 8 kg/hr primary air supplied to the burner giving PM mass loading rate of ~11 g/hr

Sample aerosol drawn from DPG exhaust downstream of DOC by ejector diluter

Iveco medium-duty diesel (MDD) engine

- 3.9 litre 4 cylinder naturally-aspirated 4 stroke diesel engine
- Run at 6.36 kW load and 1540 rpm by industrial heating furnace
- Sample aerosol drawn from exhaust upstream of Johnson Matthey CRT by ejector diluter

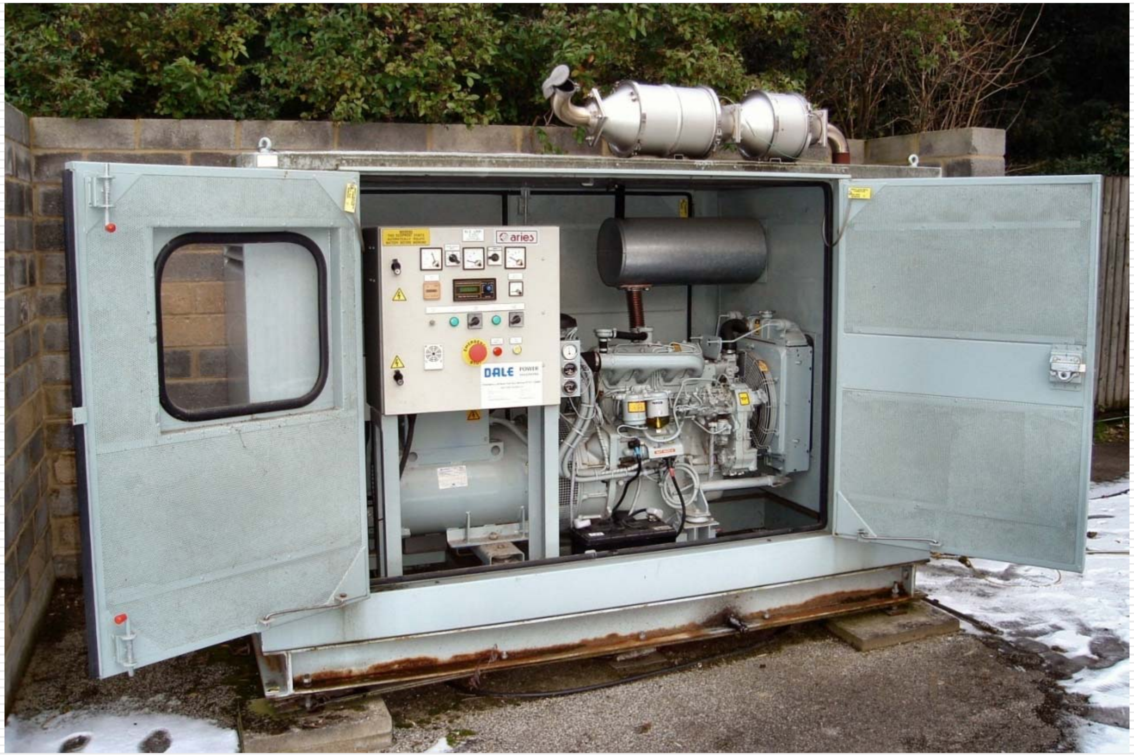

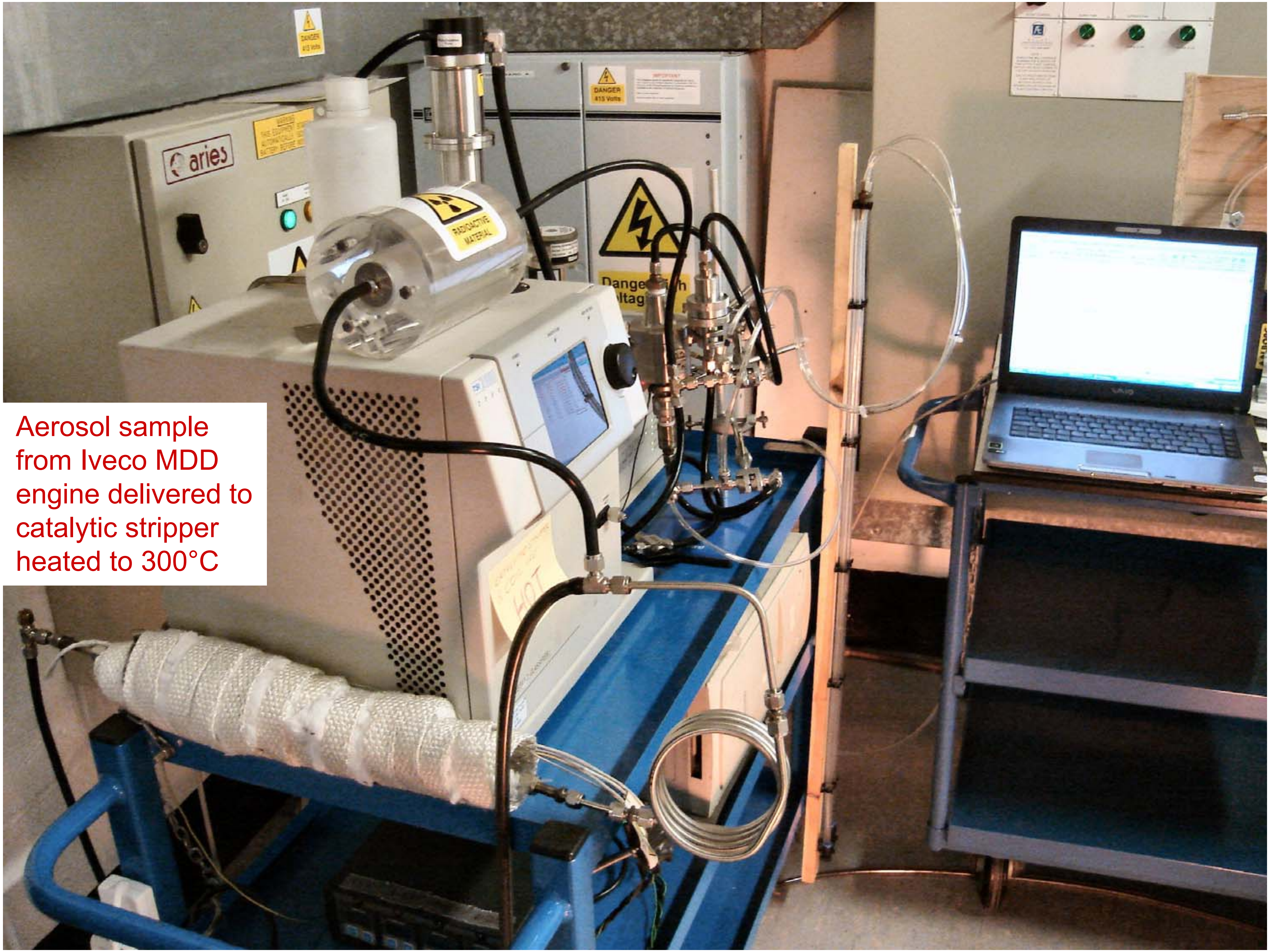

Aerosol sample from Iveco MDD engine delivered to catalytic stripper heated to 300°C

Size distributions of diesel aerosols entering SiC filter wall

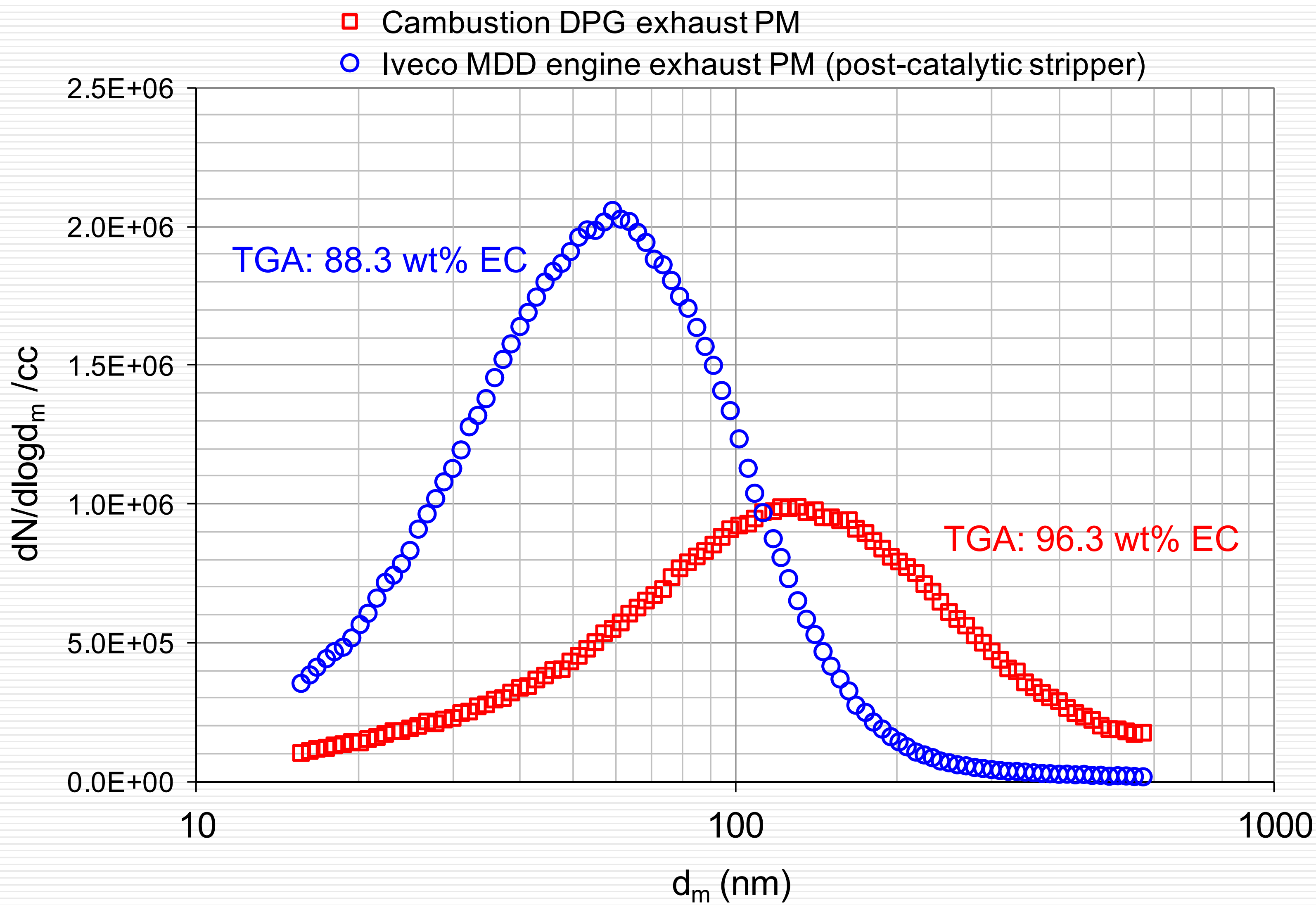

Schematic for SEM visualisation of DPF pore filling

For the **DPG** exhaust PM sample, typical no. concentration immediately upstream of wall sample was

8.5×10^5/cc = 3.12 mg/m^3

For the **MDD engine** exhaust PM sample:

9.0×10^6/cc = 1.19 mg/m^3

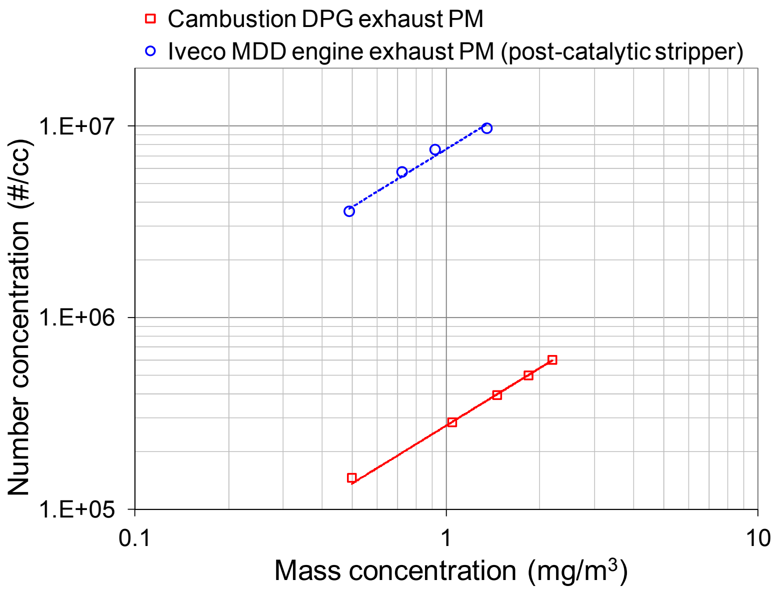

Filtration area of SEM sample is ~20mm^2 – use parallel line with filtration area of ~400mm^2 to allow total flow rate across both to be controlled in 0.5-1.5 lpm range

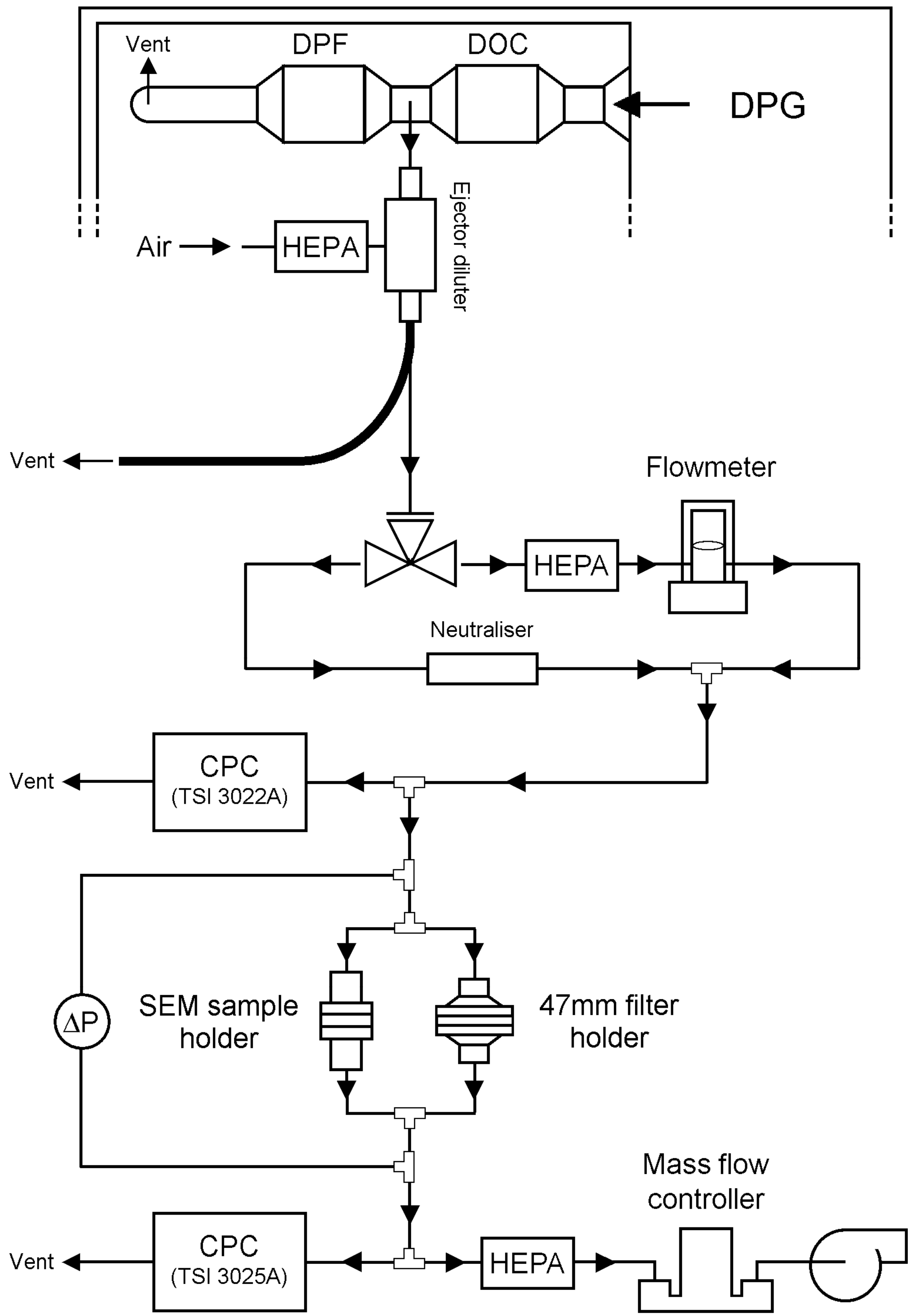

⇓ SEM sample holder and parallel filter wall

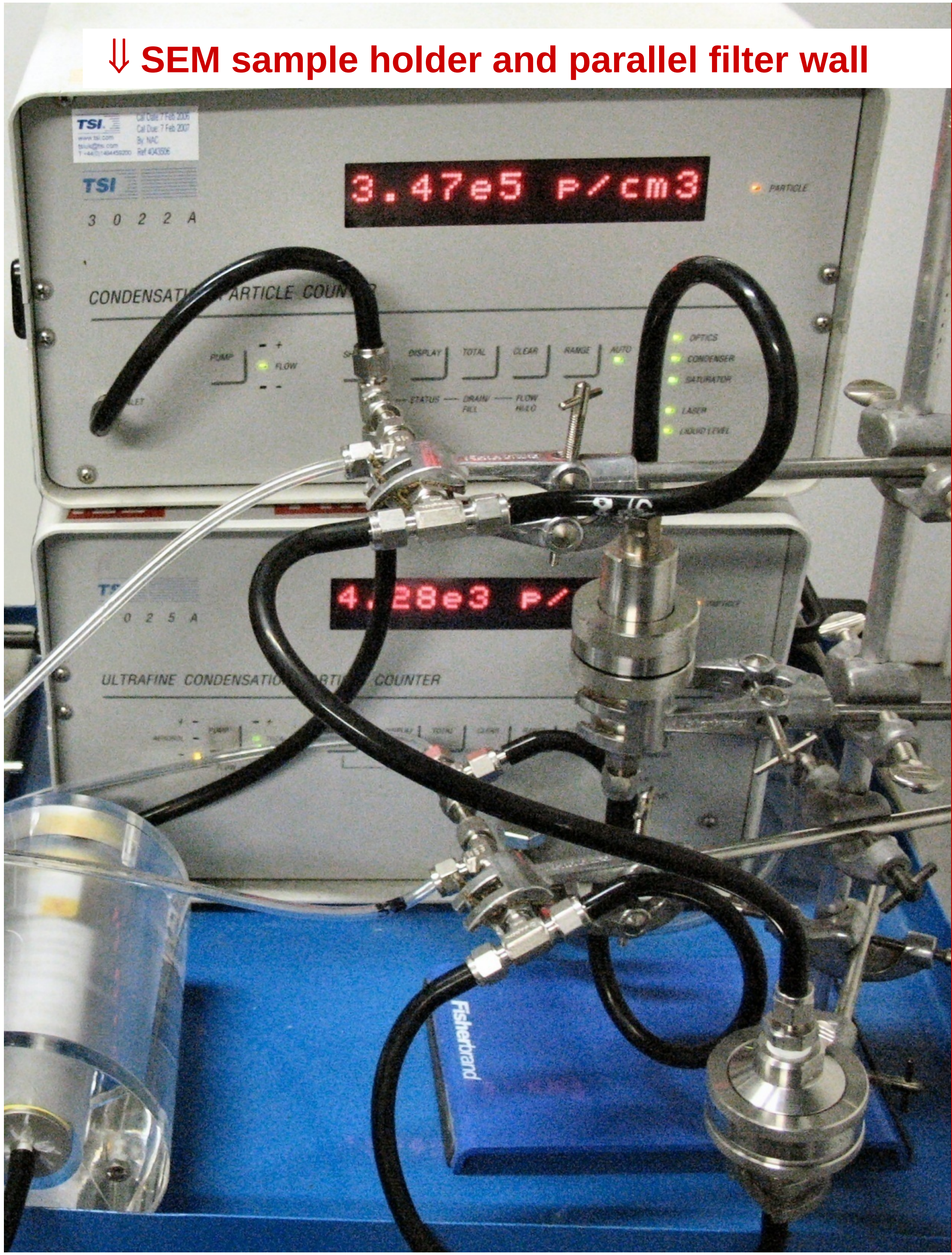

⇓ Samples mounted in SEM chamber

Pressure drop and filtration efficiency data for pore velocity of 5 cm/s (ambient)

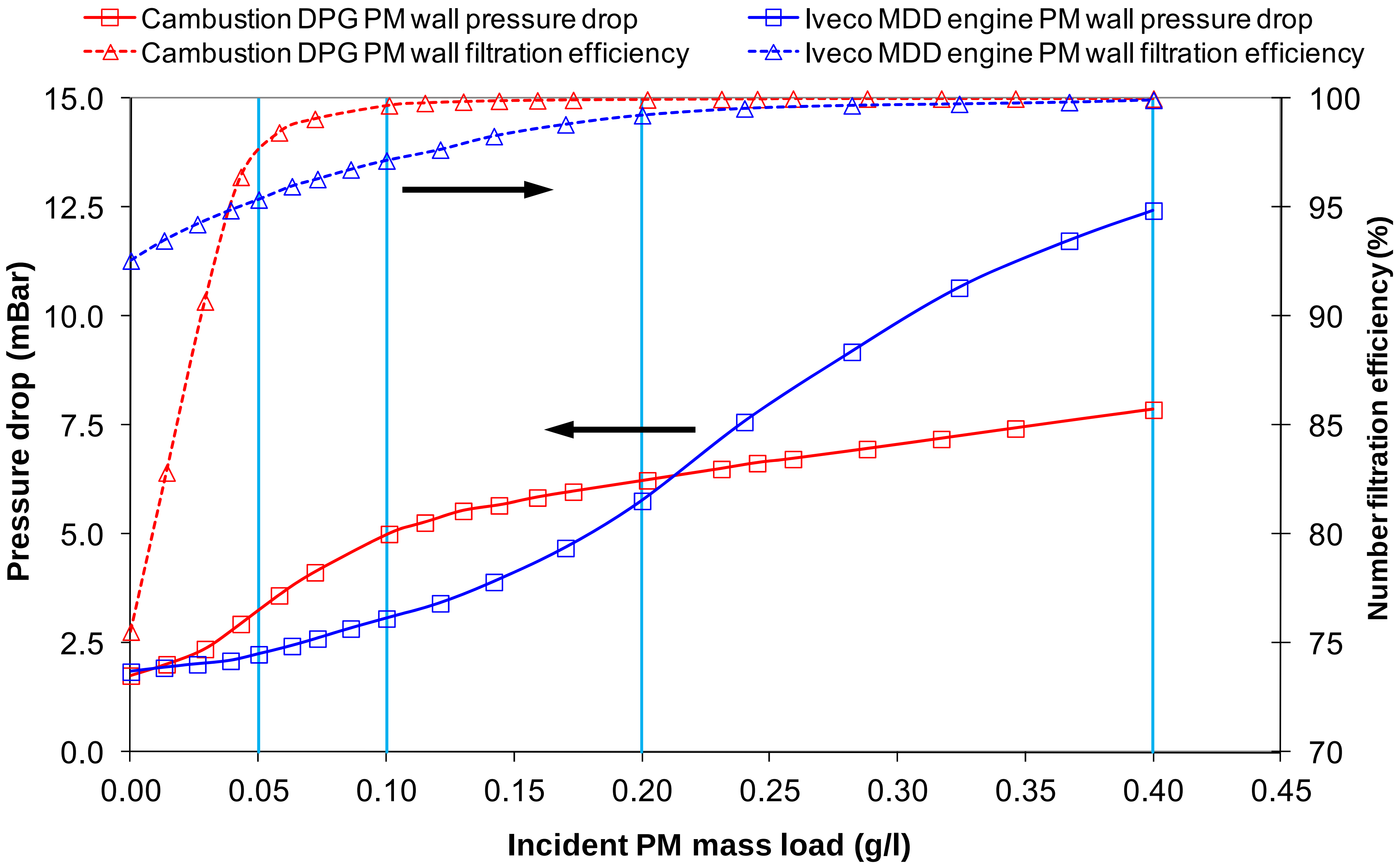

PM mass load given as grams per litre for the equivalent full-scale DPF (300 cpsi, ϕ5.66" by 6")
Loading paused at blue lines and wall sample mounted in SEM chamber

Pressure drop and filtration efficiency data for pore velocity of 5 cm/s (ambient)

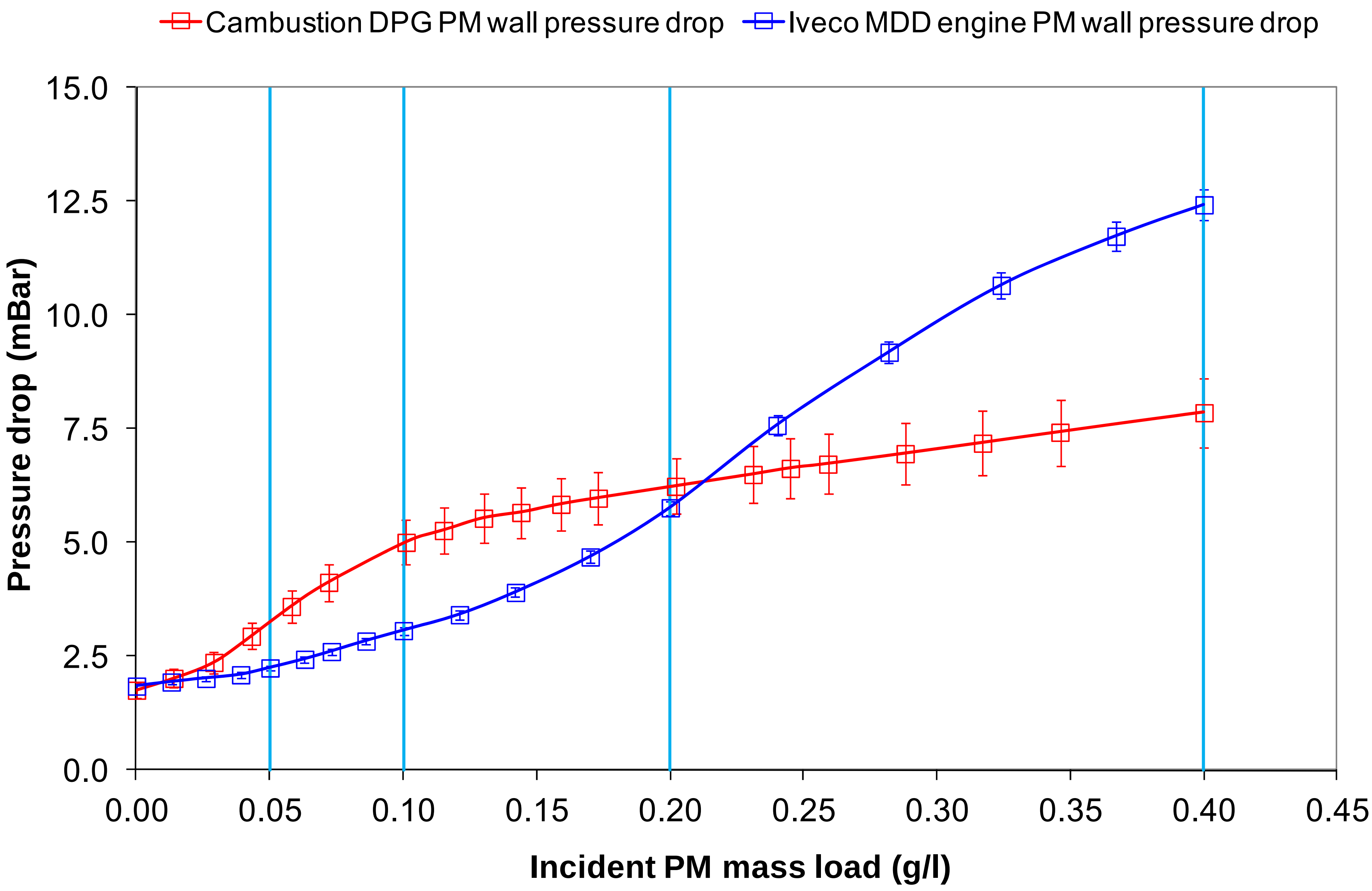

PM mass load given as grams per litre for the equivalent full-scale DPF (300 cpsi, ϕ5.66” by 6”)
Loading paused at blue lines and wall sample mounted in SEM chamber

Pressure drop and filtration efficiency data for pore velocity of 5 cm/s (ambient)

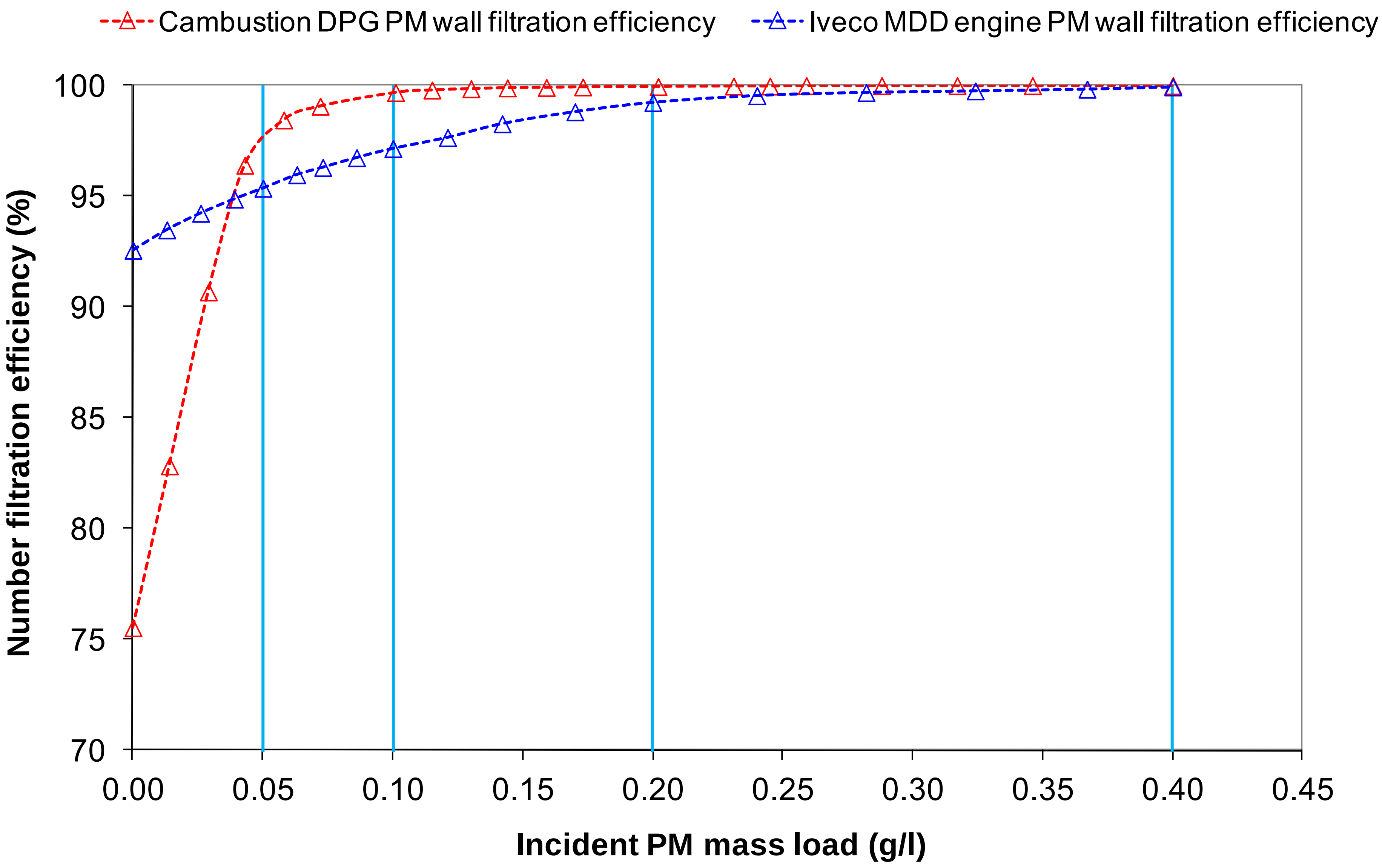

PM mass load given as grams per litre for the equivalent full-scale DPF (300 cpsi, ϕ5.66" by 6")
Loading paused at blue lines and wall sample mounted in SEM chamber

DPF wall B (silicon carbide): map of pores

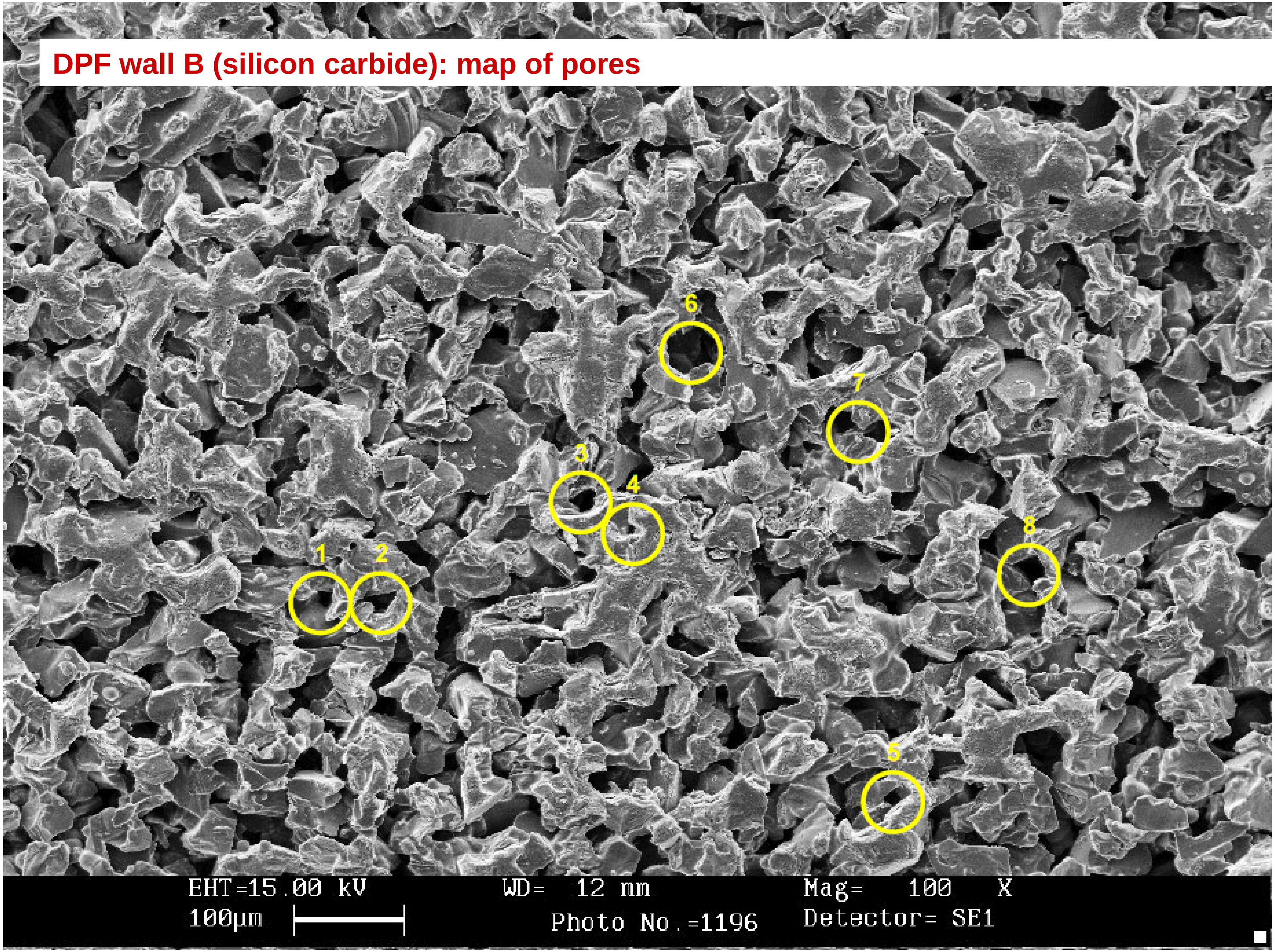

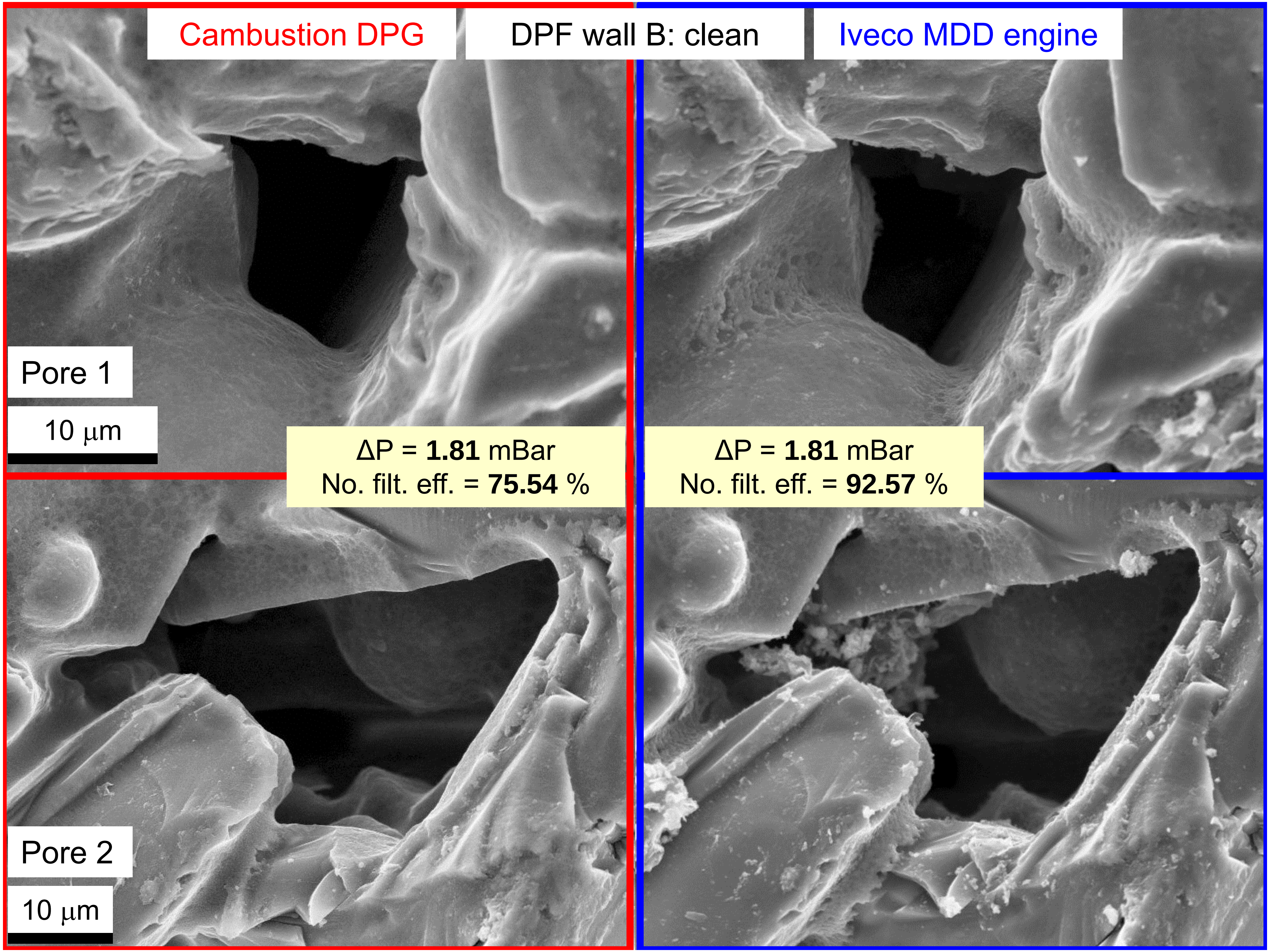
Cambustion DPG
DPF wall B: clean
Iveco MDD engine
Pore 1
10 μm
ΔP = 1.81 mBar
No. filt. eff. = 75.54 %
ΔP = 1.81 mBar
No. filt. eff. = 92.57 %
Pore 2
10 μm

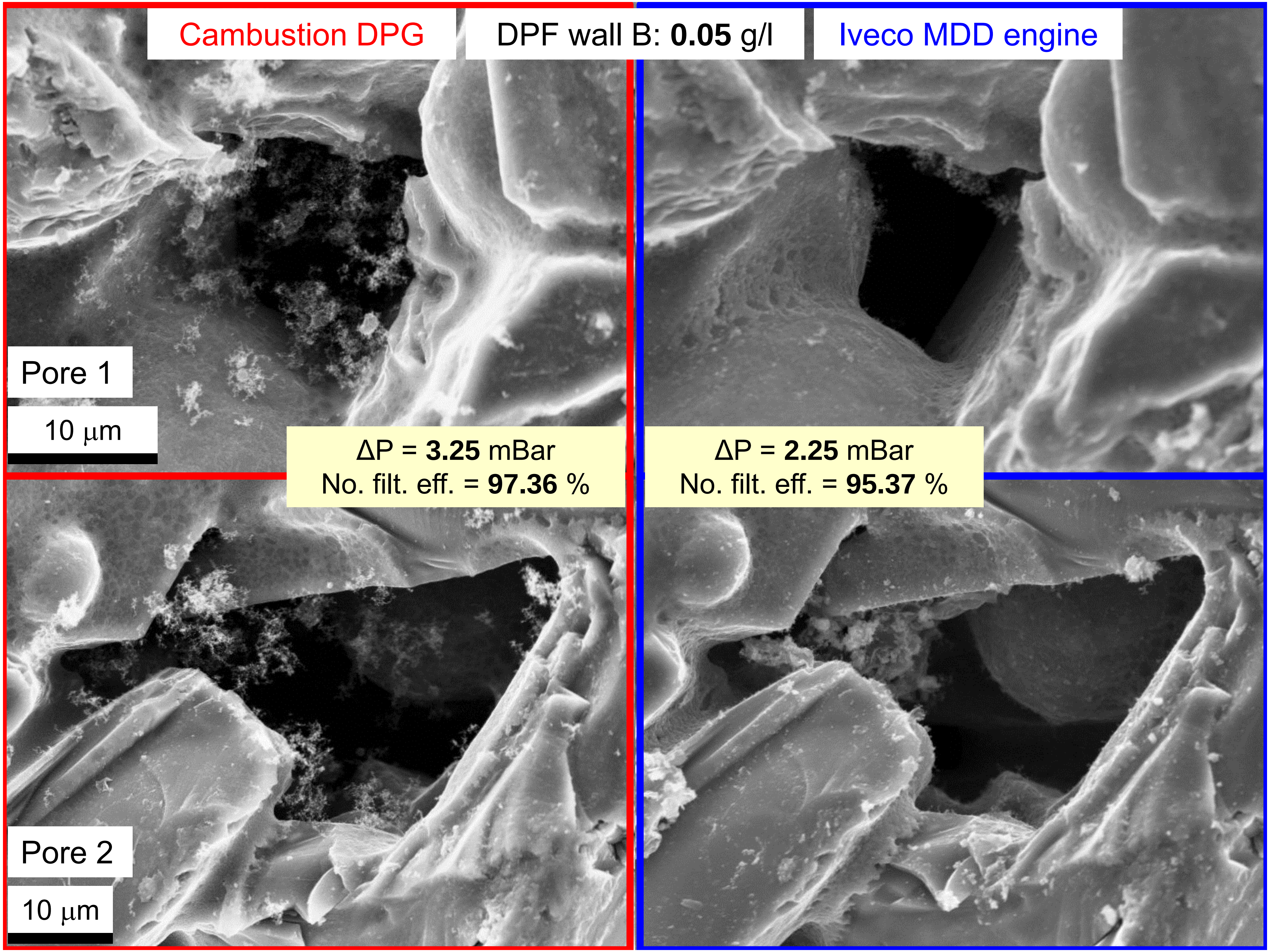

Cambustion DPG
DPF wall B: **0.05** g/l
Iveco MDD engine
Pore 1
10 µm
ΔP = **3.25** mBar
No. filt. eff. = **97.36** %
ΔP = **2.25** mBar
No. filt. eff. = **95.37** %
Pore 2
10 µm

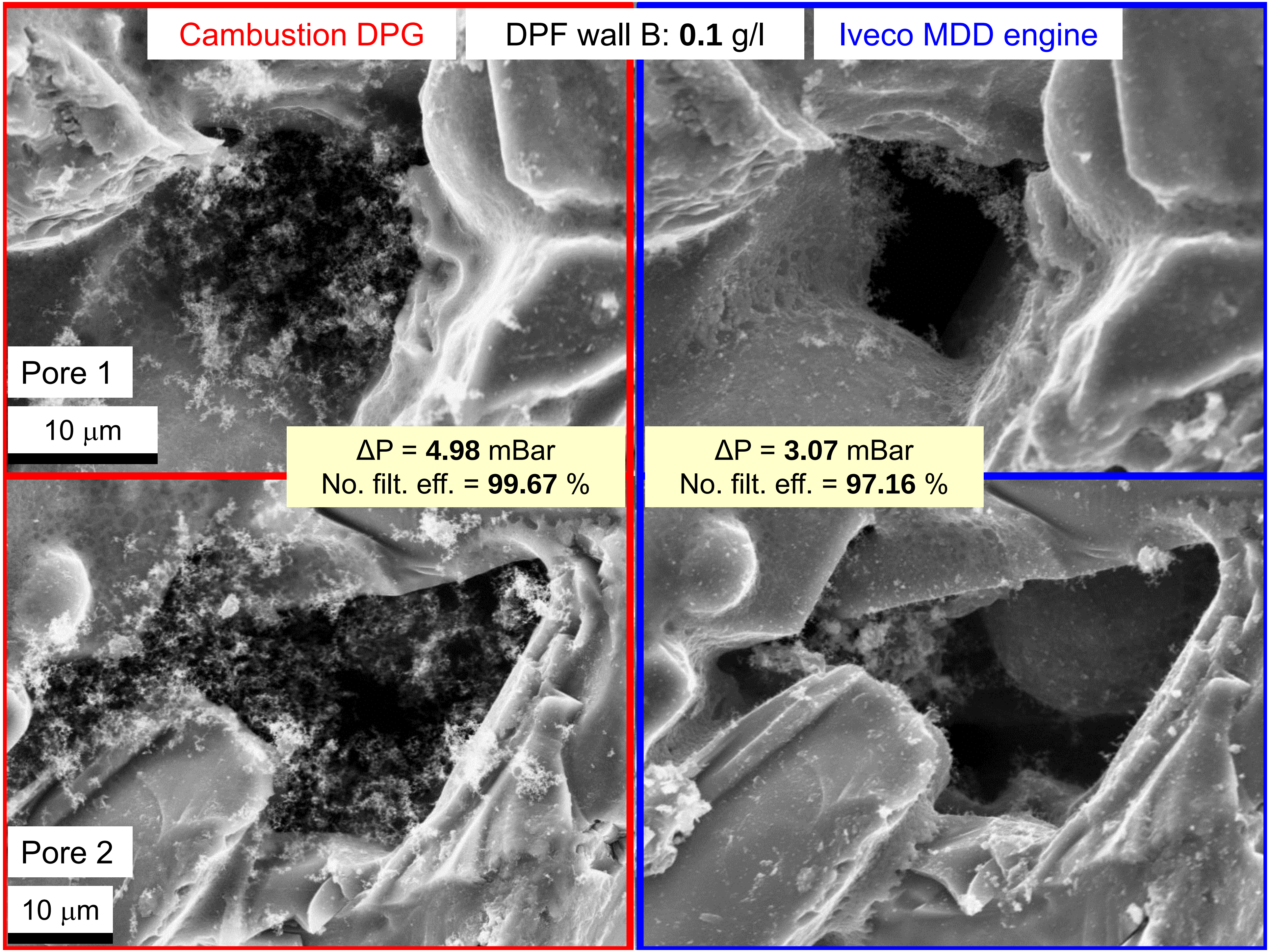
Cambustion DPG
DPF wall B: **0.1** g/l
Iveco MDD engine
Pore 1
10 μm
ΔP = **4.98** mBar
No. filt. eff. = **99.67** %
ΔP = **3.07** mBar
No. filt. eff. = **97.16** %
Pore 2
10 μm

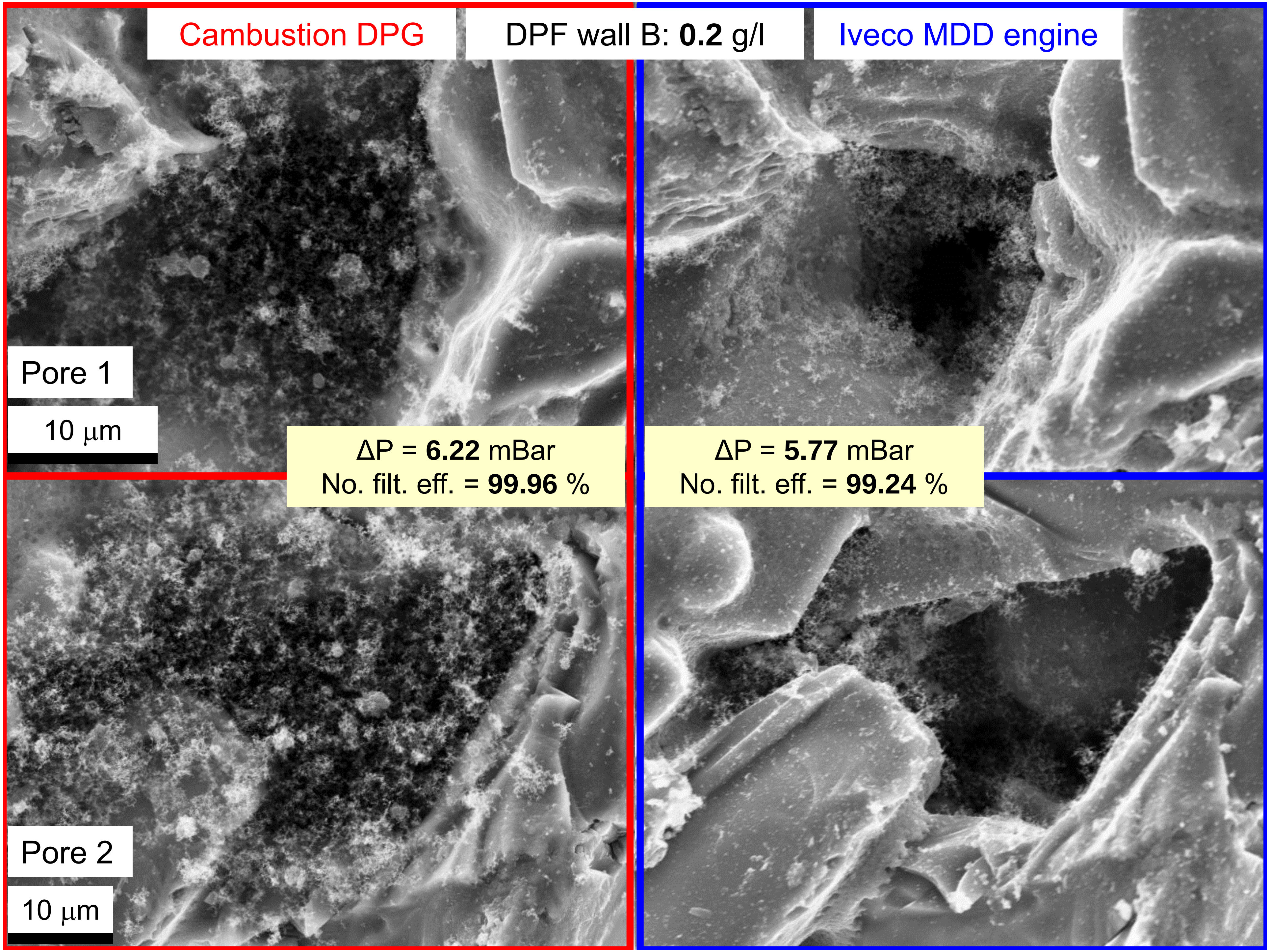
Cambustion DPG
DPF wall B: **0.2** g/l
Iveco MDD engine
Pore 1
10 µm
ΔP = **6.22** mBar
No. filt. eff. = **99.96** %
ΔP = **5.77** mBar
No. filt. eff. = **99.24** %
Pore 2
10 µm

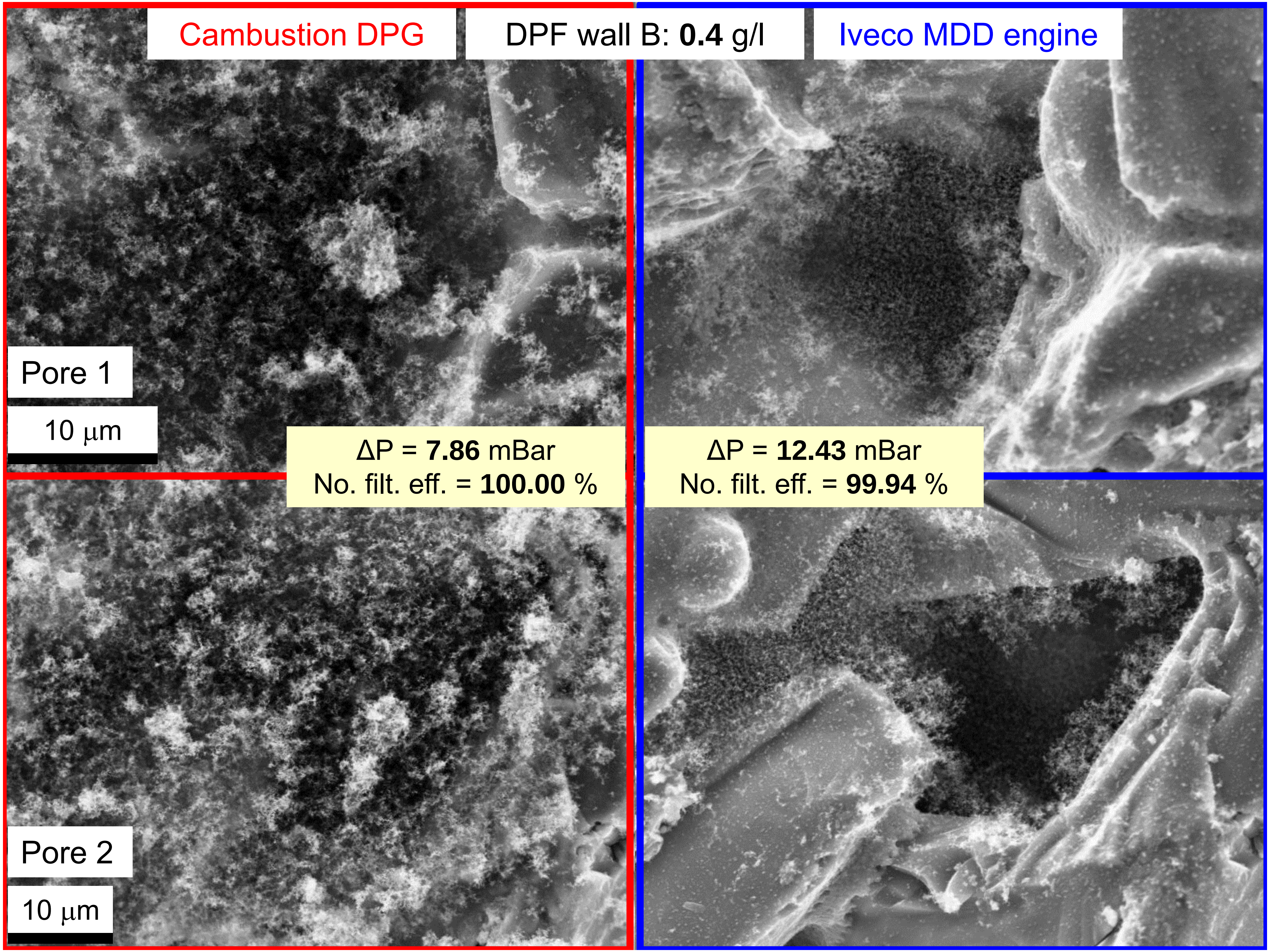
Cambustion DPG
DPF wall B: **0.4** g/l
Iveco MDD engine
Pore 1
10 μm
ΔP = **7.86** mBar
No. filt. eff. = **100.00** %
ΔP = **12.43** mBar
No. filt. eff. = **99.94** %
Pore 2
10 μm

Threshold value for *R*

- The smaller Iveco MDD engine exhaust aerosol confirms that the nature of particulate bridging increasingly approximates pore shrinking behaviour as particle size decreases or pore diameter increases

- Threshold value for R was estimated to be **0.05** from comparison of bridging with DPG and engine particles; deposition of aggregates from the right side of the DPG accumulation mode leads to the chain-like growth of dendrites that extend into the pore, altering the dynamics of pore filling

- Even larger, boulder-like agglomerates in the DPG aerosol leads to sudden blocking of pores, significantly advancing the onset of cake filtration

Laser-drilled tungsten disc

- 1” diameter disc cut from 50 µm thick tungsten foil
- 10 X 10 mm micro-channel array drilled with 20W pulsed ytterbium doped fibre laser at the University of Cambridge Institute for Manufacturing *(thanks to Prof. Bill O’Neill and Kun Li)*
- Drill entry of 32 µm diameter and exit of 20 µm achieved with 60 kHz for 0.8 ms per channel
- 100 µm channel spacing giving almost 10,000 channels total
- Disc loaded with aerosol incident on the drill exit side

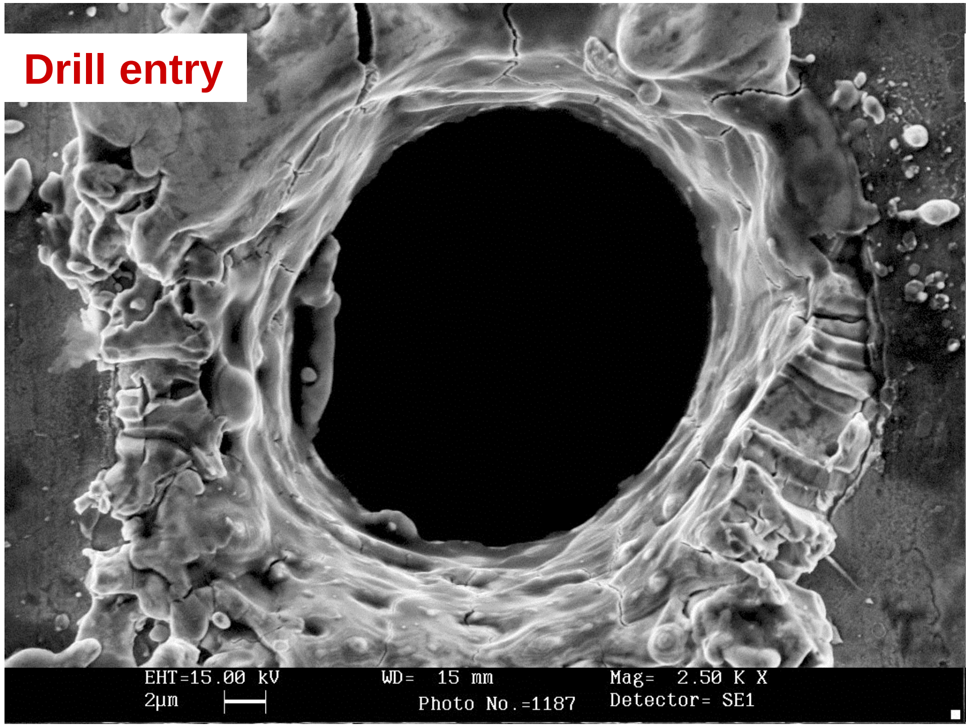

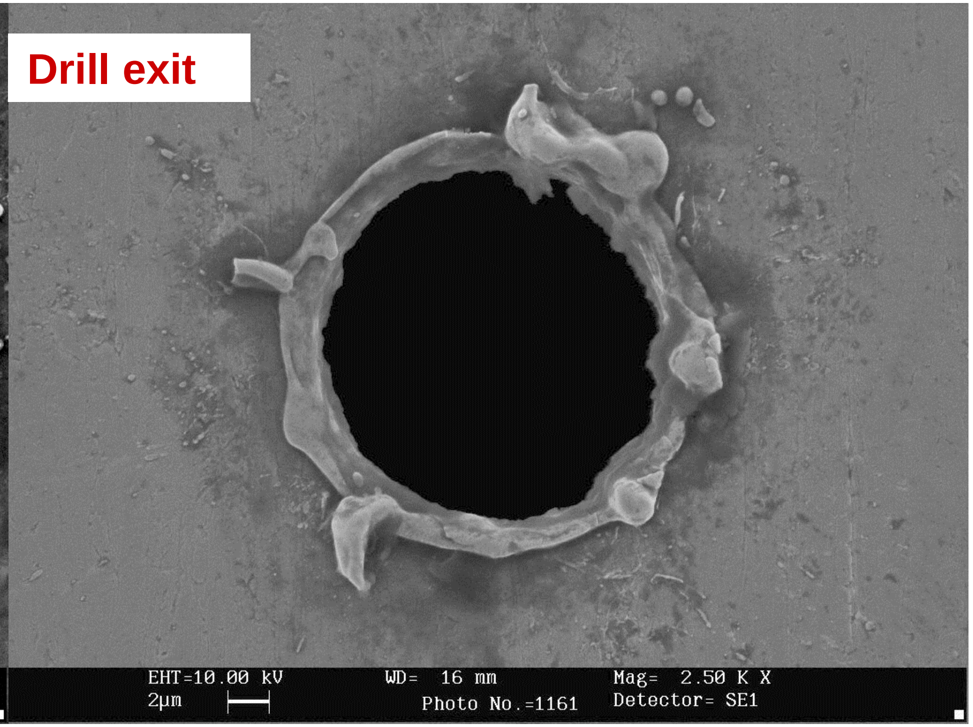

Laser-drilled tungsten disc: map of micro-channels

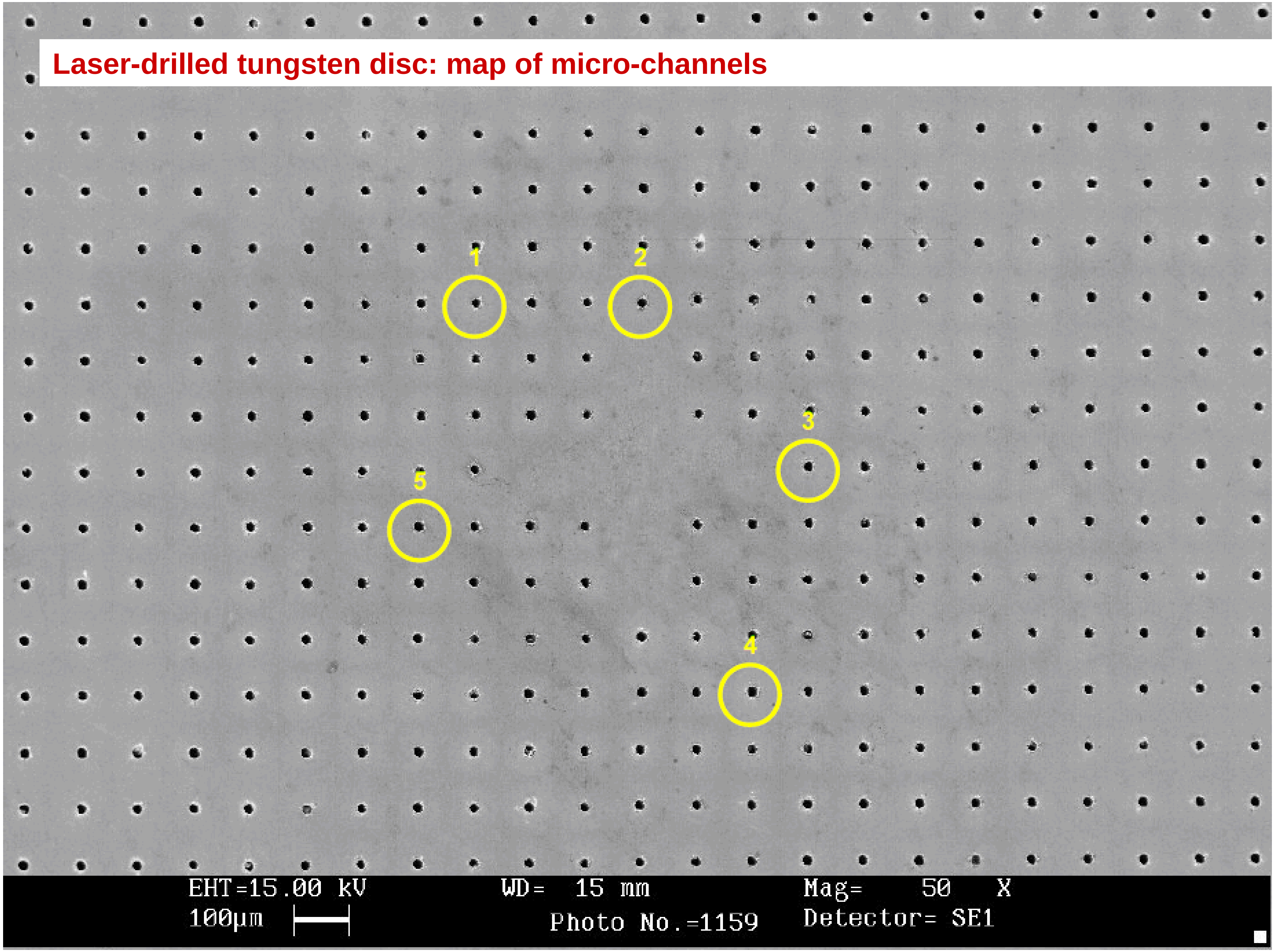

Schematic for SEM visualisation of particulate bridging of micro-channels

Iveco MDD engine used as source of PM in order to monitor bridging behaviour in absence of micro-scale agglomerates

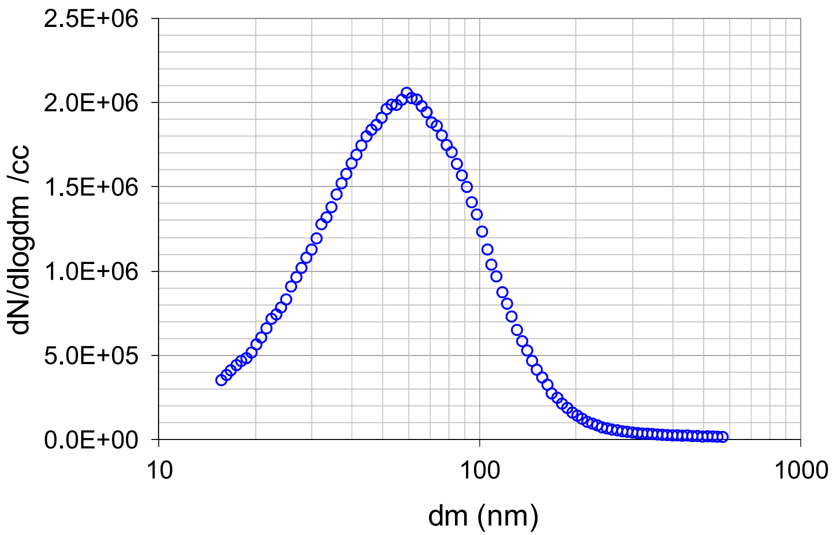

Sample flow through 9,991 channels approximately 19 cm^3/min, yielding an average flow velocity of 10 cm/s (ambient) at the clean micro-channel entrance

Almost 80 litres of diesel fuel were combusted to load the disc with 0.1 mg of engine exhaust PM over 24 hours

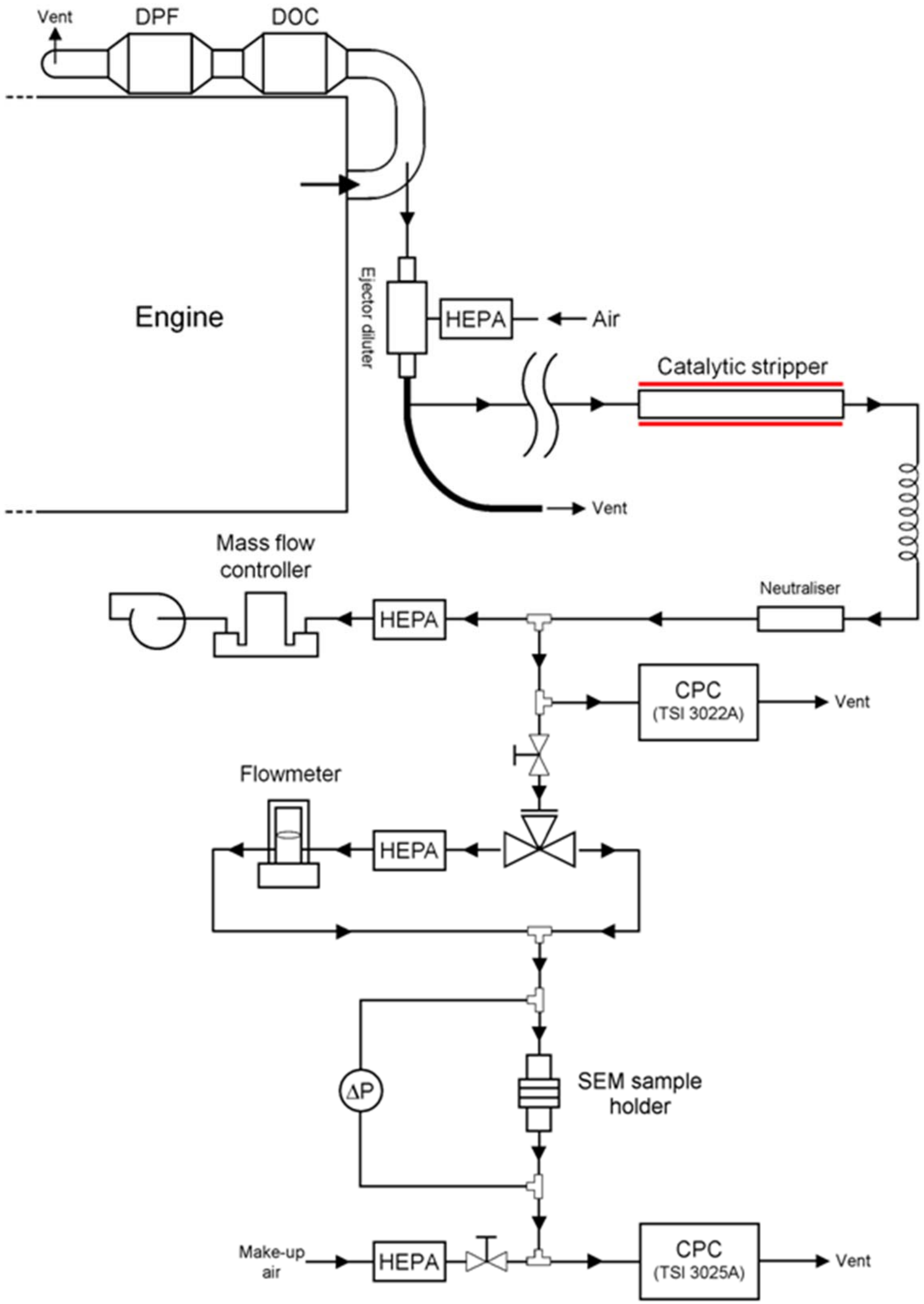

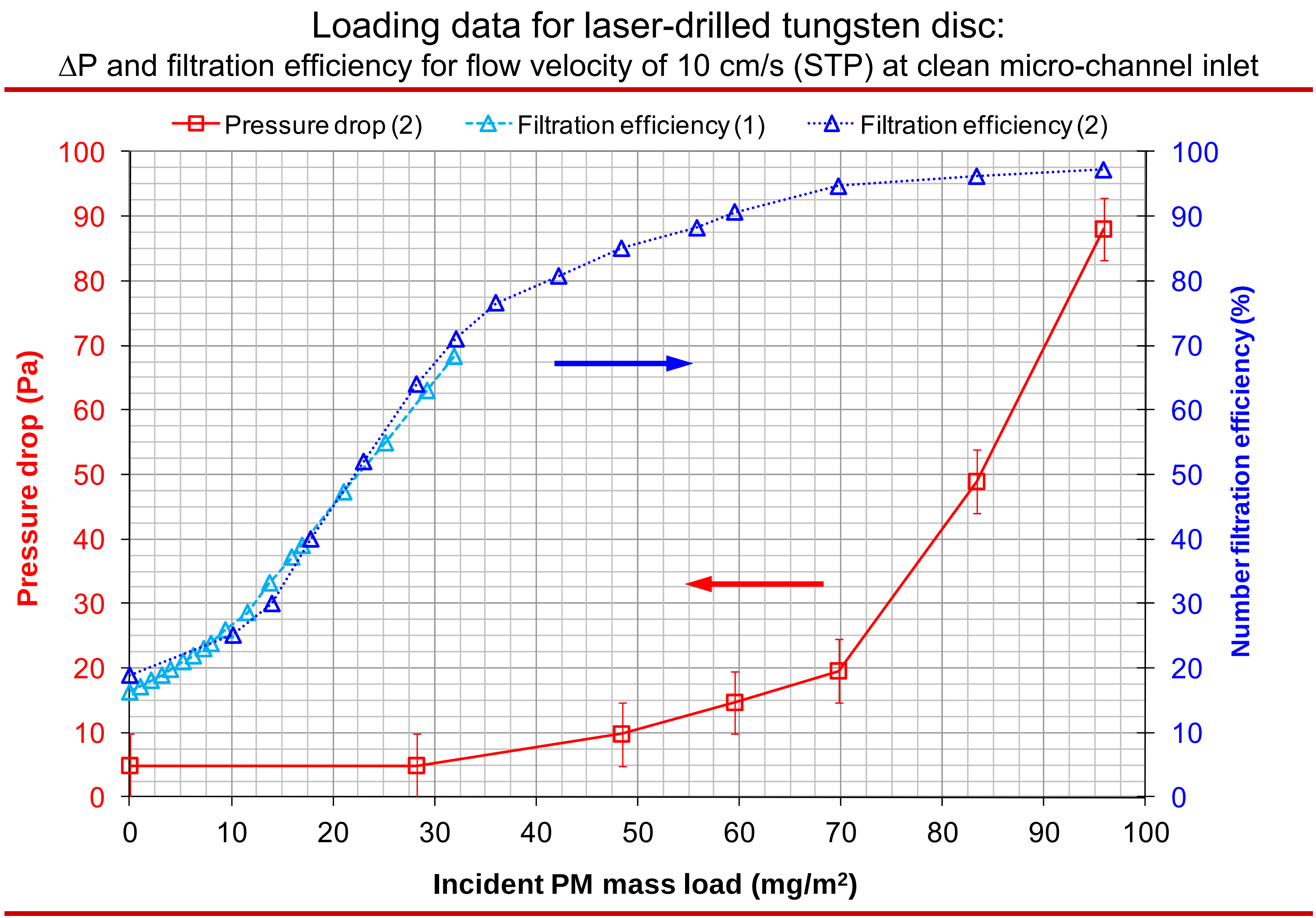

Loading data for laser-drilled tungsten disc:
ΔP and filtration efficiency for flow velocity of 10 cm/s (STP) at clean micro-channel inlet
Pressure drop (2)
Filtration efficiency (1)
Filtration efficiency (2)
Pressure drop (Pa)
Number filtration efficiency (%)
Incident PM mass load (mg/m²)
0
10
20
30
40
50
60
70
80
90
100

Loading data for laser-drilled tungsten disc:

ΔP and filtration efficiency for flow velocity of 10 cm/s (STP) at clean micro-channel inlet

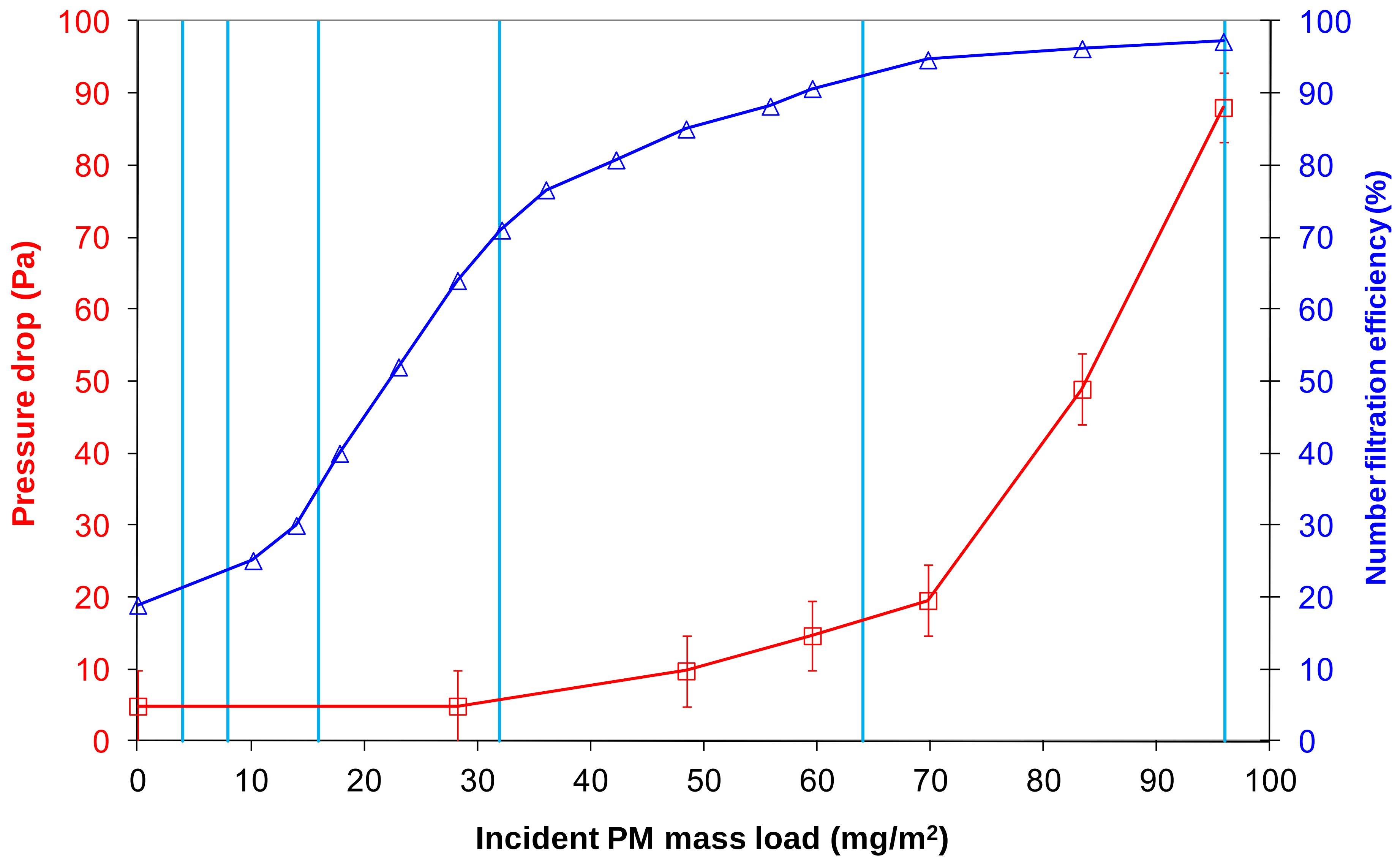

Loading paused at blue lines and wall sample mounted in SEM chamber

Tungsten micro-channel 4:
4 mg/m^3

ΔP = **5** Pa
No. filt. eff. = **21.3** %

10 cm/s average flow velocity
at clean micro-channel entrance

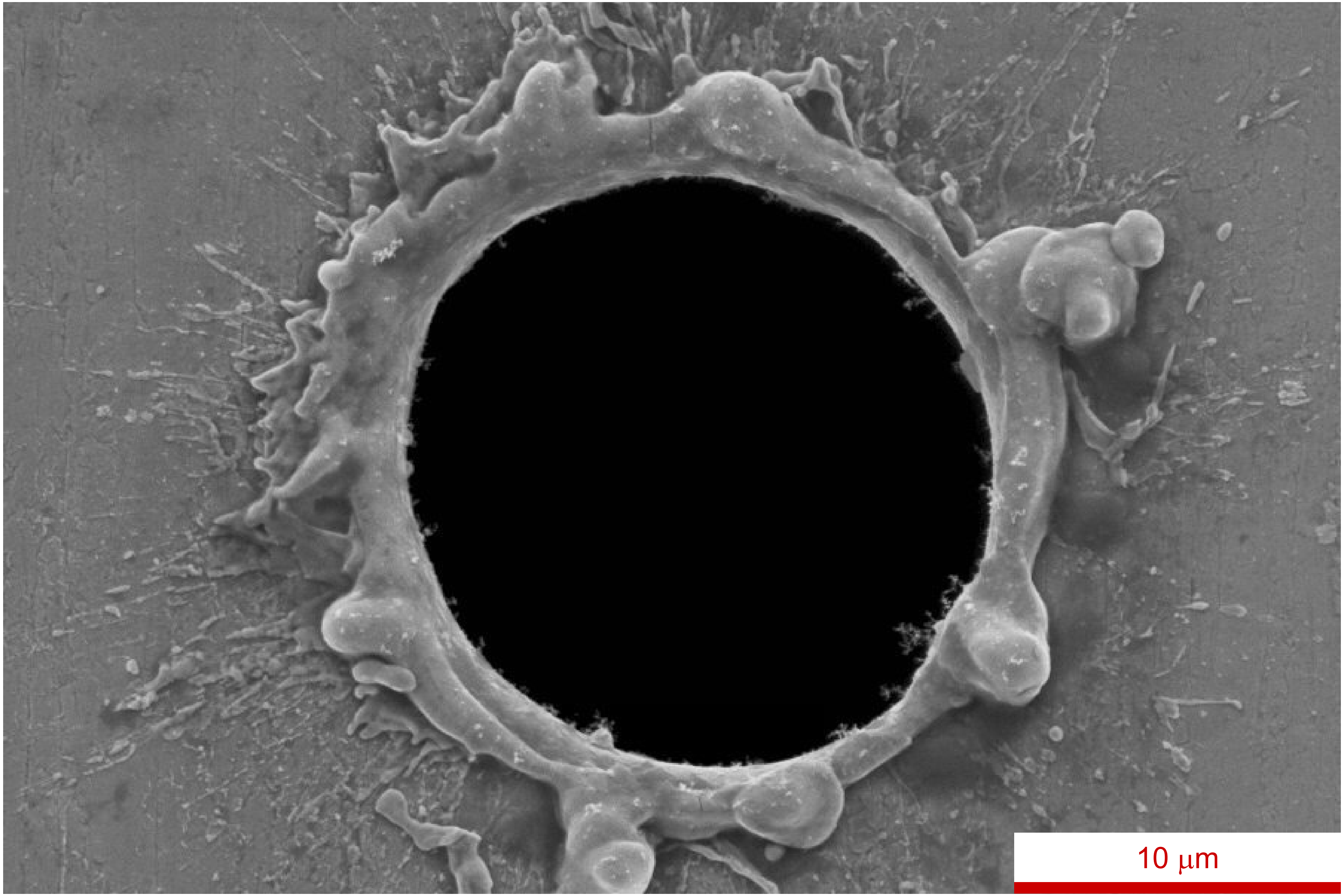

Tungsten micro-channel 4:
8 mg/m^3

ΔP = **5** Pa
No. filt. eff. = **23.8** %

10 cm/s average flow velocity at clean micro-channel entrance

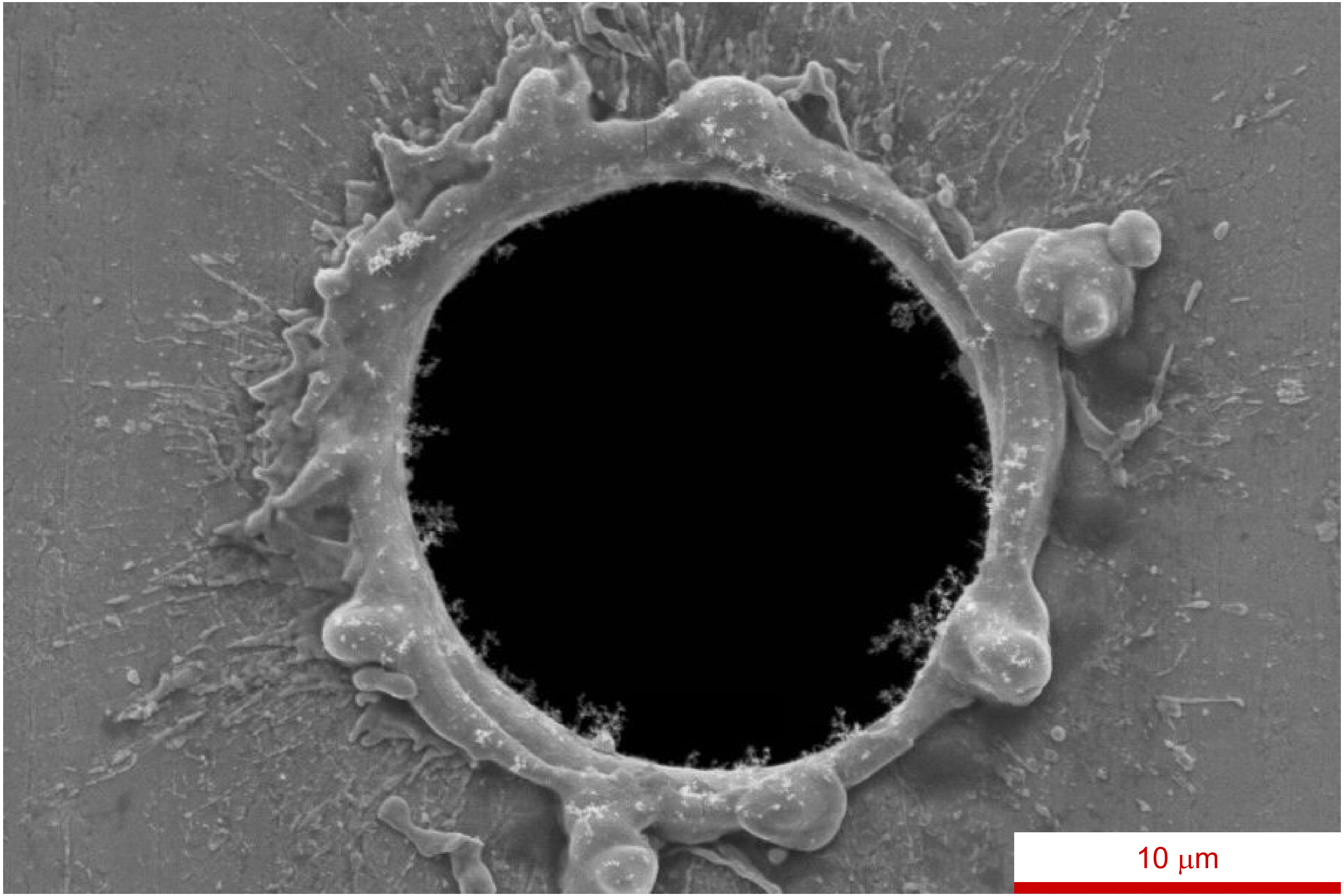

Tungsten micro-channel 4:
16 mg/m^3

ΔP = **5** Pa
No. filt. eff. = **35.3** %

10 cm/s average flow velocity
at clean micro-channel entrance

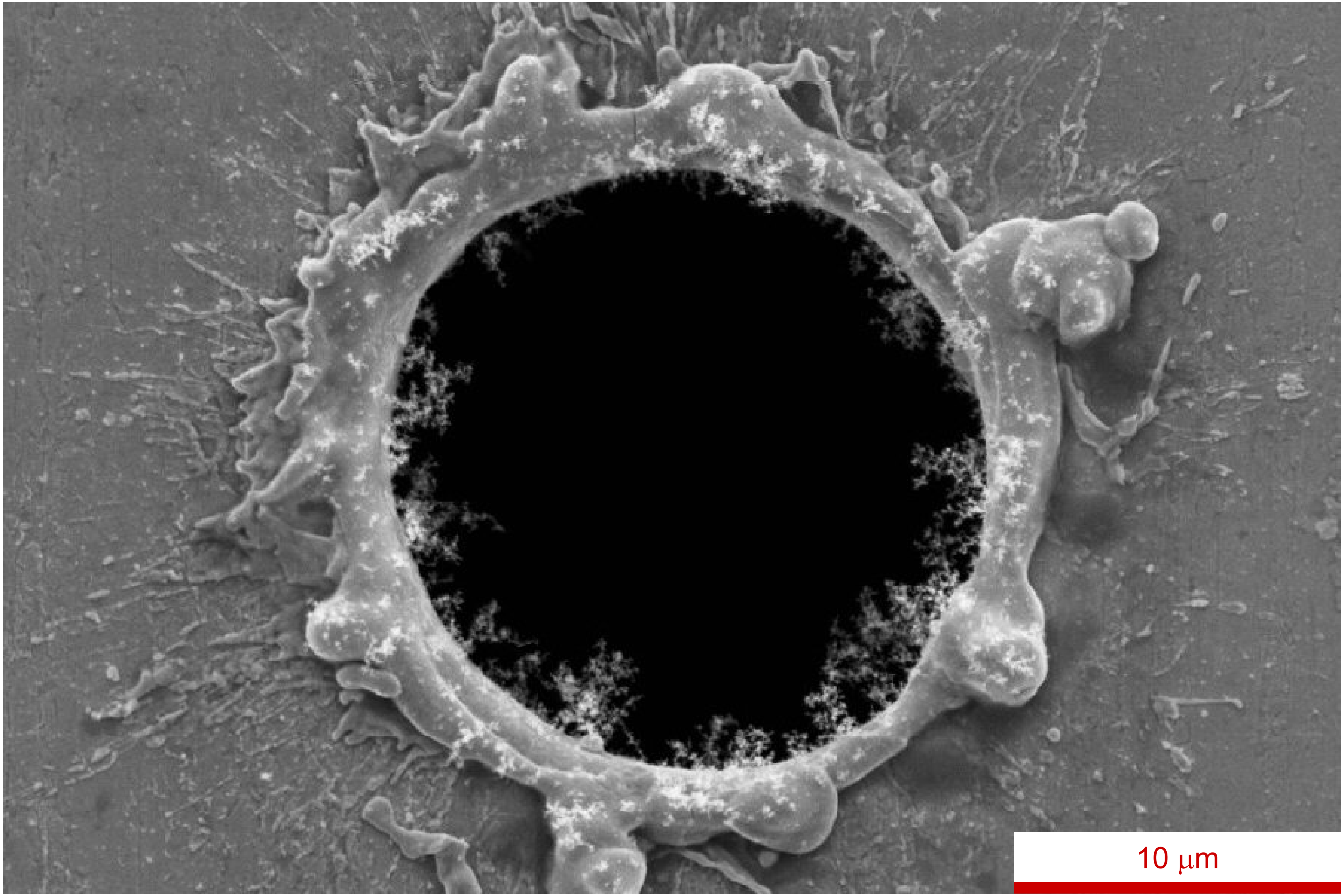

Tungsten micro-channel 4:
32 mg/m^3

ΔP = **10** Pa
No. filt. eff. = **70.8** %

10 cm/s average flow velocity
at clean micro-channel entrance

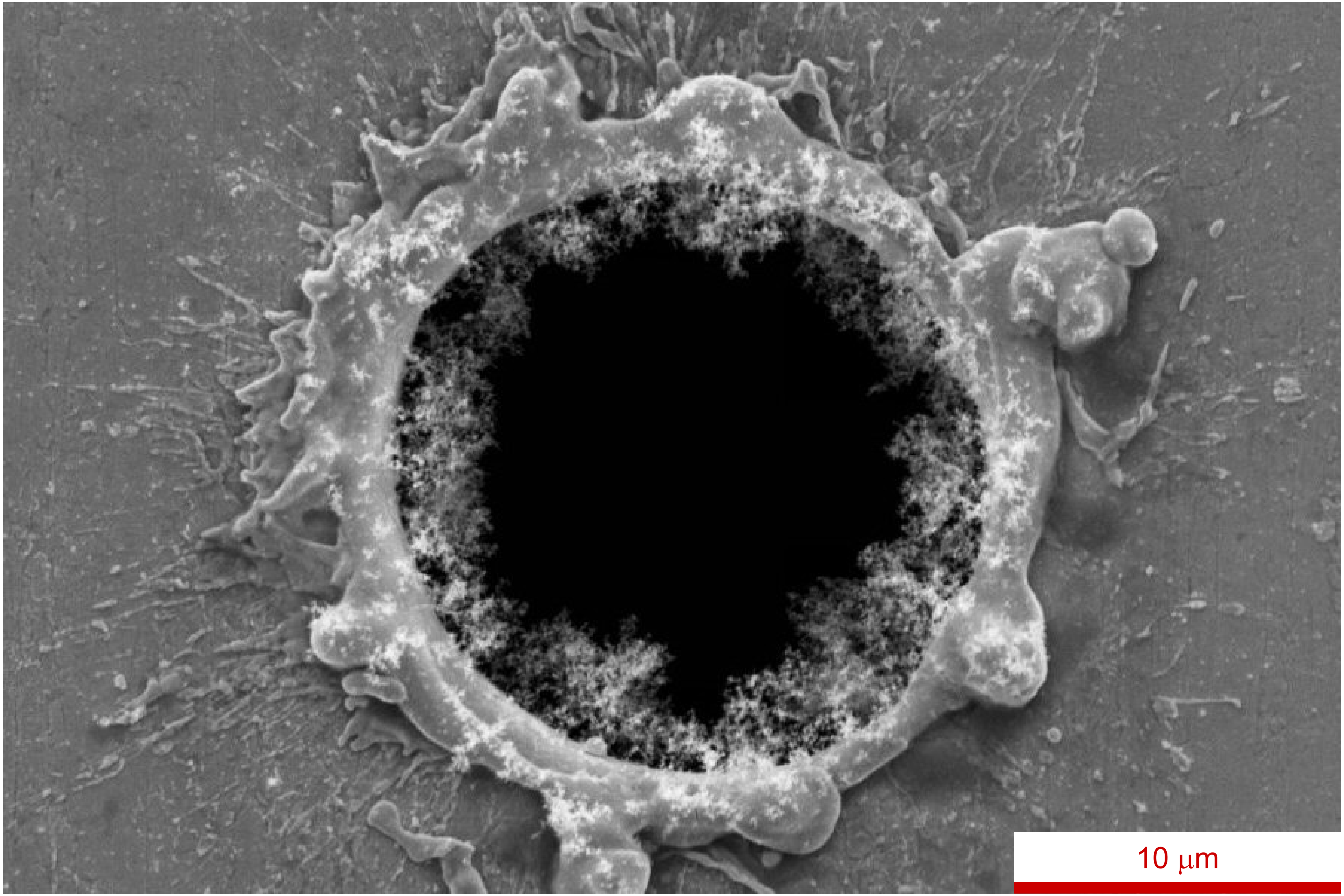

Tungsten micro-channel 4:
64 mg/m^3

ΔP = **17** Pa
No. filt. eff. = **92.4** %

10 cm/s average flow velocity
at clean micro-channel entrance

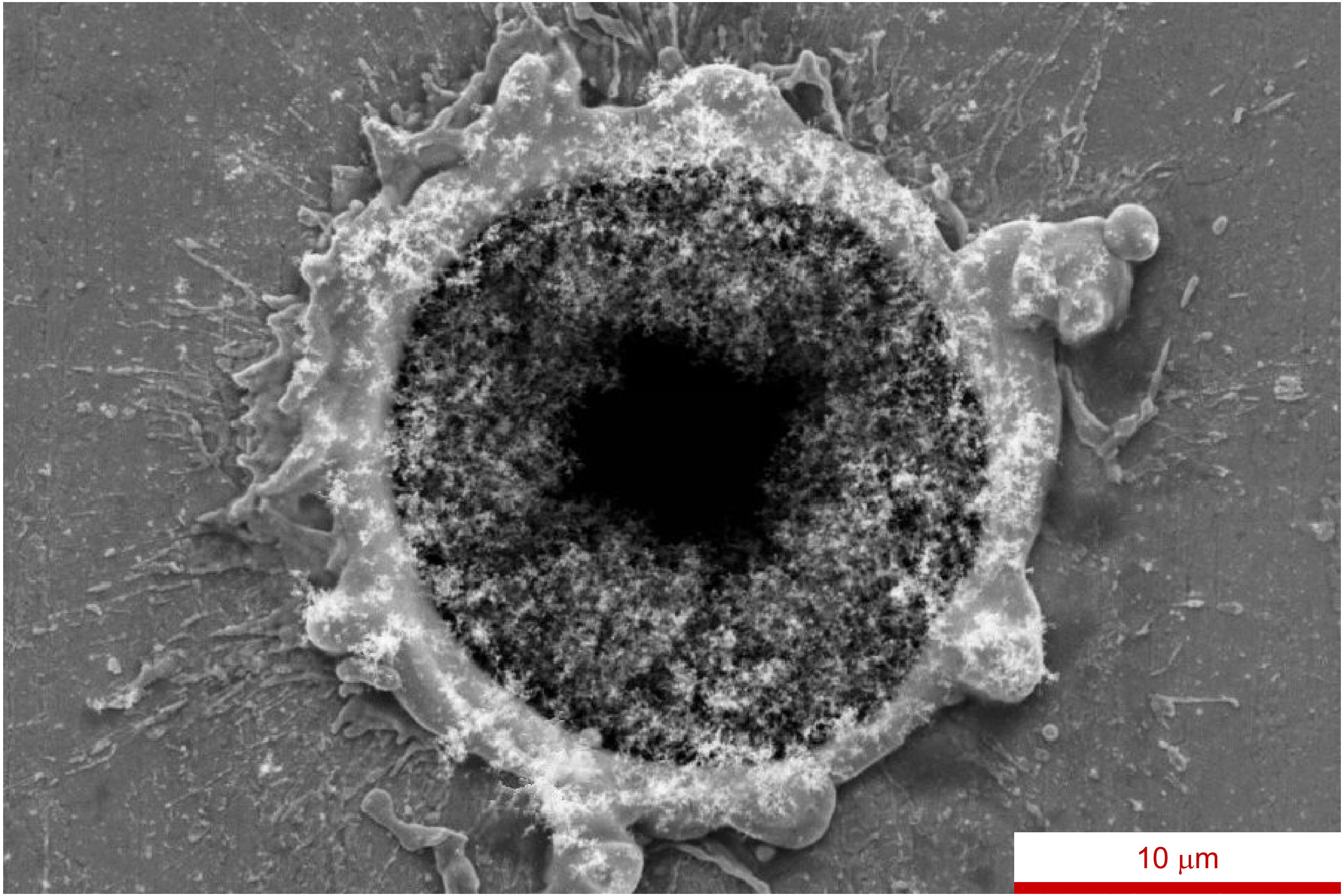

Tungsten micro-channel 4:
96 mg/m^3

ΔP = **89** Pa
No. filt. eff. = **97.2** %

10 cm/s average flow velocity
at clean micro-channel entrance

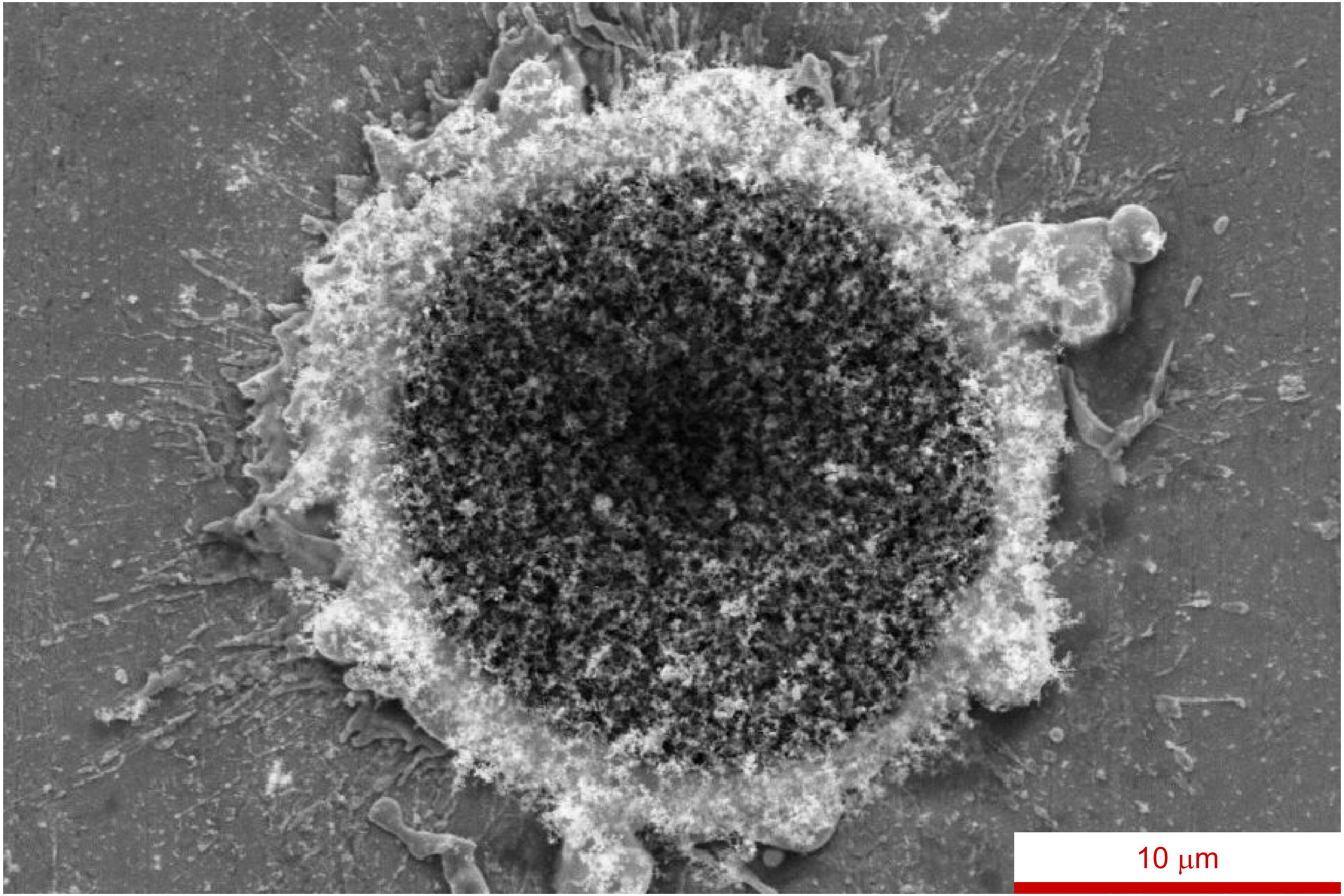

Tungsten micro-channel 4:
4 mg/m^3

ΔP = **5** Pa
No. filt. eff. = **21.3** %

10 cm/s average flow velocity
at clean micro-channel entrance

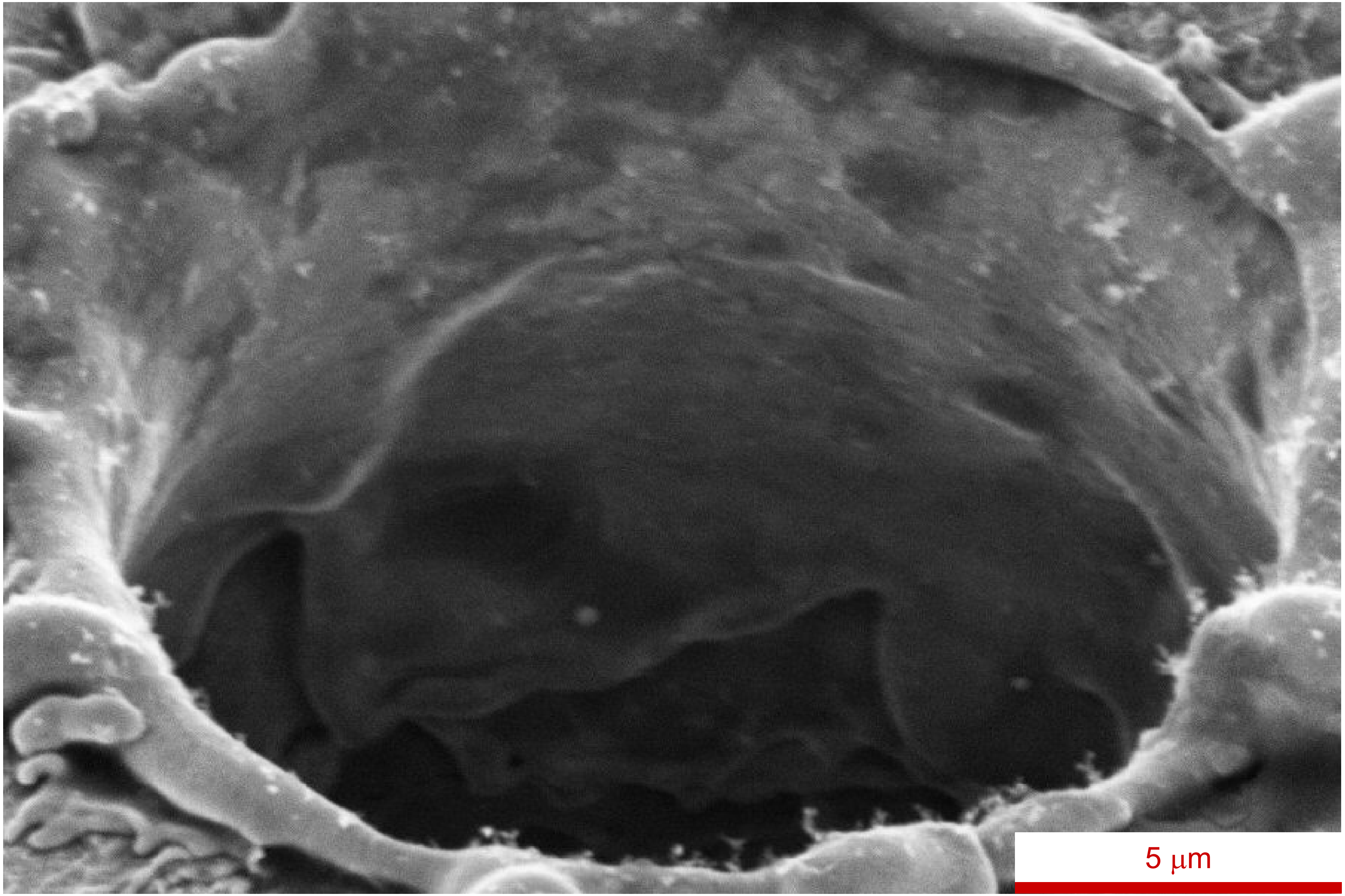

Tungsten micro-channel 4:
8 mg/m^3

ΔP = **5** Pa
No. filt. eff. = **23.8** %

10 cm/s average flow velocity
at clean micro-channel entrance

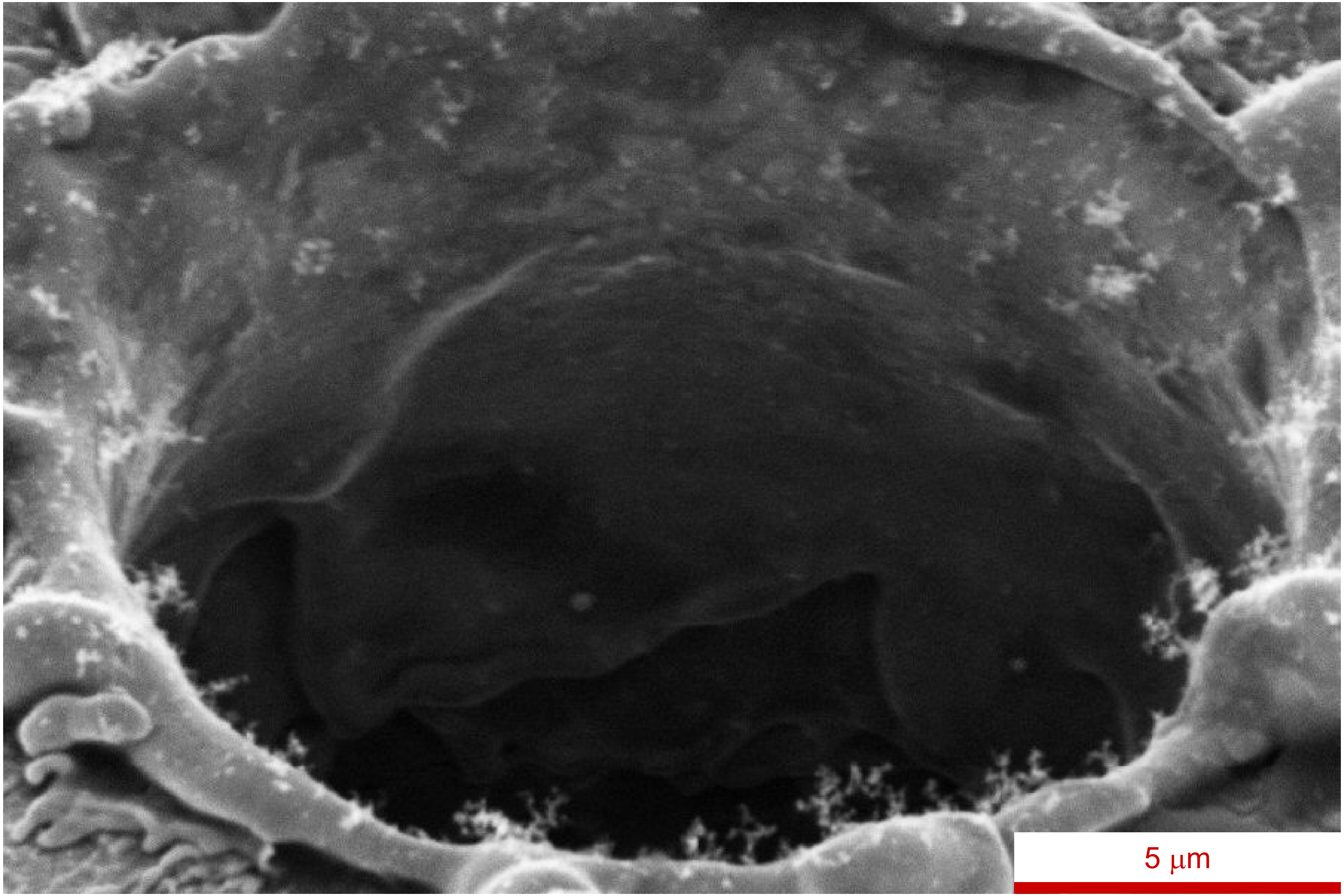

Tungsten micro-channel 4:
16 mg/m^3

ΔP = **5** Pa
No. filt. eff. = **35.3** %

10 cm/s average flow velocity
at clean micro-channel entrance

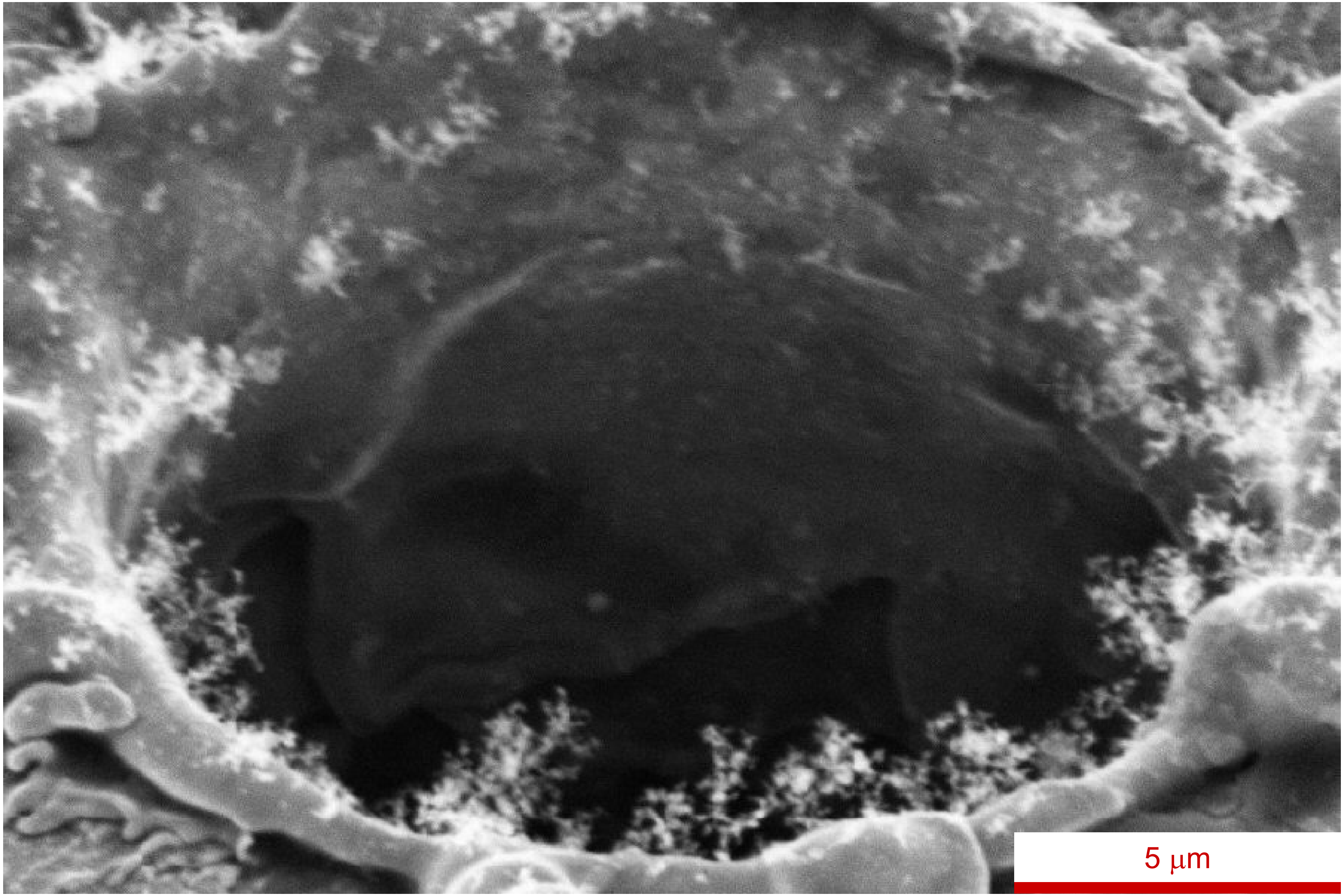

Tungsten micro-channel 4:
32 mg/m^3

ΔP = **10** Pa
No. filt. eff. = **70.8** %

10 cm/s average flow velocity
at clean micro-channel entrance

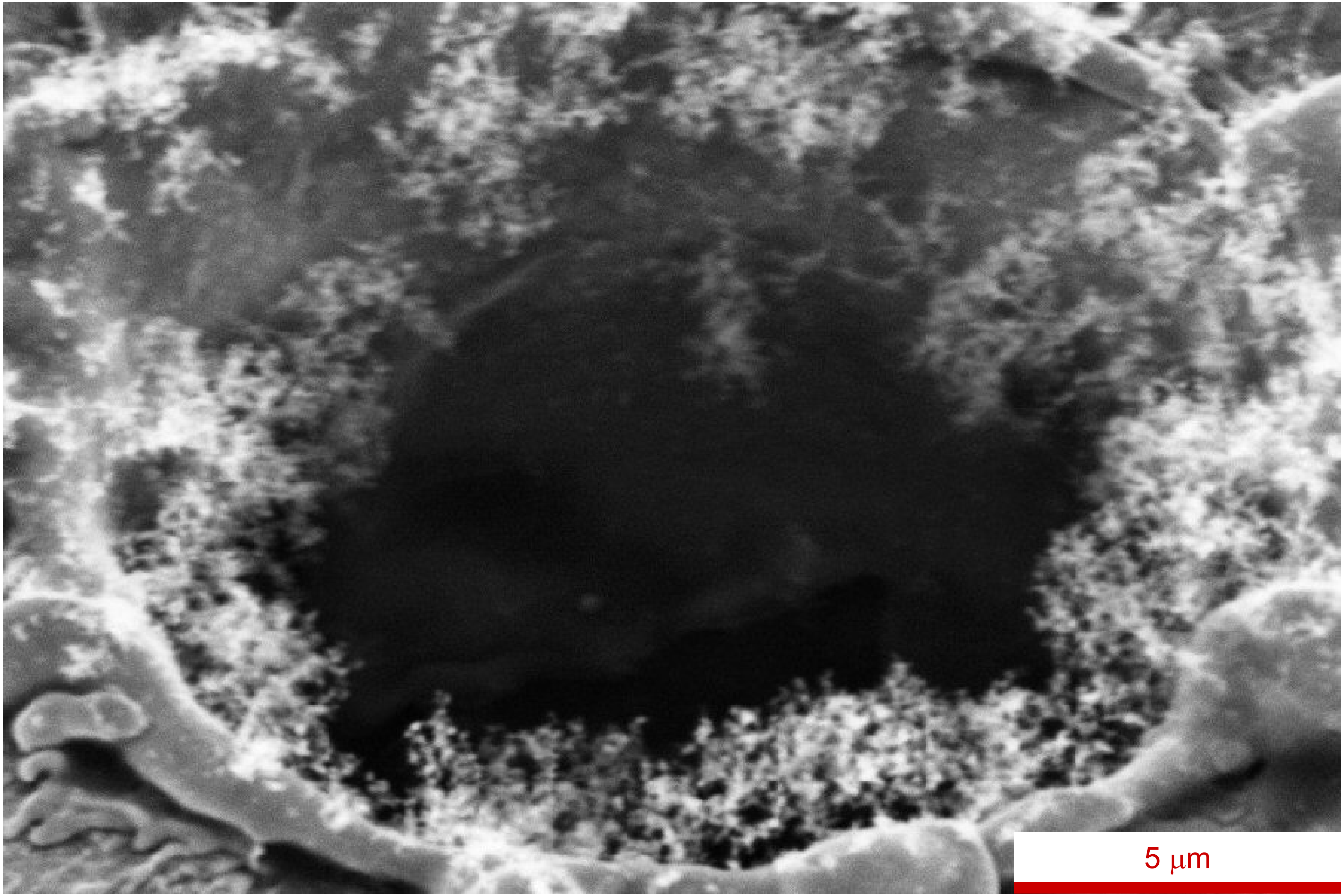

Tungsten micro-channel 4:
64 mg/m^3

ΔP = **17** Pa
No. filt. eff. = **92.4** %

10 cm/s average flow velocity
at clean micro-channel entrance

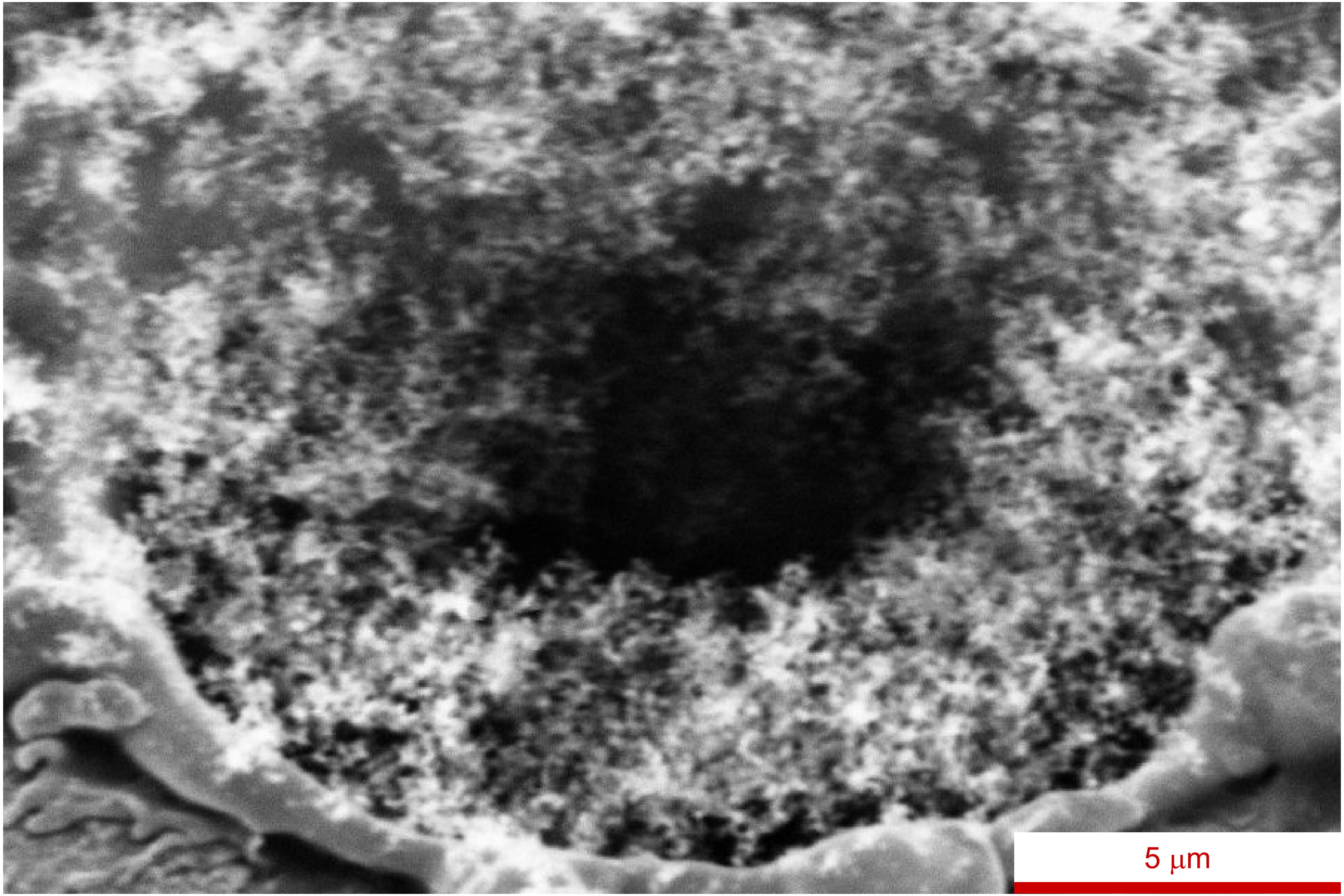

Tungsten micro-channel 4:
96 mg/m^3

ΔP = **89** Pa
No. filt. eff. = **97.2** %

10 cm/s average flow velocity
at clean micro-channel entrance

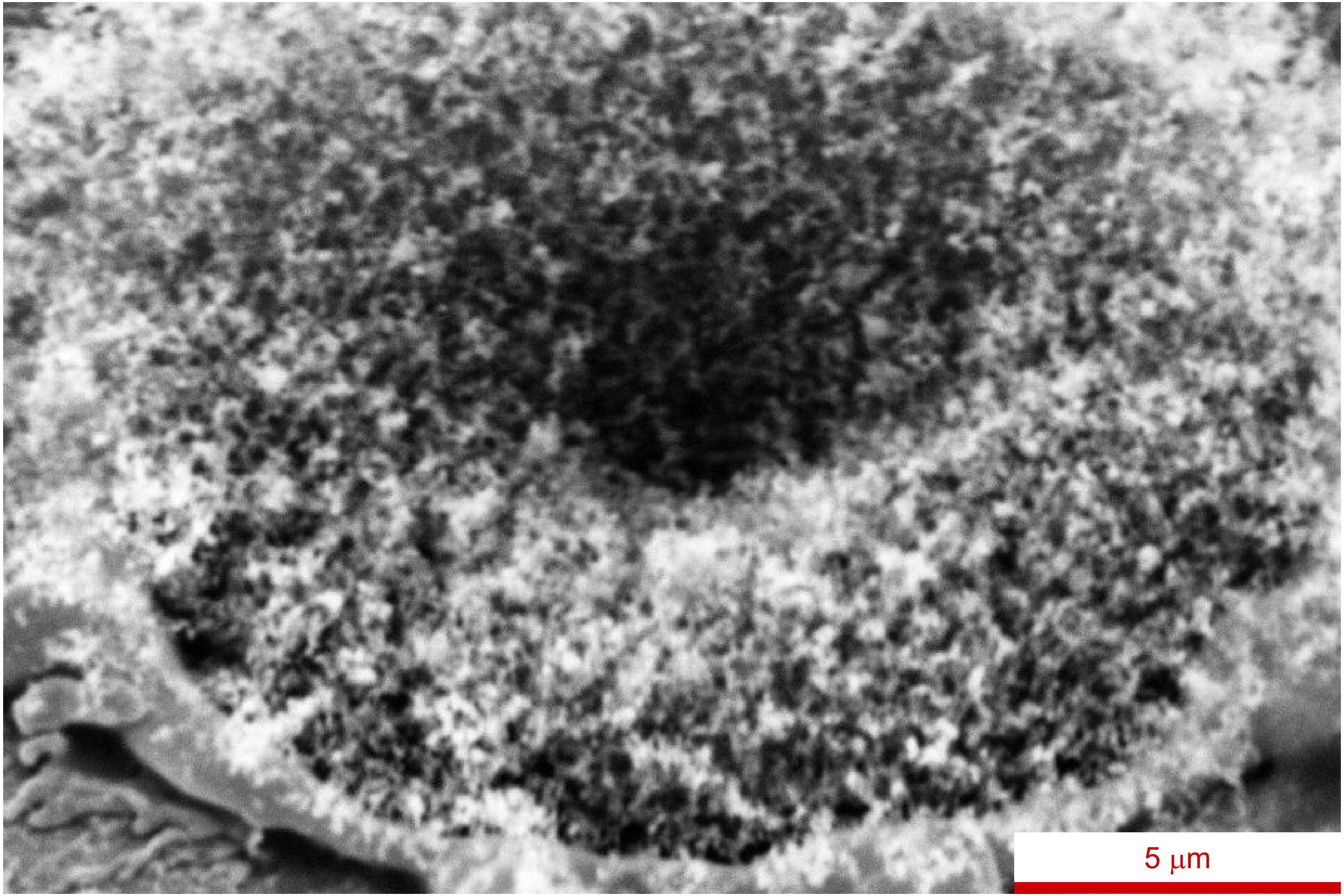

Aerosol entry side of tungsten foil at 96 mg/m^3

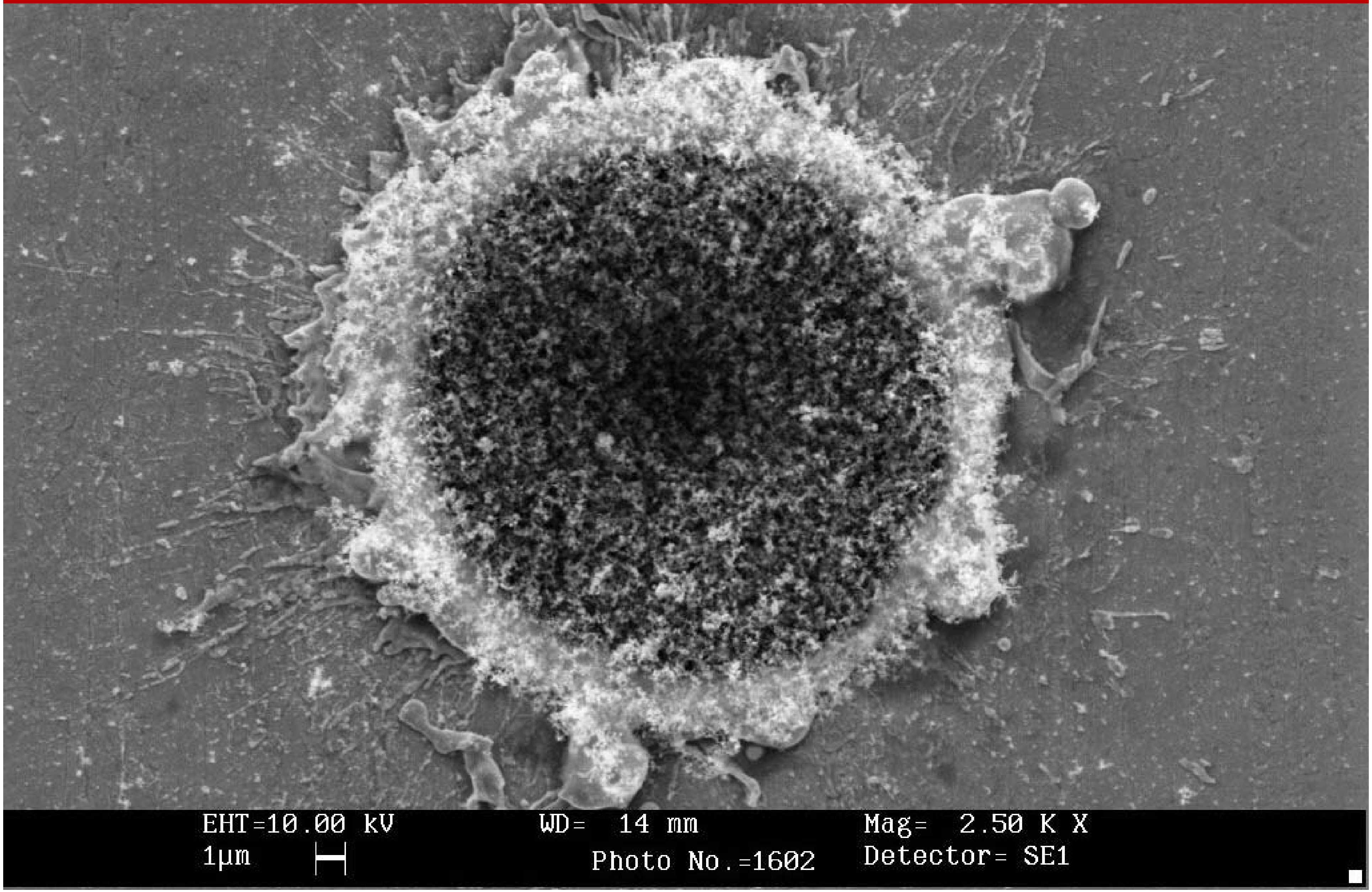

Foil reversed to show aerosol exit side at same location

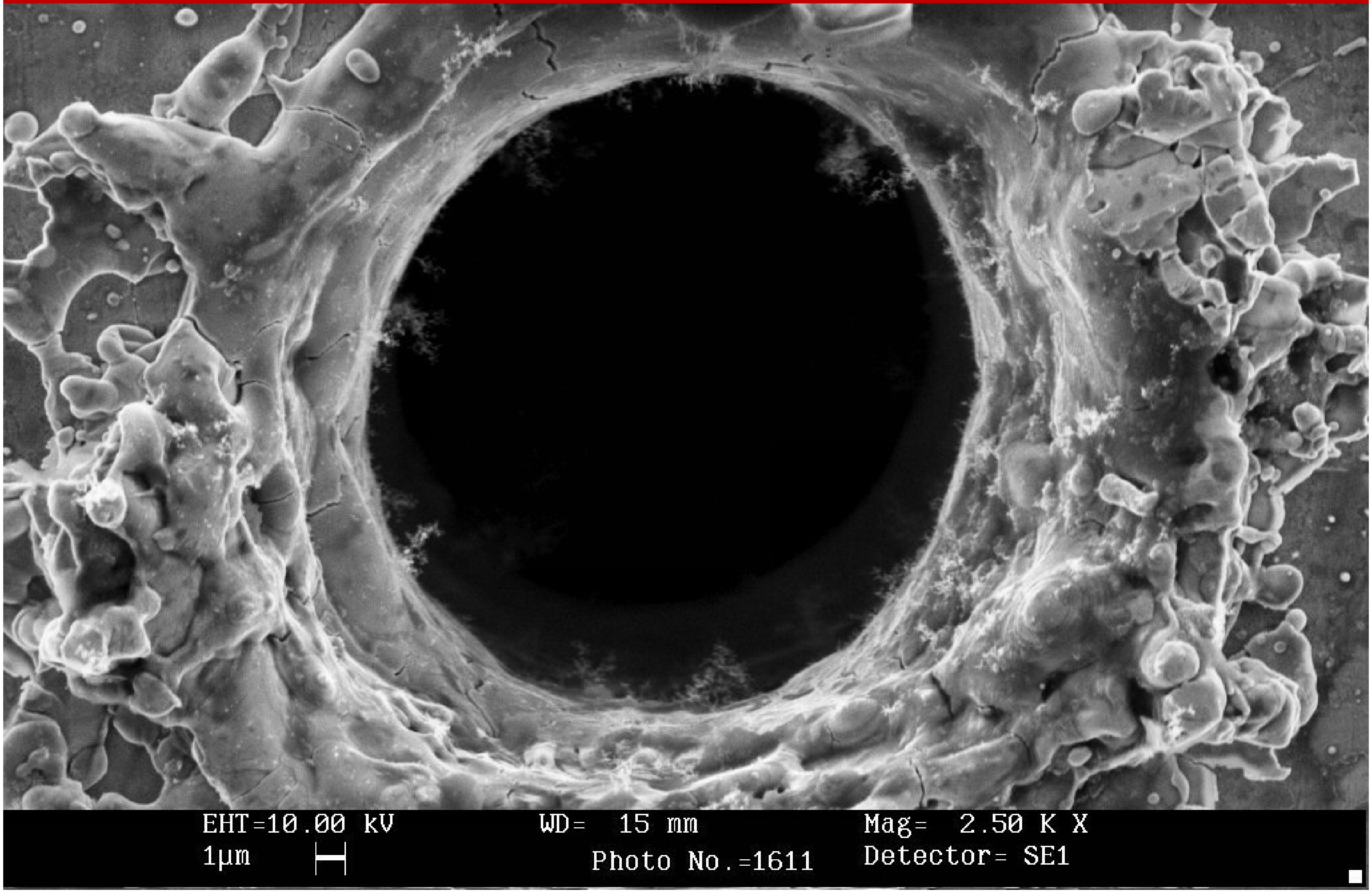

Electron beam brightness and focal depth increased to reveal underside of particulate layer

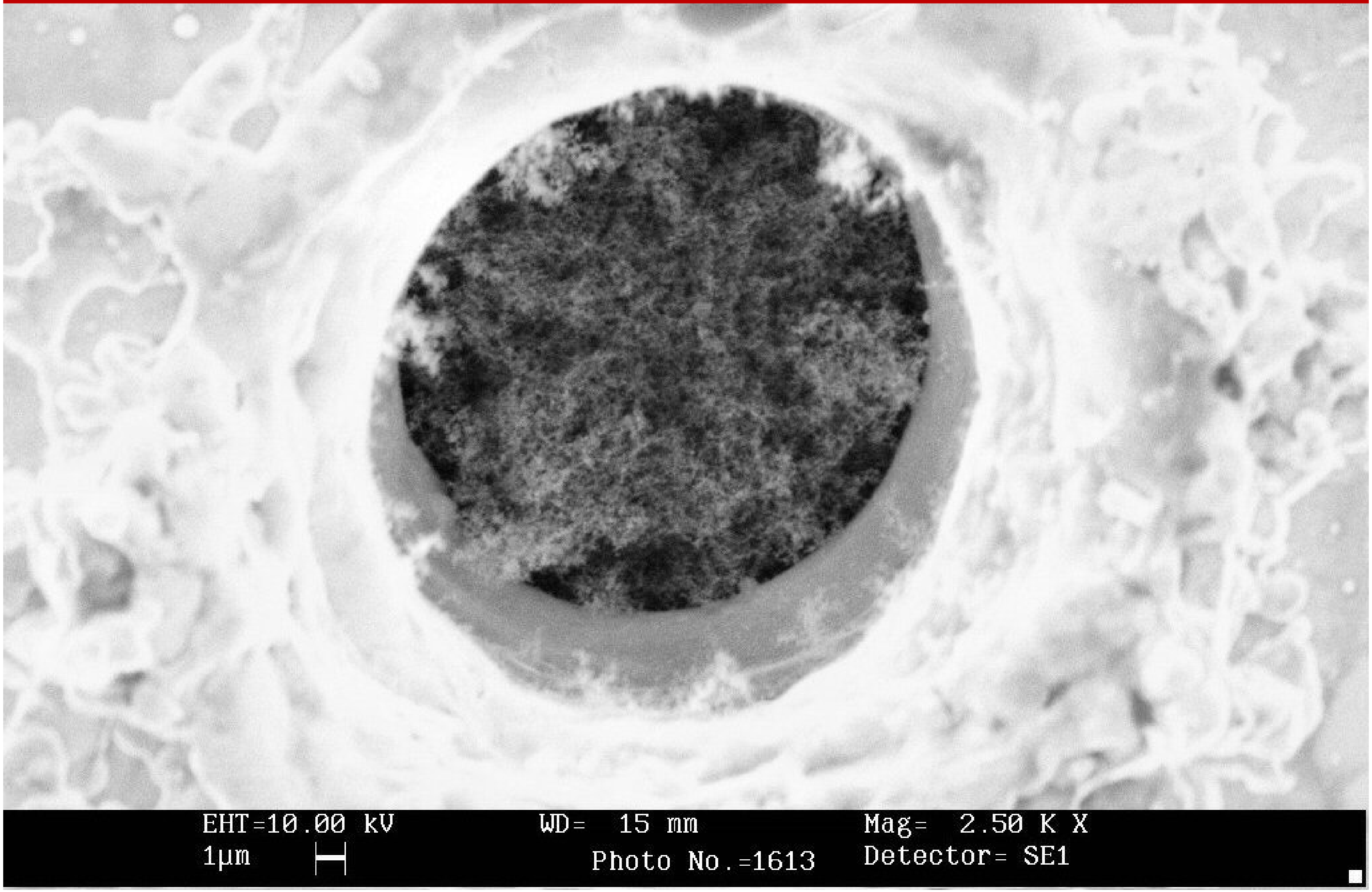

ΔP model: creeping flow ($Re \to 0$)

Pressure drop due to flow contraction/expansion through entrance/exit of circular channel into infinite plane is half that through circular orifice of zero thickness derived by Sampson (1891)*:

$$dP_\infty = \frac{3q\mu}{2r^3}$$

Weissberg's expression (1962)** for pressure drop through tube adapted to fully developed friction along element *i* of channel:

$$dP_i = \frac{8q\mu}{\pi} \cdot \frac{\delta z}{r^4}$$

Total pressure drop across clean tungsten disc can be subsequently derived:

$$\Delta P_d = \frac{q\mu}{2}\left[3\left(\frac{1}{r_1^3} + \frac{1}{r_2^3}\right) + \frac{4}{3\pi} \cdot \frac{L}{r_2 - r_1}\left(\frac{1}{r_1^3} - \frac{1}{r_2^3}\right)\right]$$

* Sampson, R. A. "On Stokes's Current Function." *Philosophical Transactions of the Royal Society of London A* 182 (1891): 449 - 518

** Weissberg, H. L. "End Correction for Slow Viscous Flow through Long Tubes." *Physics of Fluids* 5 (1962): 1033 - 1036.

Axial cross-section of single channel:

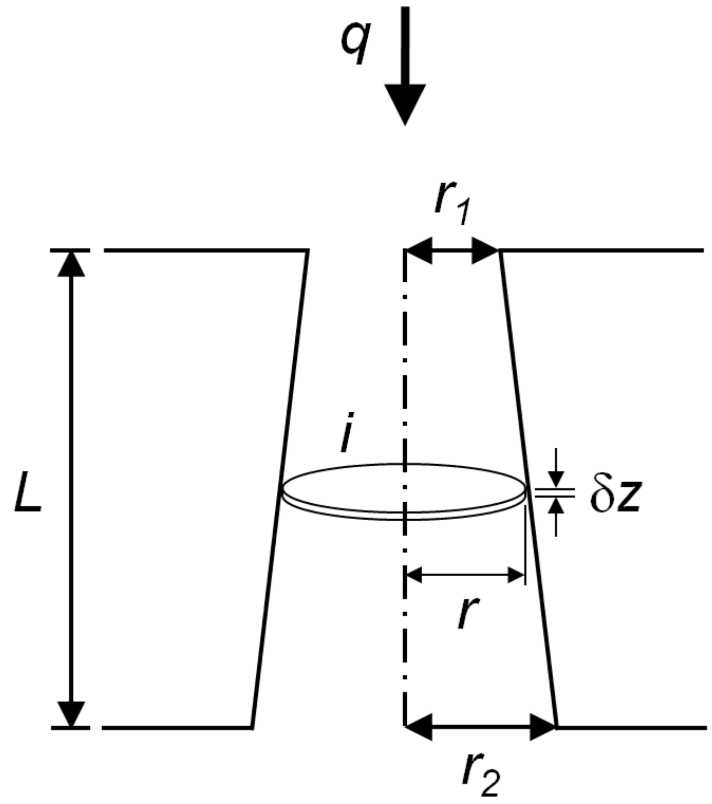

μ - gas dynamic viscosity

ΔP model: parallel electric circuit analogy

Use Ohm's Law to model pressure drop across partial particulate layer (Bear 1972):

$$V = \frac{I_1 + I_2}{\frac{1}{R_1} + \frac{1}{R_2}}$$

Resistances $R_{c,p}$, $R_{c,o}$, R_f and R_e derived from expressions on previous slide. Resistance of particulate rim deposit is:

$$R_p = \frac{w_p \mu}{A_p k_p}$$

where w_p and A_p are thickness and cross-sectional annular area of cake and k_p is permeability

** Bear, J. Dynamics of Fluids in Porous Media. New York: American Elsevier, 1972*

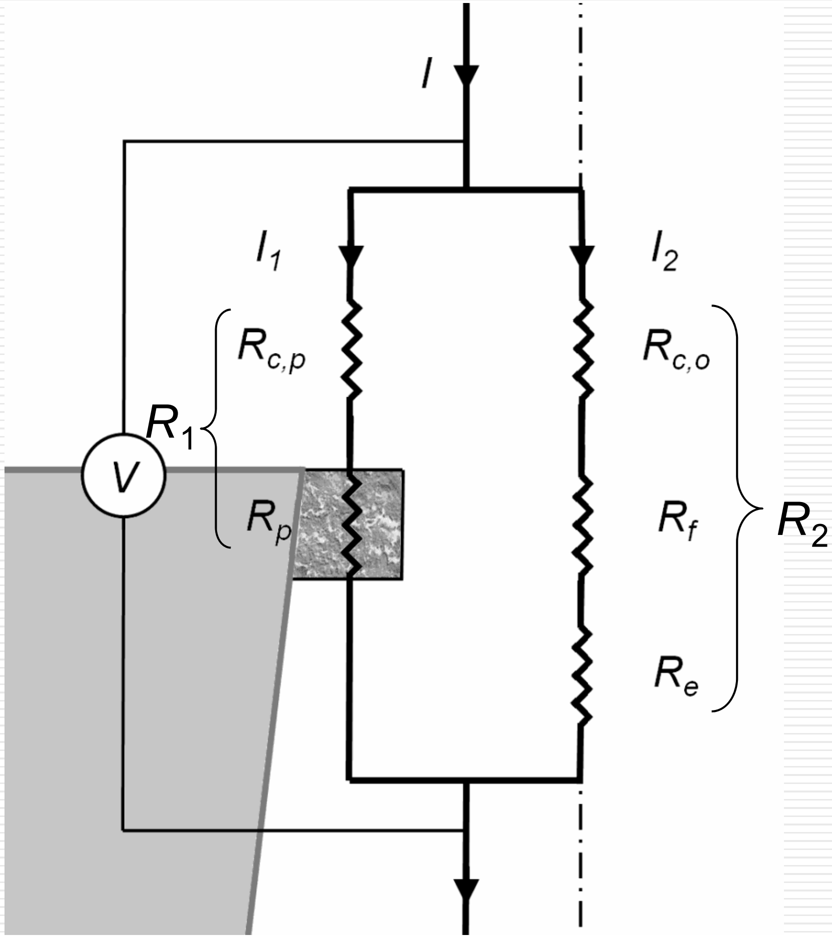

ΔP model: parallel electric circuit analogy

Incident PM mass load (mg/m^3)	Diameter of open flow area (μm)	w_p (μm)	k_p (m^2)	R_1 (Pa·s/m^3)	R_2 (Pa·s/m^3)	% flow through particulate layer
0	19.9	0.05	3×10^{-13}	9.66×10^{11}	2.74×10^{10}	2.8
8	19.5	0.2	3×10^{-13}	7.86×10^{11}	3.10×10^{10}	3.8
16	18	1	3×10^{-13}	1.01×10^{12}	5.01×10^{10}	4.7
32	14	2	3×10^{-13}	7.62×10^{11}	1.54×10^{11}	16.8
64	7	3	3×10^{-13}	6.67×10^{11}	2.06×10^{12}	75.5
96	2	4	8×10^{-14}	2.87×10^{12}	2.33×10^{14}	98.8

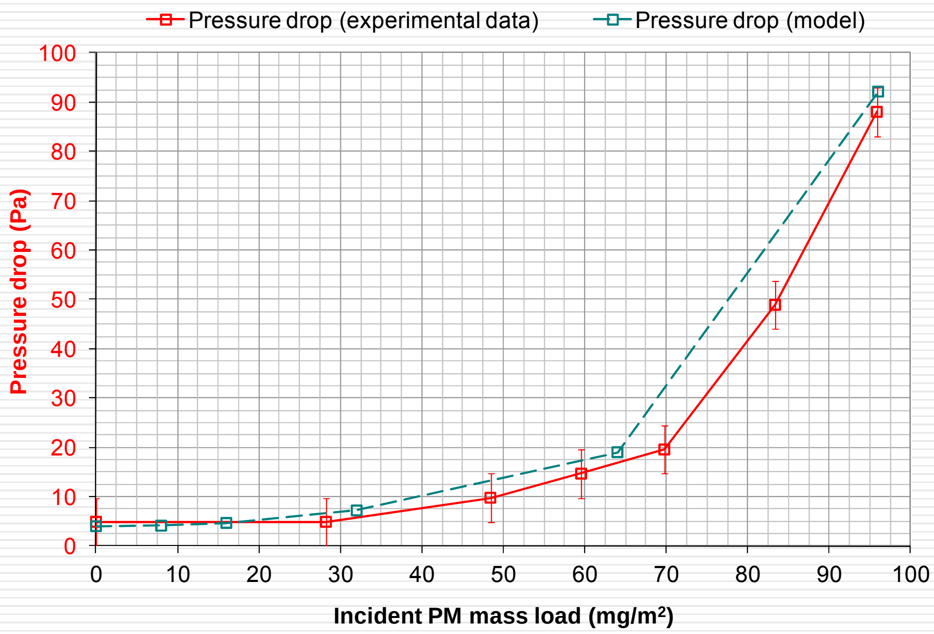

Conclusions (1/2)

- Visualisation of the transient filtration stage of DPF operation showed that small pores were rapidly filled while the bridging of larger pores was a more gradual process approximating shrinking pore behaviour; a threshold value of **0.05** for the ratio of particle to pore size was estimated

- Dendrites that extend across half the width of 10-20 µm pores grow from deposition of aggregates from the right side of the DPG accumulation mode and alter the dynamics of pore filling

- The presence of agglomerates several microns across in the same aerosol causes rapid blocking of pores and substantially reduces the pre-cake pressure drop

- While initial filtration efficiency in the SiC wall was higher with the smaller Iveco MDD engine aerosol, the transition from deep-bed to cake filtration occurred at greater particulate mass loading with the associated pressure drop penalty approximately double that with the larger DPG aerosol

Conclusions (2/2)

- Loading of the laser-drilled tungsten disc with the smaller Iveco MDD engine aerosol (devoid of micro-scale agglomerates) showed that the micro-channels are filled in a radial manner

- Little deposition beyond the entrance occurs prior to bridging; particle deposits at the rim of each channel grow as dendrites to lengths of several microns and then merge with neighbouring dendrites, leading to a nearly circular open flow area that contracts almost uniformly as loading continues

- Viewed at a 45° angle to the plane of the disc, the particulate cake, once established, is torus-shaped and begins to grow out of the channel as a dome

- Pressure drop across loaded micro-channel can be modelled using a parallel electric circuit analogy, enabling the evolving permeability of the particulate layer to be estimated

Acknowledgements

- Nick Collings (supervisor)
- Athanasios Konstandopoulos and Adam Boies
  (PhD examiners)
- Johnson Matthey (project sponsor)
  - Martyn Twigg
  - JM Orchard Laboratories:
    Neal Sutton, Russell Ableman and Dan Oakes
  - JM Autocatalyst Technology Centre:
    Owen Russell and Jeremy Gidney
- University of Cambridge IfM: Bill O' Neill and Kun Li
- Engineering and Physical Sciences Research Council

Website for SEM images of particulate bridging

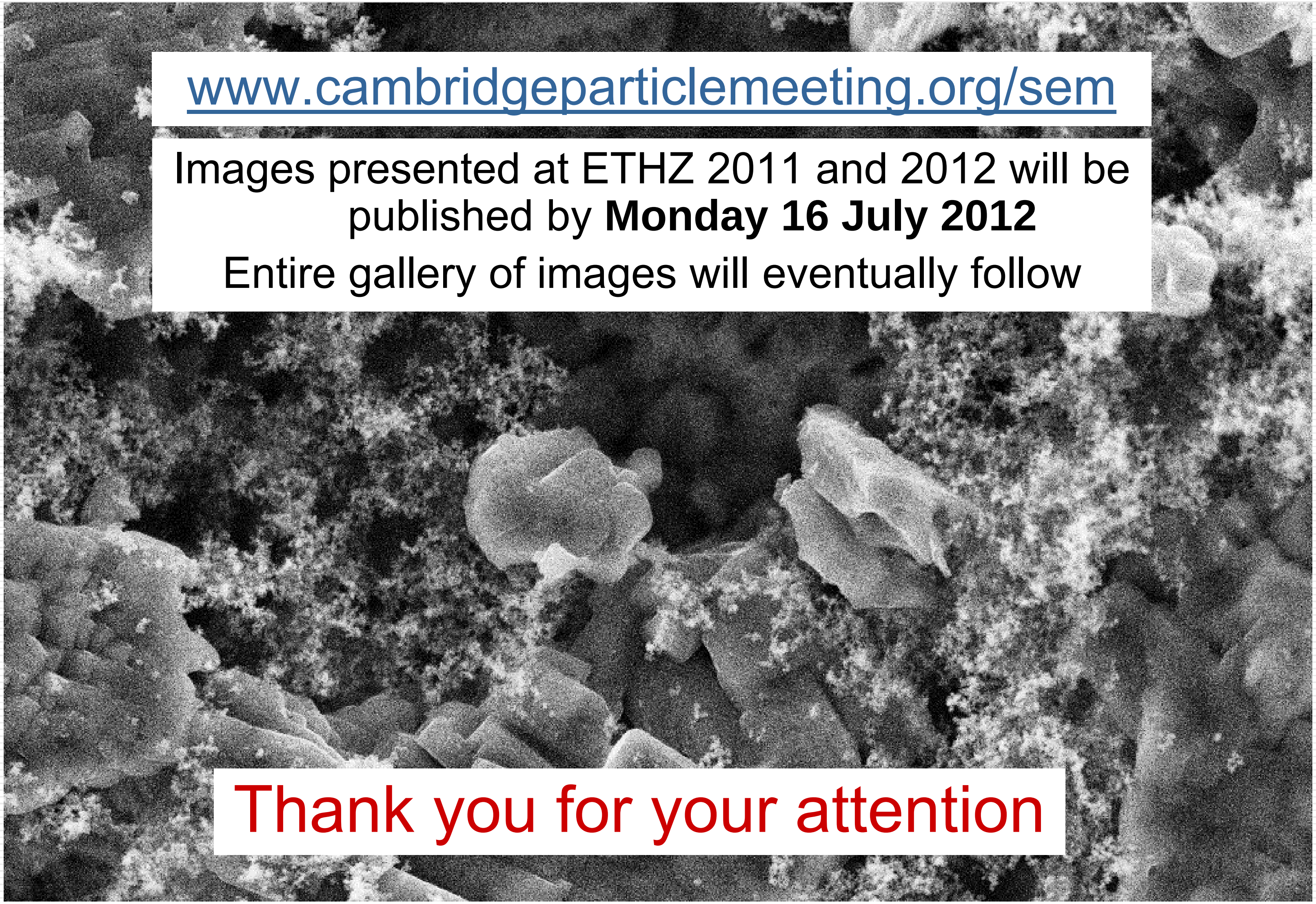

www.cambridgeparticlemeeting.org/sem

Images presented at ETHZ 2011 and 2012 will be published by **Monday 16 July 2012**

Entire gallery of images will eventually follow

Thank you for your attention

Cambustion DPG system

- Complete system for DPF testing:
  - ΔP vs soot load characteristics
  - Filtration efficiency
  - Regeneration behaviour
- Diesel burner (2-20 g/hr soot generation)
- Testing at engine exhaust flows
  - Standard load 250kg/hr at 240°C
  - Cold flow test up to 900m^3hr^{-1}
- Airflow sucked through DPF
  - Soot generator not affected by DPF backpressure
- Primary, secondary airflows and fuel flow control soot generation
  - Tertiary airflow and temperature allows independent control of DPF inlet conditions

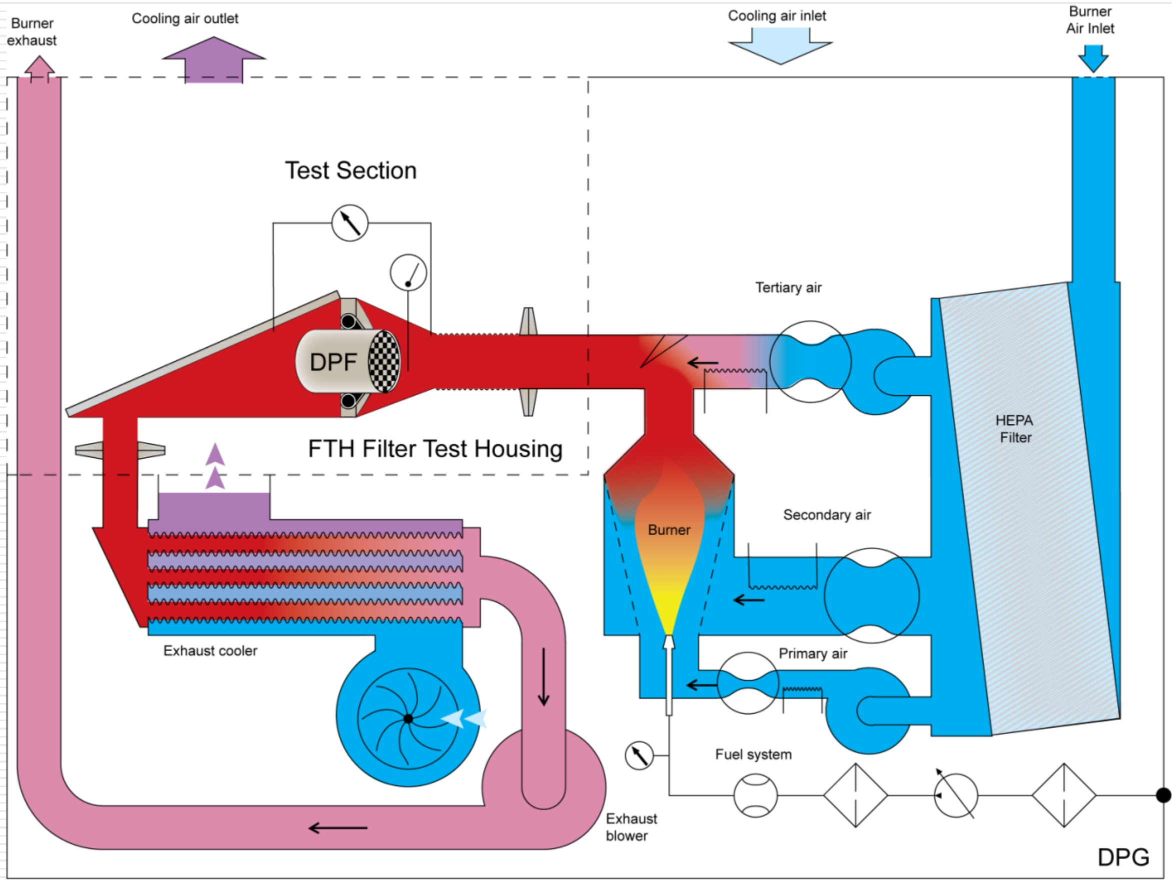

CAMBUSTION DPF TESTING SYSTEM

Checks during technique development

- Elimination of system leaks downstream of DPF wall sample
- Conservation of ratio of volumetric flow rate through the SEM sample to that through parallel wall (equal to ratio between respective filtration areas, in the range 25:1-30:1)
- Stability of particulate deposit microstructure in vacuum and under electron beam in SEM chamber
  (see images on following slides)
- Recovery of wall pressure drop between successive stages of loading

Stability of diesel particulate deposits

SiC pore 1 loaded to 0.1 g/l: SEM image captured immediately afterwards

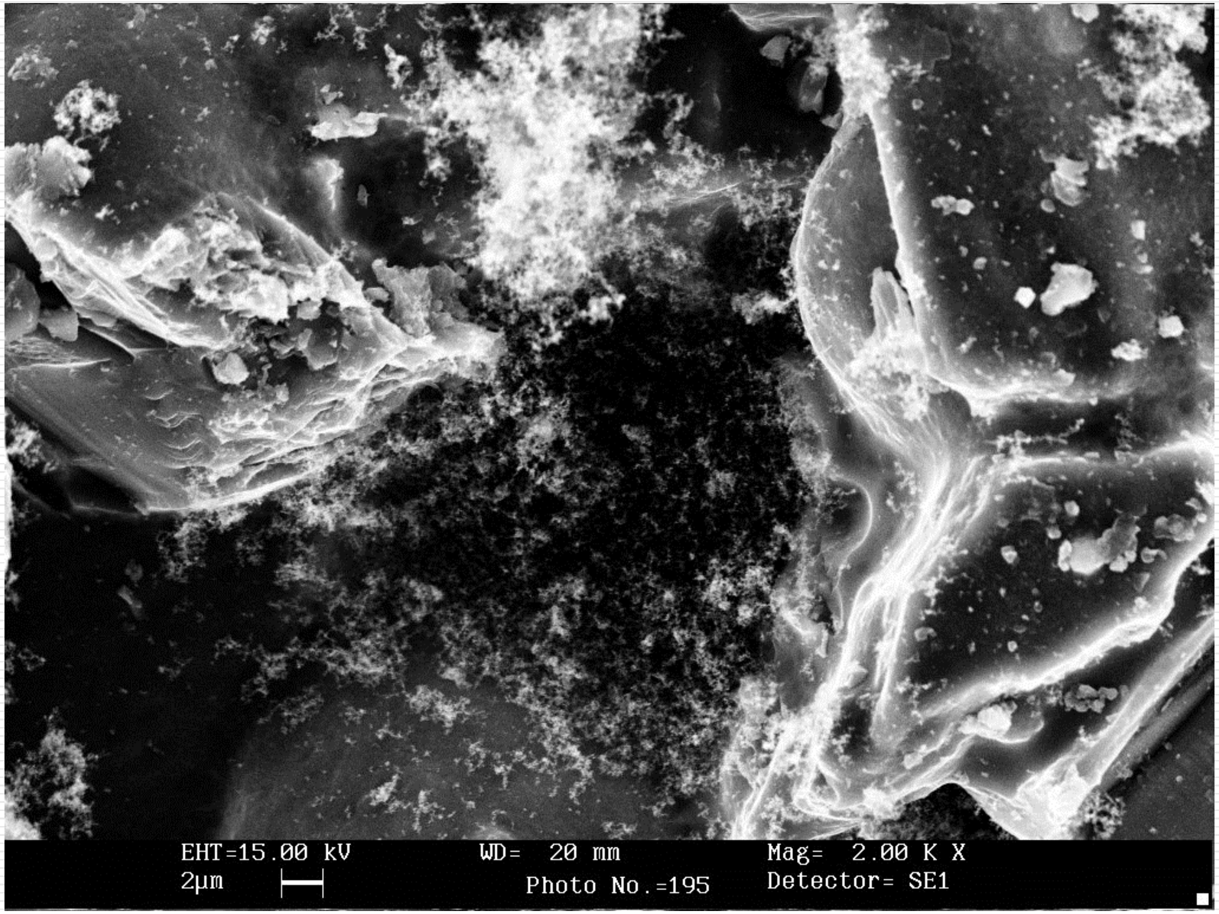

Stability of diesel particulate deposits

SiC pore 1 loaded to 0.1 g/l: SEM image captured 1 month later

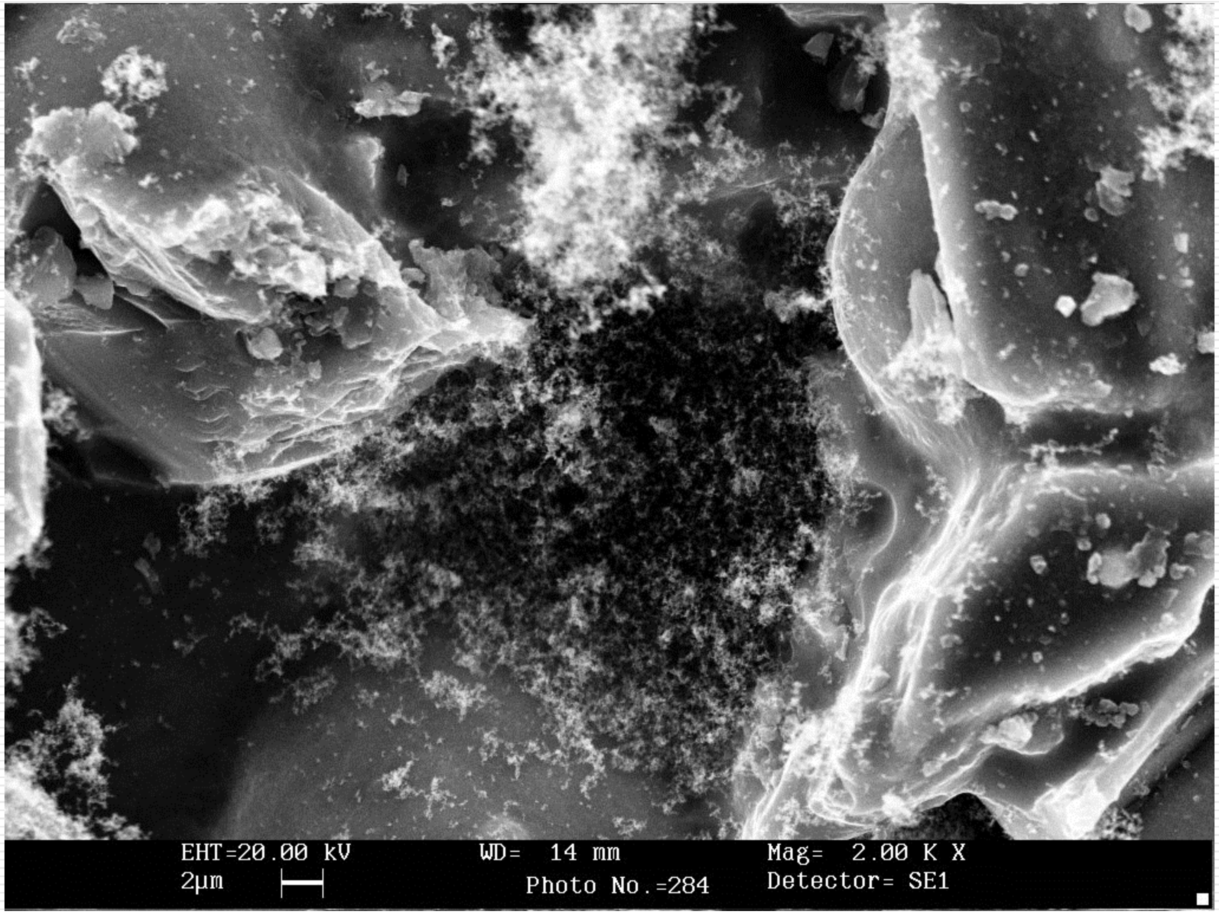

Stability of diesel particulate deposits

SiC pore 1 loaded to 0.1 g/l: SEM image captured 2 months later

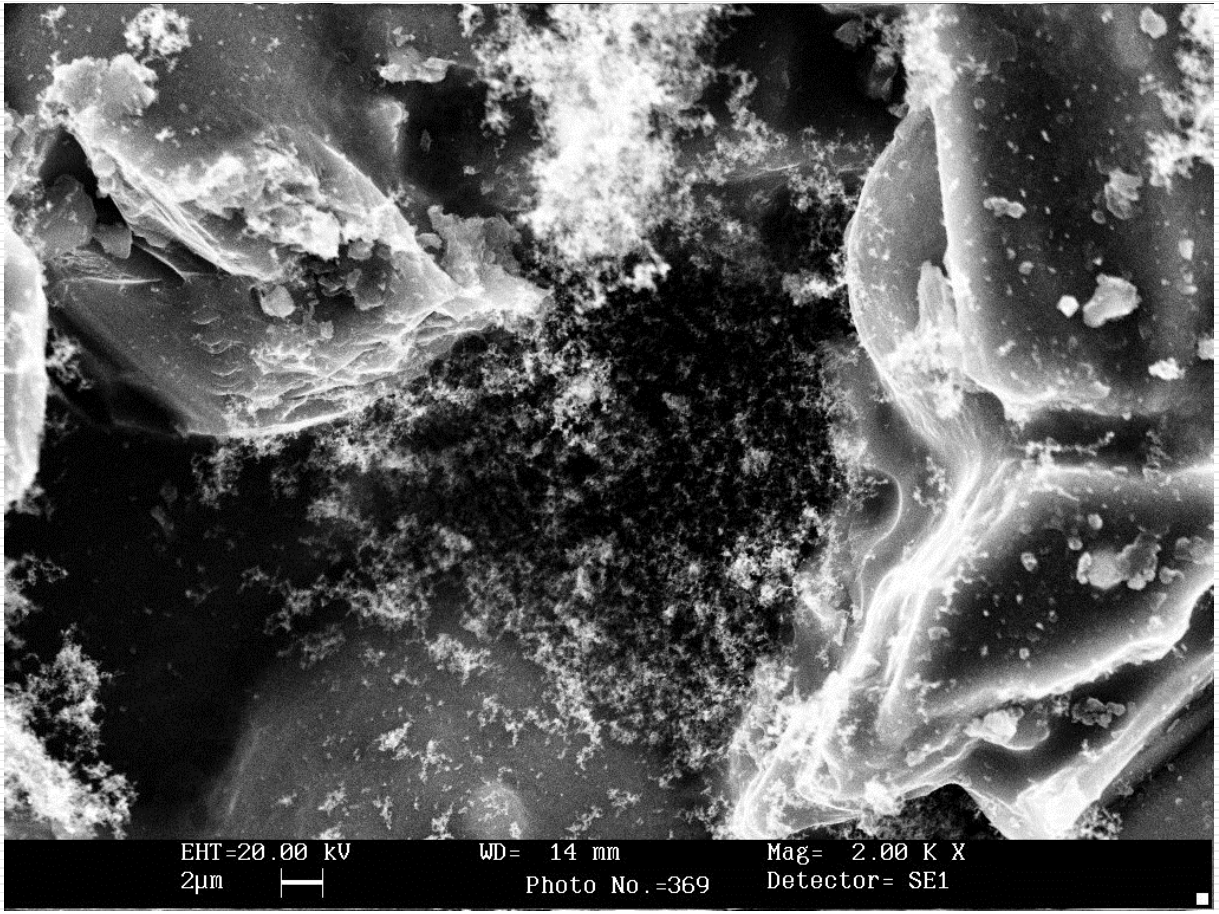

Stability of diesel particulate deposits

Same images aligned and cropped around pore (0 → 1 → 2 months old)

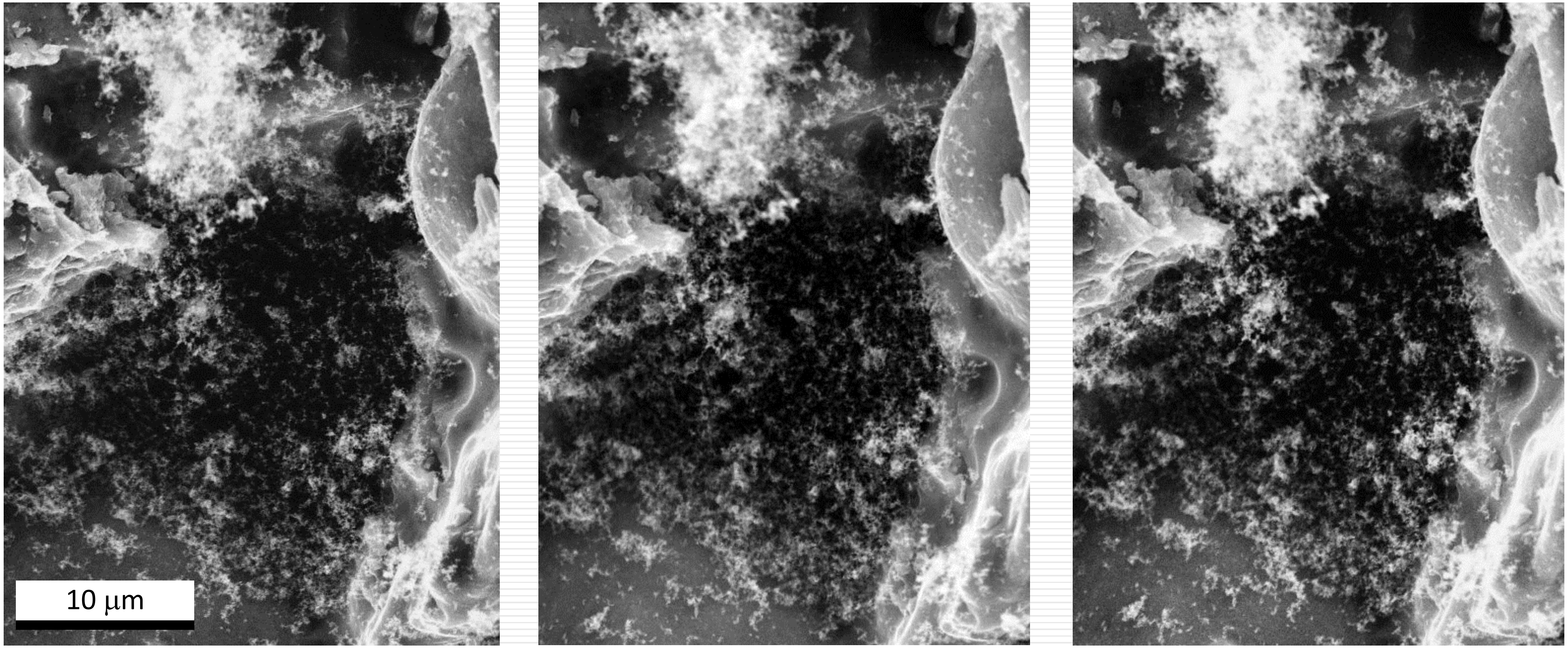

Packed bed of spheres filtration model

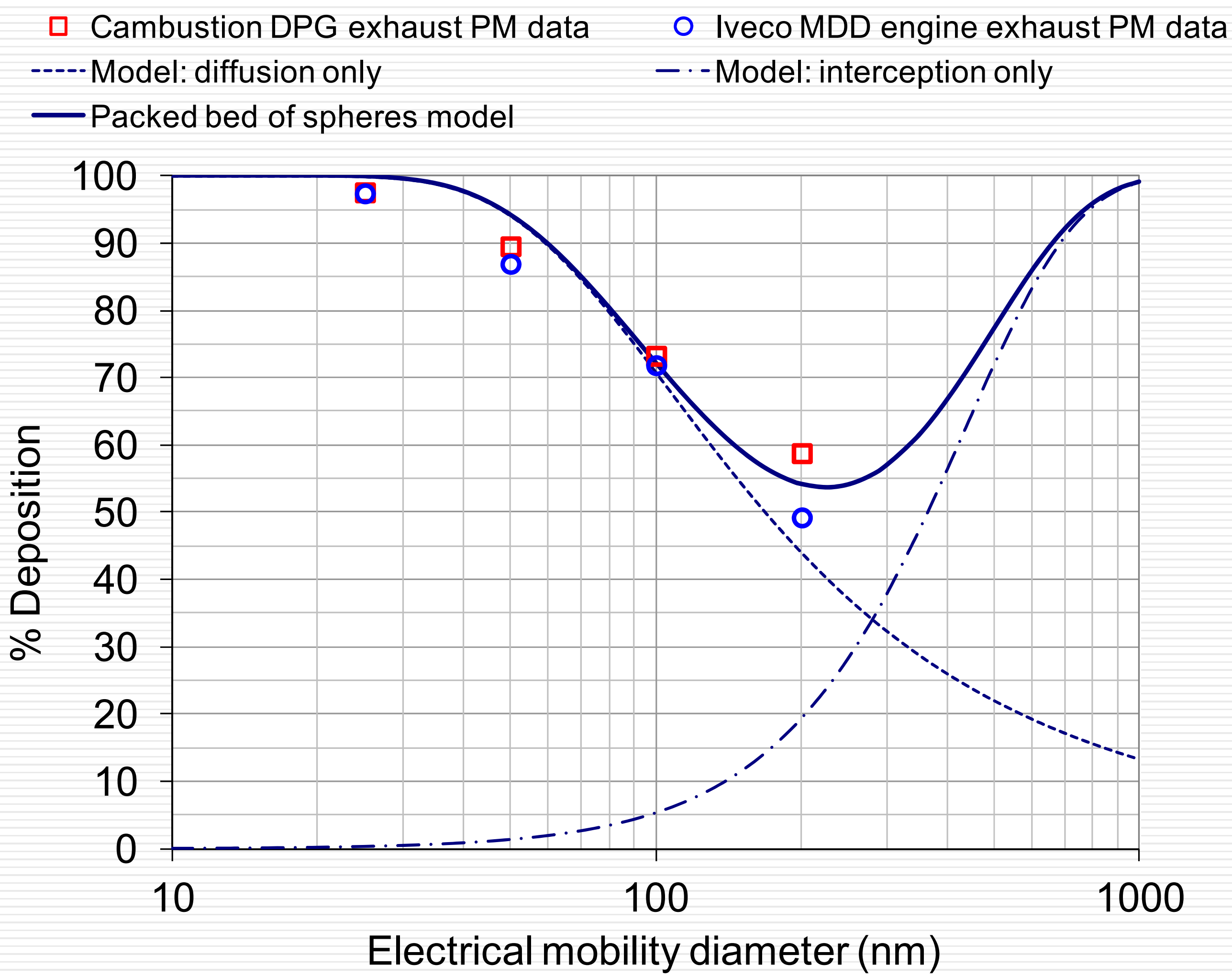

- Packed bed of spheres model (Lee and Giseke 1979*) applied to initially clean DPF porous wall by Konstandopoulos and Johnson (1989)**
- For SiC wall sample, idealised sphere diameter = 8.5μm

** Lee, K. W., and J. A. Gieseke. "Collection of Aerosol Particles by Packed Beds." Environmental Science and Technology 13 (1979): 466 – 470*

*** Konstandopoulos, A. G., and J. H. Johnson. "Wall-Flow Diesel Particulate Filters – Their Pressure Drop and Collection Efficiency." SAE Technical Paper Series, 1989: 890405*